

Hydrologic Profiles and Geospatial Trend Analysis Evaluating Recurrent Flooding at Coastal U.S. Air Force Installations

THESIS

Dylan D. Bechen, Captain, USAF

AFIT-ENV-22-M-181

DEPARTMENT OF THE AIR FORCE
AIR UNIVERSITY

AIR FORCE INSTITUTE OF TECHNOLOGY

Wright-Patterson Air Force Base, Ohio

DISTRIBUTION STATEMENT A
APPROVED FOR PUBLIC RELEASE; DISTRIBUTION UNLIMITED.

The views expressed in this document are those of the author and do not reflect the official policy or position of the United States Air Force, the United States Department of Defense or the United States Government. This material is declared a work of the U.S. Government and is not subject to copyright protection in the United States.

AFIT-ENV-22-M-181

HYDROLOGIC PROFILES AND GEOSPATIAL TREND ANALYSIS EVALUATING RECURRENT FLOODING AT COASTAL U.S. AIR FORCE INSTALLATIONS

THESIS

Presented to the Faculty

Department of Systems Engineering and Management

Graduate School of Engineering and Management

Air Force Institute of Technology

Air University

Air Education and Training Command

in Partial Fulfillment of the Requirements for the

Degree of Master of Science in Engineering Management

Dylan D. Bechen,

Captain, USAF

March 2022

DISTRIBUTION STATEMENT A
APPROVED FOR PUBLIC RELEASE; DISTRIBUTION UNLIMITED.

AFIT-ENV-22-M-181

HYDROLOGIC PROFILES AND GEOSPATIAL TREND ANALYSIS EVALUATING RECURRENT FLOODING AT COASTAL U.S. AIR FORCE INSTALLATIONS

THESIS

Dylan D. Bechen,
Captain, USAF

Committee Membership:

Dr. Christopher M. Chini, Ph.D.
Chairman

Lt Col Justin D. Delorit, Ph.D., P.E.
Member

Maj Sean-Micheal T. Kelly, Ph.D.
Member

Abstract

Military installations are exposed to numerous threats, including a changing climate, which impacts the frequency of extreme events and creates long-term changes in the environment and risk of nuisance or recurrent flooding. The four components of recurrent flooding are sea-level rise, tidal fluctuations, storm surges, and changes in rainfall event intensity. These individual events, however, do not occur in isolation. Instead, combinations of these events exacerbate the extent of the damages and create compound resilience challenges. Climate change driven combinations of these flooding events exacerbate the extent of resulting flood damage and create compound resilience challenges, which have resulted in 8 of the 10 most costly natural disasters in U.S. history. This paper analyzes 40 years of historical precipitation and tidal data for 17 coastal U.S. Air Force installations using indicators of both peak and threshold exceedance frequencies to establish hydrologic profiles.

These profiles are then used to determine long-term temporal trends in the hydrologic components that make up recurrent flood risk. Results illustrated that sea-level rise is a persistent and increasing threat which is impacting all of the coastal Air Force installations similarly. However, precipitation conditions appear to be worsening in the Mid-Atlantic region the fastest, placing these coastal installations at the greatest risk of recurrent flooding in a changing climate. This research can be used to inform U.S. Air Force decision makers when evaluating portfolio-wide adaptation strategies and aid in the prioritization of long-term infrastructure investments to combat the changing recurrent flood risk at coastal installations.

For my loving wife and daughters...

Table of Contents

Page

Abstract iv

List of Figures viii

Acknowledgements xi

I. Introduction 1

1.1 Background 1
1.2 Langley AFB, Hurricane Isabel 2003 2
1.3 Problem Statement 4
1.4 Research Objectives 6

II. Literature Review 8

2.1 Flood Event Measurement and Infrastructure Design Scale 8
2.2 Coastal Recurrent Flooding & Climate Change 13
Sea Level Rise (SLR) 15
Precipitation 18
Storm Surge 25
Tidal Fluctuations, Astronomical Tides 27
Multi-modal Recurrent Flooding 28

III. Methodology 31

3.1 Indicator Selection 31
3.2 Precipitation Data 32
Data Retrieval and Analysis in RStudio 33
Precipitation Indicators 35
3.3 Tidal Data: SLR, Tidal Fluctuations 39
Data Retrieval and Analysis in RStudio 39
SLR and Tidal Indicators 42
3.4 Data Analysis & Normalization 45
Simple Linear Regression 45
Normalization 46
3.5 Analysis Structuring and Synthesizing Results 47
1. Single Installation Analysis 47
2. Multi-Installation Trends 48
3. K-means Clustering Analyses 48

Page

IV. Results 50

4.1 Single Installation Analysis 50
Precipitation Results 50
Tidal Results 56
4.2 Multi-Installation Trends 58
Tidal Trend Analysis 58
Precipitation Trend Analysis 59
1. Distinct Zones 62
2. Significant Indicator Identification 62
3. Installation- Positive & Negative Indicator Magnitudes 63
4. Single Installation Trends 63
4.3 K-means Clustering Analyses 64
Quantitative Analysis: RStudio 65
4.4 Key Takeaways 69

V. Discussion 70

5.1 Hurricane Isabel, Langley AFB and Adaptation Effectiveness 70
5.2 Air Force Application of Hydrologic Profiles 73
1. DOD Risk Identification and Analysis 73
2. Adaptation Efforts 75
3. Prioritizing Installations for Adaptation 76

VI. Conclusions 78

VII. Appendix 79

Bibliography 107

List of Figures

Figure		Page
1	NOAA Hurricane Isabel Storm Surge, September 2003	3
2	Coastal U.S. Air Force Installations & USGS Total Annual Precipitation	6
3	Intensity-Duration-Frequency Curves[22]	10
4	Precipitation-Frequency Atlas- 100-Year 24-Hour Rainfall (inches) [22]	11
5	Hydrologic Design Scale- % Estimated Limiting Value (ELV)[22]	12
6	Generalized Design Criteria for Water-Control Structures [22, 28]	13
7	Riverine Flood Hazard Area (100-Year Floodplain) [26]	14
8	CO2 Emission Pathways Until 2100- RCPs [30]	15
9	2100 Mean Temperate Change Forecasts- RCP2.6 and RCP8.5l [4]	15
10	NOAA Global Mean Sea-Level Rise, 1993-2021 [32]	17
11	North American VLM Trend Estimates (mm/year)-NASA Jet Propulsion Laboratory [32]	17
12	IPCC AR6 WGI Reference Regions- Heavy Precipitation Map [4]	19
13	IPCC AR6- Global 24 hr 10-year Event Frequency and Intensity [4]	20
14	Nine Principle Climate Oscillations Map [39]	21
15	NOAA Multivariate ENSO Index Version 2, 1980-2021 [40]	22
16	NOAA- ENSO Pacific Basin Schematic [40]	22
17	Atlantic Multidecadal Oscillation Index [39]	23

Figure Page

18 Precipitation and AMO Seasonal Correlation Maps- May-to-Jun & Aug-to-Oct [41] . . . 24

19 NOAA Storm Surge Diagram . . . 25

20 NOAA Peak Storm Surge Map, Hurricane Katrina, 29 August 2005 . . . 26

21 Astronomical diagram of tidal extremes . . . 28

22 Tide Surge and Precipitation Interaction Results- Wahl et. al 2015 [23] . . . 30

23 Precipitation Indicators . . . 35

24 National Water Level Observation Network (NWLON) Tidal Station [49] . . . 40

25 API Parameters and Example Concatenation . . . 41

26 Selected Tidal Stations . . . 42

27 Sea-Level Rise and Tidal Indicators . . . 43

28 Total Annual Precipitation . . . 51

29 Maximum Accumulation by Period . . . 52

30 Max Monthly Precipitation & Month . . . 53

31 # Threshold Exceedances by Duration- Threshold 1 & 2 respectively . . . 54

32 # Threshold Exceedances by Duration- Threshold 3 & 4 respectively . . . 54

33 Number Threshold Exceedances by Threshold for 24hr & 48hr Periods . . . 55

34 Number Threshold Exceedances by Threshold for 72hr Period . . . 55

35 Mean Sea Level & Peak Tides . . . 57

36 Number of 90 & 95% Quantile Exceedances and Maximum Tide Differential . . . 58

Figure Page

37 Tidal Indicators- Rates of Change Results Table 58

38 Precipitation Indicators- Rates of Change Results Table 61

39 Precipitation Results- Euclidean Distances Heat Maps 65

40 K-Means Optimal Number of Clusters- Elbow Charts 66

41 Cluster Results 67

42 Cluster Results Summary Table 68

43 Electricity Infrastructure Flood Analysis – Florida USAF Installations 74

44 Electricity Infrastructure Line-of-Effort Matrix for Flood Mitigation 75

Acknowledgements

I would like to thank all of the GEM faculty and AFIT instructors for their outstanding instruction in such a challenging teaching environment. A special thanks to my faculty advisor, Dr. Chini, who guided me throughout this academic endeavor and supported me as our family welcomed in our baby girl.

Finally, I would like to thank my loving wife for all of her encouragement and understanding over the last 18 months. You could have timed the whole baby-thing a little better, but I am so glad that we have been able to have this adventure together.

Dylan D. Bechen

HYDROLOGIC PROFILES AND GEOSPATIAL TREND ANALYSIS EVALUATING RECURRENT FLOODING AT COASTAL U.S. AIR FORCE INSTALLATIONS

I. Introduction

1.1 Background

Military installations across the globe are exposed to numerous threats ranging from terrorist attacks, host-nation instability, cyberattacks, near-peer conflicts, and natural disasters, each of which poses serious risk of severely disrupting or even halting an installation's ability execute their mission. In recent history, natural disasters have shown to be one of the most disruptive, destructive, and persistent threats to our modern military installations and their ability to operate. A natural disaster is any hurricane, tornado, storm, flood, high water, tidal wave, tsunami, earthquake, volcanic eruption, mudslide, snowstorm, drought, fire, or other catastrophe that may cause damage or injury to civilian property or people [1]. A changing climate impacts both the frequency and magnitude of many of these natural disasters including hurricanes, tornadoes, and flooding events, resulting in more devastating and widespread extreme events. The increasing prevalence of such events has caused numerous mission disruptions to military installations and requires a greater emphasis on the implementation of climate change adaptations throughout the Department of Defense's (DoD) infrastructure portfolio to ensure our military's ability to operate in all current and future threats.

Nationwide, recurrent flooding events result in the greatest damage costs of all

natural disaster types; 8 of the 10 most expensive natural disasters in U.S. history were due to recurrent flooding, 7 of which occurred at coastal locations due to Extreme Weather Events (EWEs)[2]. Damage caused during EWEs events such as hurricanes are typically caused by two vectors: wind and flooding. The impacts of wind damages can be severe, but the vast majority of infrastructure damage and fatalities are driven by water intrusion and flooding.

In the 2019 Report on Effects of a Changing Climate to the Department of Defense and the 2019 Inspector General's Audit of the DoD's Preparation for Natural Disasters, both reports noted that climate change is having significant effects on current and future installation vulnerabilities. This report found that of the 79 installations evaluated, 53 of them are currently battling recurrent flooding and an additional 7 are expected to experience impacts in the immediate future. While this particular threat evaluation was limited to only the next 20 years, sea-level rise is expected to continue until at least 2100 at an increasing rate due to climbing global temperatures [1, 3–6].

The impacts of recurrent flooding on U.S. Air Force Installations and their missions can vary wildly. While the relatively minor costs and inconveniences of the occasional pooling or over-topping of a coastal road on our installations may seem inconsequential, these symptoms may be indications that our installations are not adequately prepared to withstand the compound flood conditions that come with extreme weather events (EWEs) which can devastate an ill-prepared installation, as was the case in 2003 when Hurricane Isabel swamped Langley AFB.

1.2 Langley AFB, Hurricane Isabel 2003

At Langley AFB, VA, the installation's low elevation waterfront placement at the mouth of the Chesapeake Bay makes it no stranger to recurrent flood risk. This

area has seen a number of storms thorough its long history, with varying degrees of damage due its fairly well protected positioning within Chesapeake Bay [7]. Like many hurricanes, Hurricane Isabel originated off the coast of North Africa as a tropical depression at the beginning of September 2003 and rapidly grew to a Category 5 storm as it approached the Bahamas. The storm turned north and lost some steam, making landfall on the 18th of September as a strong Category 2 storm at Hatteras Village, NC, approximately 150 miles south of Langley [7–9].

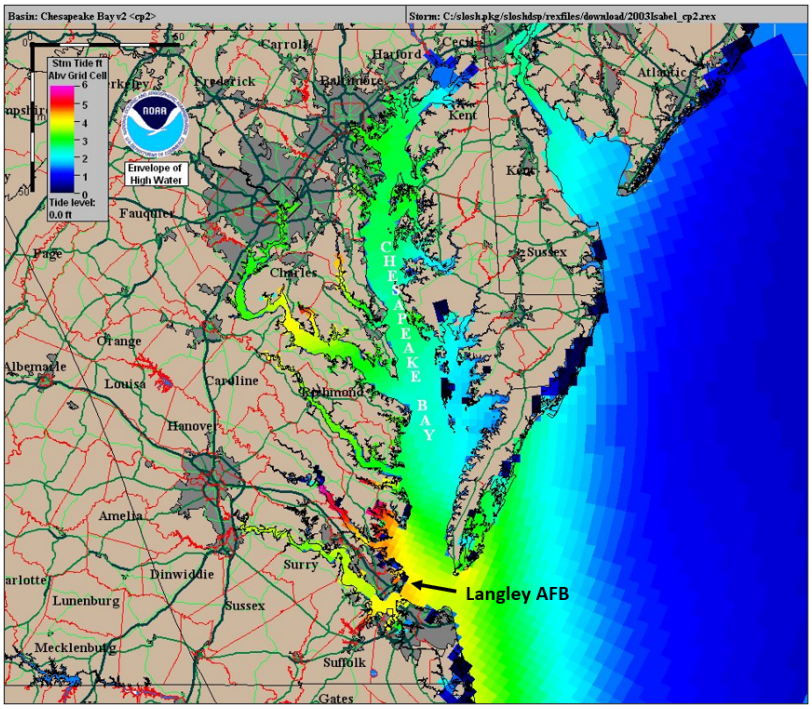


Figure 1. NOAA Hurricane Isabel Storm Surge, September 2003

The storm's incredibly wide and persistent storm bands dumped 8-12 inches of rain on the area, with isolated areas experiencing over 20 inches over the course of the storm event. However wind driven storm surge was the cause of much of the damage in the region, resulting in damages costing over $1.85B, 33 casualties and left 4.3 million people without power for up to 5 days [8, 10, 11]. The wind bands were perfectly aligned with the mouth of Chesapeake Bay, slamming Langley with

over 7.9ft of storm surge. With much of the installation sitting at only a few feet above sea-level the damage was extensive at over $146M. Damage and flooding was so extreme, that it took 4 days just to recover the airfield and more than 10 days for the installation to re-open [7, 10, 12, 13]. However, the installation's successful implementation of flood resilience adaptations following the event allowed them to fair significantly better in subsequent storms [14]. Further discussion of Langley AFB and their adaptations are provided in Chapter 5.

1.3 Problem Statement

The four components of recurrent flooding are sea-level rise, tidal fluctuations, storm surges, and changes in rainfall event intensity. These individual events, however, do not occur in isolation. Instead, climate change driven combinations of these events exacerbate the extent of the flood damages and create compound resilience challenges [15, 16].

Several studies have evaluated the combination of these events, including storm surge/precipitation and sea-level/storm surge [17, 18]. These compound climate events are combinations of multiple hazards, and significantly increase risk, which have increased over the past century. In addition, both the magnitude and frequency of each of these hydrologic components vary along the coast [19, 20]. Due to its proximity to the Caribbean and average tropical storm path, south-eastern states such as Florida see a higher number of storms making landfall than more northern states such as Virginia or New York, resulting in patterns of higher frequency of storm surge and rainfall events in the region. Location, along with a number of factors that are influenced by climate change make up an area's hydrology or hydrologic patterns as they relate to recurrent flooding. Hydrology is defined as "the science that treats the water of the Earth, their occurrence, circulation, and distribution, their chemical and

physical properties, and their reaction with the environment, including the relation to living things, the domain of hydrology embraces the full history of water on Earth" [21, 22]. Weather patterns are the most commonly experienced forms of hydrology. It has been shown that that weather patterns vary widely along the United State's East Coast due to a number of meteorological variables such as average temperatures, humidity, proximity to trade winds, and simple latitude [23]. It varies so much in fact, that the East Coast contains all 5 of the major climate zones, but do the hydrologic components vary regionally as well? Are each of the component changing at similar rates or is there a "controlling" component that is changing faster than the others?

Extensive Department of Defense funds have been put into modeling the impacts of climate change, such as sea level rise [20, 24]. However, there has been minimal implementation of these results by installation planners and decision makers due to a lack of data synthesis and understanding over the major modalities of hydrologic failure. Therefore, this study focuses on three questions to investigate flooding indicators:

1. How have hydrologic patterns along the east and gulf coasts changed over time?

2. Can k-means clustering techniques be applied both spatially and temporally on hydrologic characteristics to identify at-risk DoD installations and infrastructure?

3. What infrastructure adaptations or policy changes should be implemented by Air Force at coastal installations to increase resilience and protect our installations from changing flood threats?

1.4 Research Objectives

This research will establish the methodology to aggregate and synthesize large amounts of hydrologic data from multiple DoD and federal databases to establish normalized hydrologic profiles for 17 the coastal U.S. Air Force installations shown in Figure 2 below. I develop the statistical and data tools necessary to assess historical (1985 to 2020) hydrologic patterns by analyzing historical precipitation and tidal data to identify spatio-temporal hydrologic trends.

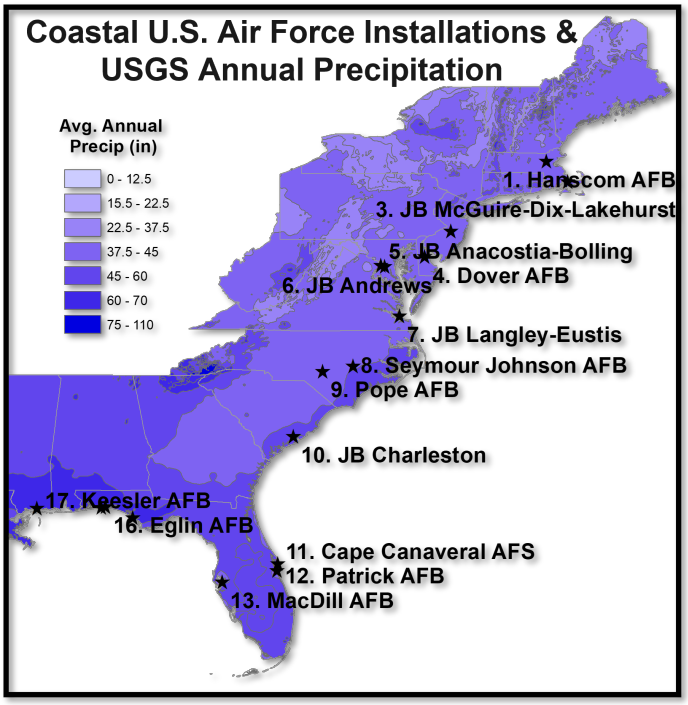


Figure 2. Coastal U.S. Air Force Installations & USGS Total Annual Precipitation

I develop of series of hydroloic indicators using both peak and threshold exceedance frequencies that allow for the identification of trends in each of the hydrologic components. Together, the rates of change for each indicator make up a location's hydrologic profile. This will enable the identification of DoD installations that have statistically similar hydrologic trends and will highlight installation's with the most rapidly changing risk of recurrent flooding.

Together this research's findings can be used to better inform U.S. Air Force Senior leaders and decision makers when evaluating portfolio-wide adaptation strategies and prioritization of long-term infrastructure investments to combat climate change driven flood risk. It can be used at the installation level to establish a comprehensive understanding of the changing recurrent flood risk and enable the selection of appropriate design standards for flood prevention infrastructure.

II. Literature Review

In this chapter, I will define the four hydrologic components of recurrent flooding (sea-level rise, tidal fluctuations, storm surge, and precipitation), identify how each component causes or impacts flooding events, summarize how climate change is expected to impact the magnitudes and frequencies of each component, and describe how combinations of these hydrologic components compound damage totals and create complex challenges for resiliency and crisis management actions.

2.1 Flood Event Measurement and Infrastructure Design Scale

The definition of recurrent flooding is simply "flooding that happens repeatedly in the same areas, typically leading to economic loss" [25]. When a flooding event occurs, there are 6 mechanisms of flooding at work that can result in widespread damages: depth, duration, velocity, wave action, impacts from debris and ice, and erosion or scour [26]. The drivers of recurrent flooding vary by location due to the geography and hydrologic threats present in a particular area. Some of these threats may be seasonal as is the case for snow-melt runoff and extreme weather events that often occur during a "stormy" or "rainy" season, whereas others are more persistent threats such as sea level rise.

The Federal Emergency Management Agency (FEMA) 543, the Design Guide for Improving Critical Facility Safety from Flooding and High Winds, was established in the aftermath of Hurricane Katrina (2005) to capture the costly lessons learned from the extreme flood and wind conditions that resulted in approximately 80% of the City of New Orleans being flooded. This devastating event resulted in over $40B in damage and caused an estimated total economic losses of over $150B, the most expensive natural disaster in U.S. history. The severity of this event as well as the

botched response and recovery efforts, brought flood preparedness to center-stage for coastal communities across the United States. Floods represent about one-third of all natural disasters and 77% of economic losses from 1980 to 2006 were caused by flooding during extreme weather events such as hurricanes [27]. Katrina brought added scrutiny to how the United States' defines floods, determined flood zones, and to how the historical adoption of definitions and evaluation techniques have hampered the progress necessary to provide adequate flood resilience.

In 1961, Dr. Hershfield of the U.S. Department of Commerce, Weather Bureau, developed a standardized methodology for quantifying flood risk from precipitation events across the United States using intensity-duration-frequency (IDF) curves which was rapidly adopted and became the foundation of water-control infrastructure design standards. This flood risk metrics, flood zone maps, and even building codes and design standards are based on Dr. Hershfield's work so it is important to understand the methods and key assumptions made that may impact the usable life of the Air Force's water-control infrastructure in a changing climate. Dr. Hershfield's research first began by creating rainfall hyetographs, or time-intensity graphs, for every rainfall event recorded prior to 1960 for a single monitoring station. All of the rainfall events were then plotted on a time scale allowing him to calculate a return period for each categorical storm intensity and enabled him to generate IDF curves such as those shown in Figure 3.

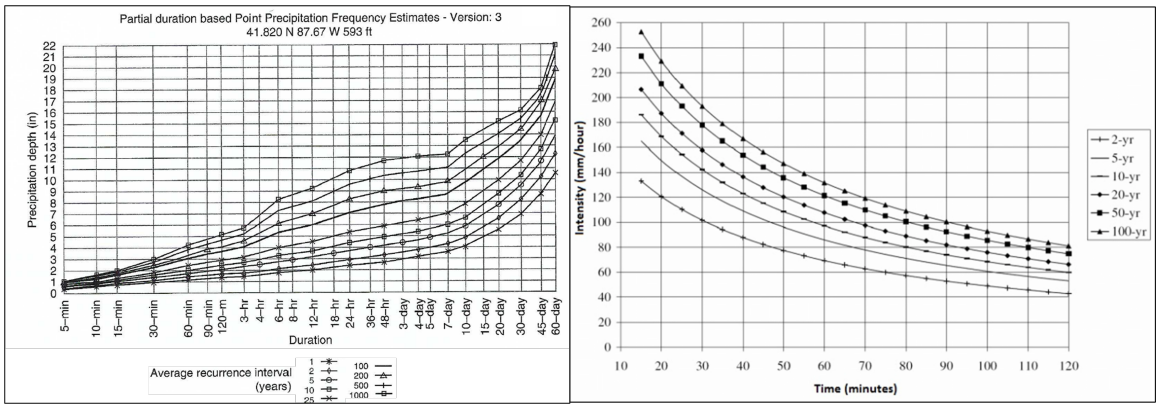


Figure 3. Intensity-Duration-Frequency Curves[22]

In 1970, the National Oceanic Atmospheric Administration (NOAA) was established and enveloped much of the U.S. Department of Commerce, Weather Bureau's meteorological work. NOAA went on to apply Dr. Hershfield's methodology across the United States. The resulting IDF curves were compiled geospatially to develop a comprehensive Precipitation-Frequency Atlas of precipitation events known as the NOAA Atlas 2, where each map within the atlas illustrates the rainfall intensity of a specific IDF curve. For example, Figure 4 below illustrates the historical rainfall intensities across the United States for a 100-year (frequency) 24-hour (duration) rainfall event.

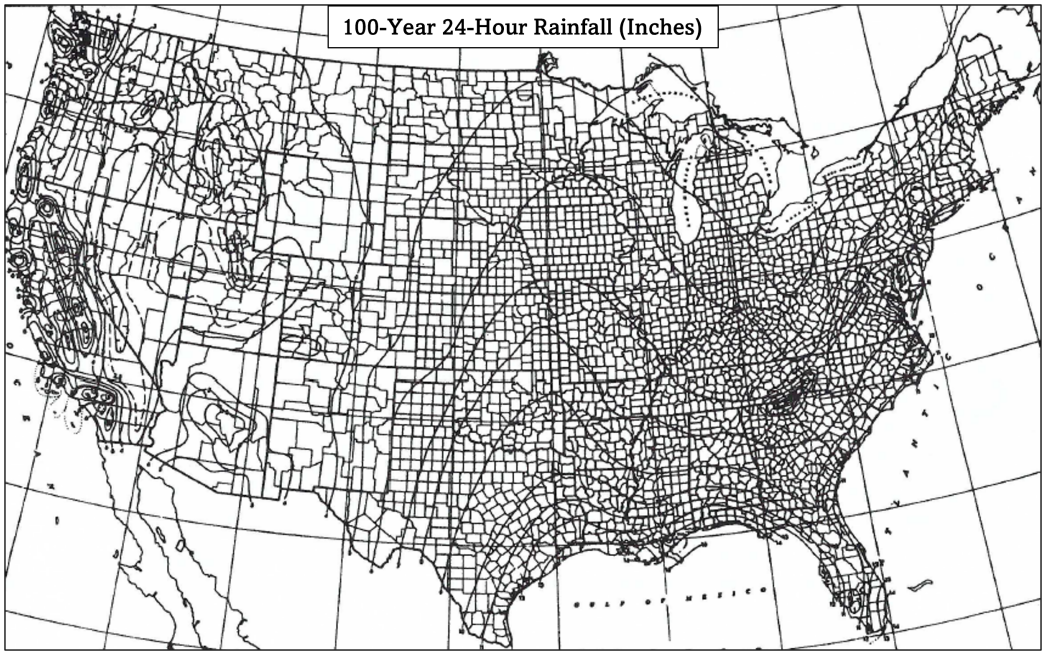


Figure 4. Precipitation-Frequency Atlas- 100-Year 24-Hour Rainfall (inches) [22]

Once established, this atlas became the primary reference for establishing a project's hydrologic design scale, by which all manners of water-control structures such as flood prevention and protection infrastructure ranging from road ditches to major flood canals and dams are designed to. Determining project's hydrologic design scale is often done by either selecting an appropriate return period or Estimated Limited Value (ELV) to meet the controlling hydrologic threat present for that project. ELV is defined as "the largest magnitude event at a given location, based on the available hydrologic information." Figure 5 below illustrates that the design metric used is dependent upon the size of the project and the risk of failure with respects to potential loss of life and economic impacts.

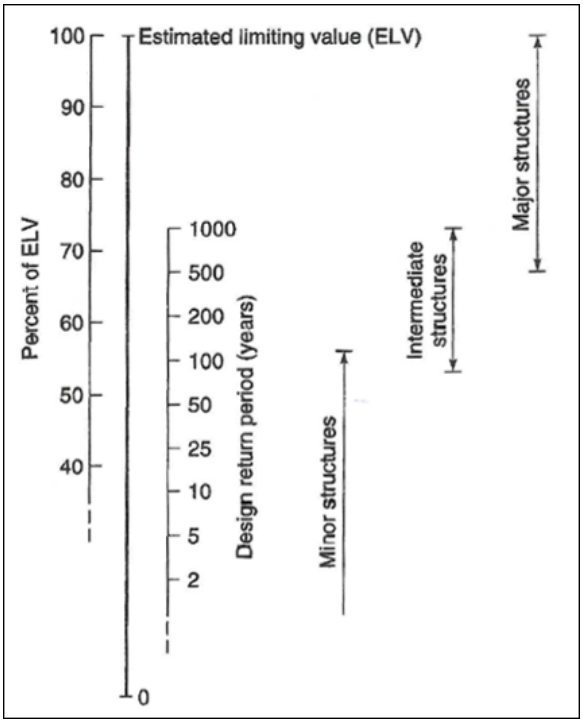


Figure 5. Hydrologic Design Scale- % Estimated Limiting Value (ELV)[22]

Figure 6 below illustrates the generalized design criteria for a number of water-control structures. Many of our coastal Air Force Installations are critically reliant upon a number of these types of structures. However, these design scales are based on data that was collected prior to the 1968 under the critical assumption that precipitation IDF curves would remain constant indefinitely. Due to this continued assumption of stochasticity in a rapidly changing climate, the flood risk to coastal installations today is actually much higher than the design scales portray. Climate change has dramatically influenced the hyrdologic threats with which Air Force designs its water-control infrastructure to because the frequencies (return-periods) and magnitudes of extreme hydrologic events are rapidly increasing [3, 5]. This puts the Air Force's current water-control portfolio at a significant disadvantage to withstand the extreme weather events of the future and decreases the expected usable life of our infrastructure.

Type of structure	Return period (Years)	ELV (%)
Highway culverts		
Low traffic	5–10	—
Intermediate traffic	10–25	—
High traffic	50–100	—
Highway bridges		
Secondary system	10–50	—
Primary system	50–100	—
Farm drainage		
Culverts	5–50	—
Ditches	5–50	—
Urban drainage		
Storm sewers in small cities	2–25	—
Storm sewers in large cities	25–50	—
Airfields		
Low traffic	5–10	—
Intermediate traffic	10–25	—
High traffic	50–100	—
Levees		
On farms	2–50	—
Around cities	50–200	—
Dams with no likelihood of loss of life (low hazard)		
Small dams	50–100	—
Intermediate dams	100+	—
Large dams	—	50–100
Dams with probable loss of life (significant hazard)		
Small dams	100+	50
Intermediate dams	—	50–100
Large dams	—	100
Dams with high likelihood of considerable loss of life (high hazard)		
Small dams	—	50–100
Intermediate dams	—	100
Large dams	—	100

Figure 6. Generalized Design Criteria for Water-Control Structures [22, 28]

In the following sections I will describe each of the hydrologic components that drive coastal recurrent flooding, how climate change is impacting these components, and how these changes are influencing flood risk at coastal Air Force installations.

2.2 Coastal Recurrent Flooding & Climate Change

Coastal recurrent flooding is flooding that occurs at or near coastlines. Evaluating recurrent flooding for coastal locations tends to be quite complex because coastal locations experience all of the same hydrologic threats as inland locations, but also face

the massive threats posed by the sea which can vary wildly during extreme weather events. Figure 7 diagrams the three types of coastal flood zones (V, Coastal A, and A) that may experience water intrusion during extreme weather or tidal events. The 4 hydrologic components of recurrent flooding are: sea-level rise (SLR), precipitation, storm surge, and tidal fluctuations.

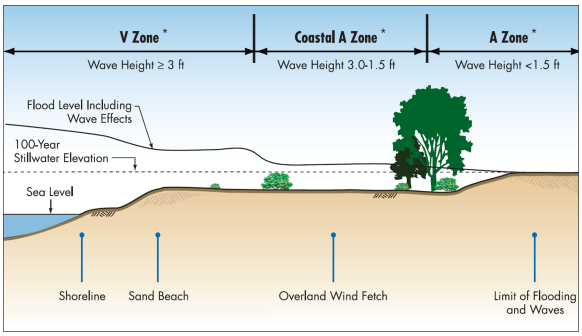


Figure 7. Riverine Flood Hazard Area (100-Year Floodplain) [26]

Carbon dioxide emissions since the industrial revolution have resulted in a rapid increase in Earth's mean temperature which in turn is altering climate variables and weather patterns globally. Climate change is resulting in increasingly warmer atmospheric and sea surface temperatures (SSTs) which enables tropical storm systems to grow rapidly and fuels the heavy precipitation and wind-driven storm surges that are experienced along the coast [1, 29–32]. Probability based forecast models of carbon dioxide known as Representative Concentration Pathways (RCPs) shown in Figure 8 illustrate that this warming trend is expected to continue through 2100 (Figure 9). It is imperative that emergency managers, community planners, federal support agencies, and all levels of government help build awareness of these growing threats and enable the implementation of adaptations to mitigate future recurrent flooding disasters [32, 33].

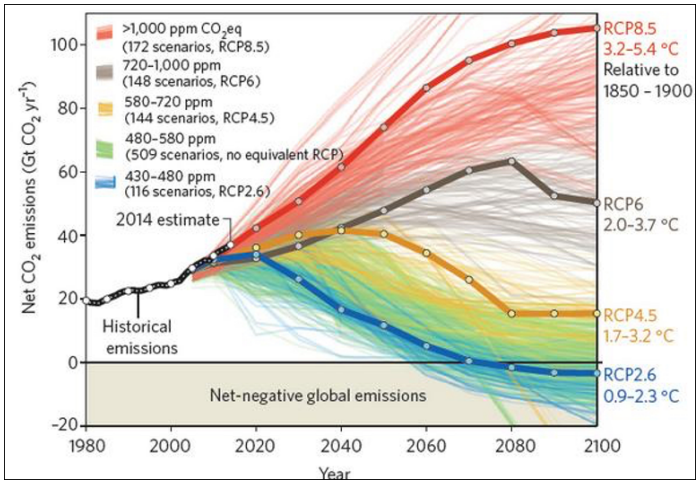


Figure 8. CO2 Emission Pathways Until 2100- RCPs [30]

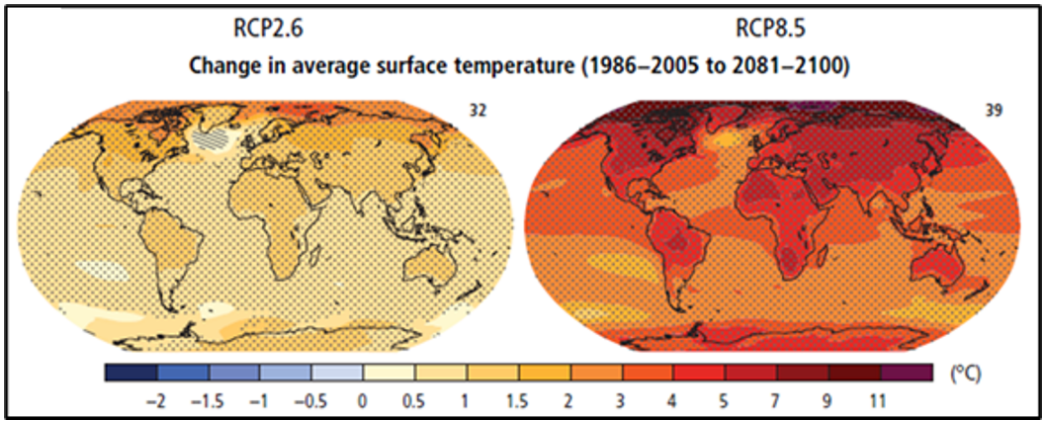


Figure 9. 2100 Mean Temperate Change Forecasts- RCP2.6 and RCP8.5l [4]

Sea Level Rise (SLR).

The first, and arguably the most impactful hydrologic component is sea-level rise (SLR). Sea level is measured in two ways; the first is through a global network of tide monitoring stations that consist of both affixed coastal stations as well as open-water buoy stations. Accurate and complete sea level readings can date back as far as the 1800s for certain monitoring locations. The second and much newer method of monitoring sea levels is through the use of satellite laser altimeters thorough the use of LIDAR) techniques, which use satellite based Light Detection and Ranging

(LIDAR) techniques to bounce lasers off of ocean's surface to record surface elevations across wide areas [12, 34]. These techniques for monitoring global sea level were first used by NASA and NOAA in 1993 and is actually a very minor capability that the entire altimeter satellite constellation provides; they are the primary source for global weather pattern tracking, topography mapping, sea surface temperatures, environmental imagery and much more.

The term "sea level" and "sea level rise" are often used inappropriately to describe any and all references to water levels such as tide levels, storm surges, and even wave heights. Sea level, appropriately used, is actually the mean sea height with respects to a specified datum, over a set period of time, typically one year due to the oscillating nature of tidal fluctuations that we discussed previously, for a given location or area. In research and application, sea level is more specifically referred to as either Local Sea Level (LSL) and Global Sea Level (GSL). This distinction is important to make because changes in LSL are often not the same as changes in GSL.

Global sea level rise has two main contributors: (1) thermal expansion caused by the warming of the ocean, and (2) an increase in water volume due to the melting of land-based ice, such as glaciers and ice sheets [32, 35]. Thermal expansion occurs when molecules absorb energy, causing the molecule to vibrate at high frequency and occupying a larger volume of space. The gradual warming of the Earth's atmosphere subsequently increases the mean ocean water temperature causing the water volume and water level to rise. In addition, rising atmospheric temperatures has also caused large amounts of land-based ice masses in our polar regions to melt and increase the total volume of water being held in our oceans. Research indicates that the impacts of all of these factors combined has resulted in a Global Mean Sea Level rise rate which has seen an SLR rate of around 3.4 millimeters (0.14 inches) per year since the 1990's, which is roughly twice the rate experienced in the previous 100 years (Figure

10) [4, 32].

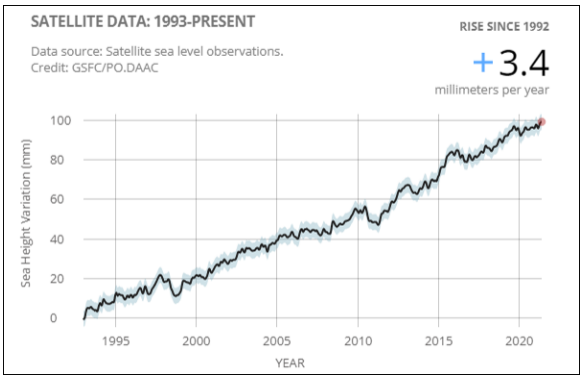


Figure 10. NOAA Global Mean Sea-Level Rise, 1993-2021 [32]

However, it is important to note that the magnitude of sea-level rise is not the same everywhere. Vertical Land Movement (VLM) caused by the shifting of tectonic plates and even the extraction of sub-surface materials such as water or natural resources can lead to increased VLM at different locations [32, 33, 36]. Variations in of these factors result in unequal experienced sea level rises as shown in Figure 11 below and illustrate that the coastal installations evaluated in this study are experiencing an additional 1-4 millimeters per year of experienced SLR.

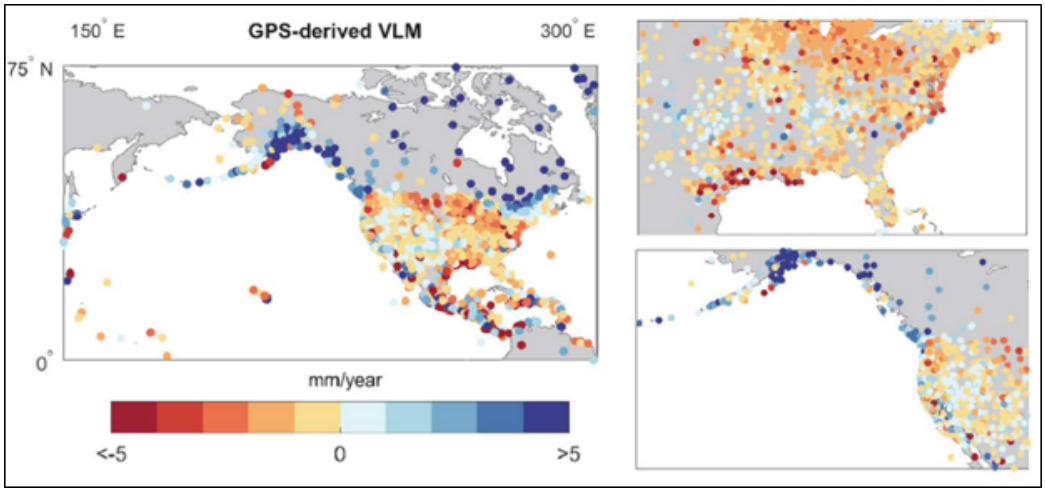


Figure 11. North American VLM Trend Estimates (mm/year)-NASA Jet Propulsion Laboratory [32]

Precipitation.

Precipitation is the hydrologic component that is shared between inland and coastal locations with respects to flooding. However, in addition to the jet stream driven thunderstorms that cause extreme precipitation events inland, Atlantic coastal locations also experience heavy rainfalls from extreme weather events (EWEs) such as tropical storms, hurricanes, and typhoons that are fed by warm equatorial waters. Powerful Nor-Easter storms also impact the Northeastern United States and supply large rainfalls and strong winds that can also lead to flooding [25, 32].

EWEs often result in heavy precipitation within a very short period, sometimes with accumulations of multiple feet in a period of only 1-2 days. Rainfall events that result in flooding are due to "rainfall excess" which is rainfall that is neither retained on the land surface or infiltrated into the soil, causing water to flow across a watershed surface [22]. If any part of the watershed (i.e. channels, ditches, basins, storm water infrastructure, or rivers) do not have the capacity to handle the rainfall excess, flooding of low-lying areas ensues.

The Intergovernmental Panel on Climate Change 6th Assessment Report (IPCC AR6) warned that the warming of the Earth's atmosphere is indisputable and scientific consensus forecasts that the magnitudes and number of EWEs globally are expected to rise [4]. The projected increase in such climate threats poses significant societal threats, given that large proportions of global populations live near coastlines [37]. Climate change projections indicate adverse impacts on worldwide coastlines from EWEs, such as high-intensity tropical storms and increased rainfall events coupled with rising sea levels, will continue to form complex challenges for coastal communities and infrastructure systems.

Figure 12 is the IPCC AR6's Working Group I (WGI) Reference Regions synthesized map of heavy precipitation already being experienced by region as along

with the statistical confidence of human contribution to such events. My study looks at the United State's Gulf and East coasts which are WGIs: NEN- North-Eastern North America, CNA- Central North America, ENA- Eastern North America. Both the CNA and ENA regions have already shown to be experience significant increases in heavy precipitation events while the North-Eastern region has too limited data at this time to make a formal observation. In my study I hope to provide further insight on precipitation events in these regions.

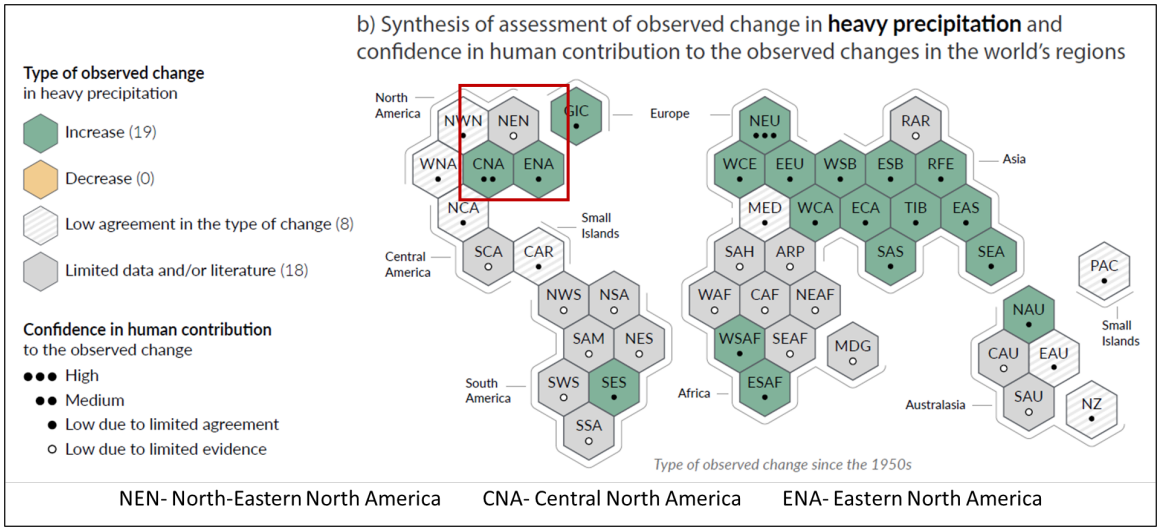


Figure 12. IPCC AR6 WGI Reference Regions- Heavy Precipitation Map [4]

Figure 13 below illustrates the IPCC AR6's forecasted heavy precipitation frequencies under each of the three future global warming levels. It is important to note that globally heavy precipitation events occur 30% more frequently that the baseline period, but is expected to more than double by 2100 under RCP 8.5. This means that globally, experiencing a once in 10-yr or 10-yr return period rainfall event will become a 3 in 10-yrr event and these frequency increases are expected to impact all intensity levels to include 100-yr events that only our critical infrastructure is designed to.

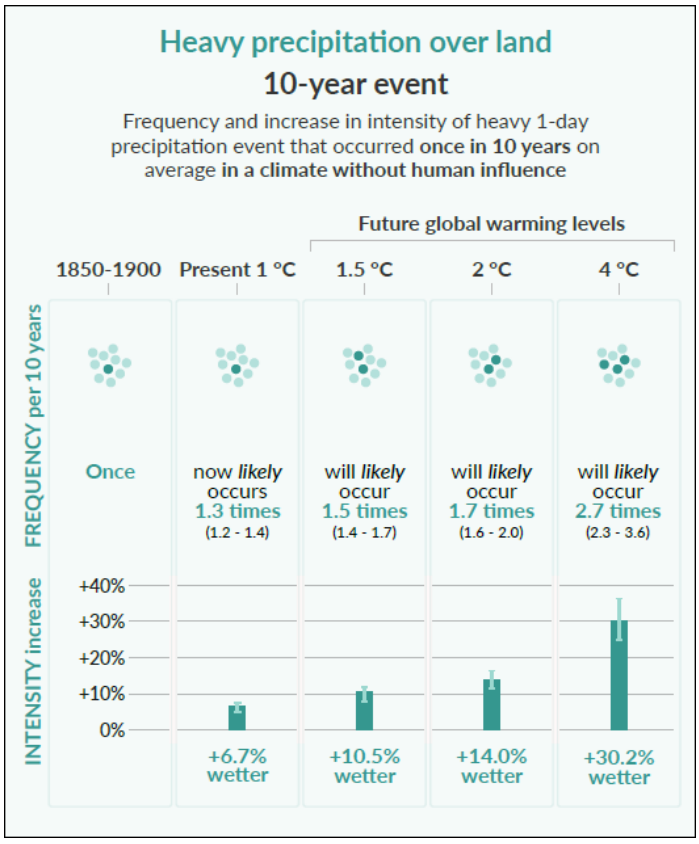


Figure 13. IPCC AR6- Global 24 hr 10-year Event Frequency and Intensity [4]

Precipitation amounts can also be affected by changes in naturally-occurring climate patterns often referred to as climate oscillations that describe major changes in atmospheric and oceanic conditions such as mean air temperatures, wind speed and direction, sea-surface temperatures, and jet-stream intensities over very large areas [38, 39]. The nine principal climate oscillations that cover different regions of the globe as shown in Figure 14 below and each of them function or oscillate at different frequencies some fluctuating every few years to multi-decadal periods such as the 70 period for the Atlantic Multidecadal Oscillation [39].

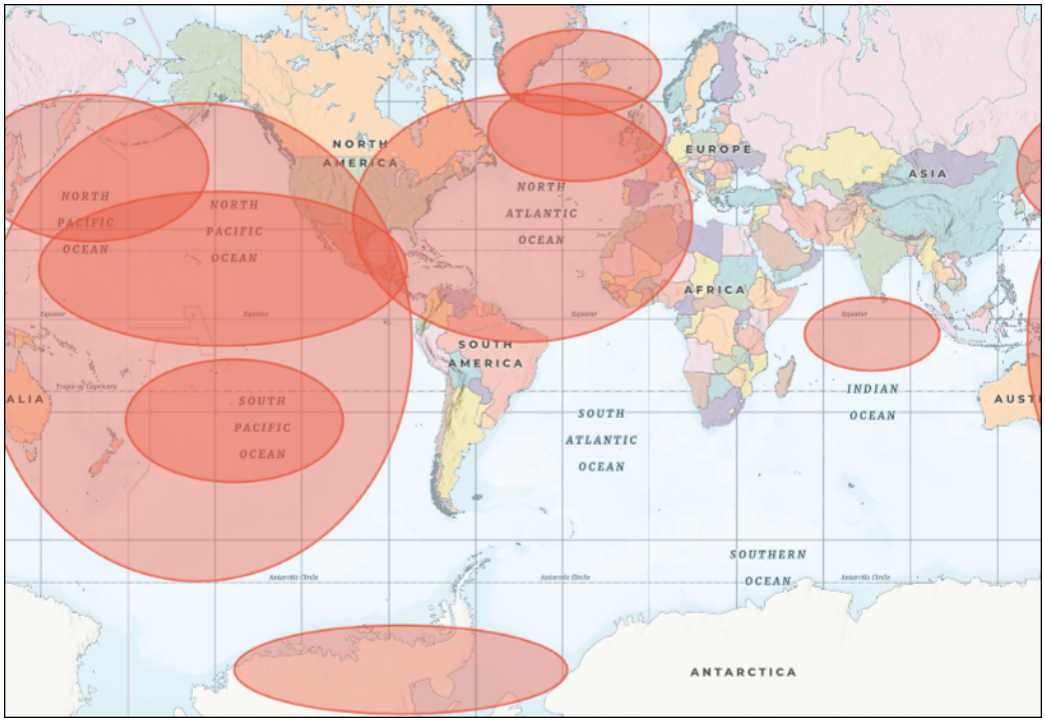


Figure 14. Nine Principle Climate Oscillations Map [39]

The most well-known of which is the El Niño/Southern Oscillation (ENSO). ENSO is a measure of 5 different variables over the Pacific basin: sea level pressure (SLP), sea surface temperature (SST), zonal and meridional components of the surface wind, and outgoing longwave radiation (OLR). Together, these variables make up a relatively cyclical pattern that rotates every 3-5 years and can dramatically impact weather patterns and rainfall amounts across the Pacific coastal regions. Figure 15 below shows the multivariate ENSO Index Version 2, which is effectively an "ENSO score" with high values indicating strong El Niño conditions and low values showing strong La Niña conditions [40]. As you can see from Figure 15 over the course of this study period (1985-2019) the ENSO Index shows relative similar magnitudes and durations of El Niño vs. La Niña overall. In Chapter 3, we will normalize our results to a 5-year (1985-89) baseline and Figure 15 shows that the mean MEI value for this period is $\tilde{0}$, so we won't be normalizing to an extreme El Niño or La Niña baseline period which

could otherwise skew the interpretation of our precipitation indicator results.

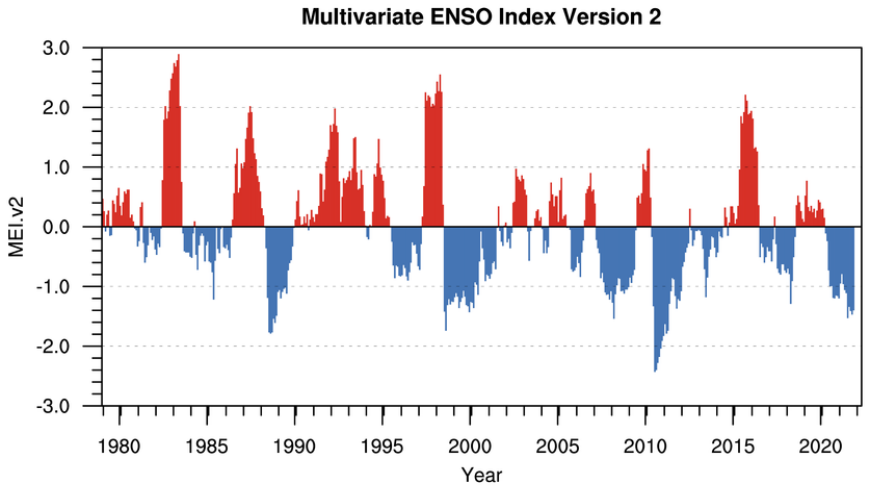


Figure 15. NOAA Multivariate ENSO Index Version 2, 1980-2021 [40]

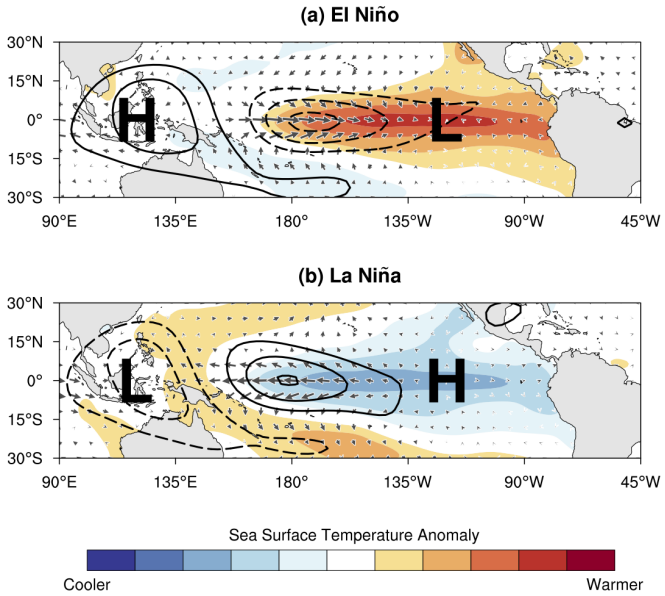


Figure 16. NOAA- ENSO Pacific Basin Schematic [40]

EWEs such as hurricanes are more frequent during La Niña episodes due to weaker vertical wind shear and less atmospheric stability [40]. Figure 16 below illustrates the

ocean-atmosphere El Niño and La Niña conditions. These patterns can dramatically vary the frequency, magnitudes, and storm paths of EWEs, ultimately impacting precipitation amounts.

Since my study is focusing on U.S. Air Force Bases on the East and Gulf coasts, two other oscillations, the Atlantic Multidecadal Oscillation (AMO) and North Atlantic Oscillations (NAO) also have significant impacts on the precipitation and EWE generation in this region. The NOA is a climate pattern that "refers to a redistribution of atmospheric mass between the Arctic and the subtropical Atlantic, and swings from one phase to another producing large changes in surface air temperature, winds, storminess and precipitation over the Atlantic as well as the adjacent continents" [38]. This pattern has more of a seasonal frequency with much of its impact on water and storm systems taking place in the winter months where this jet stream can cause atmospheric disturbances between North America and Europe.

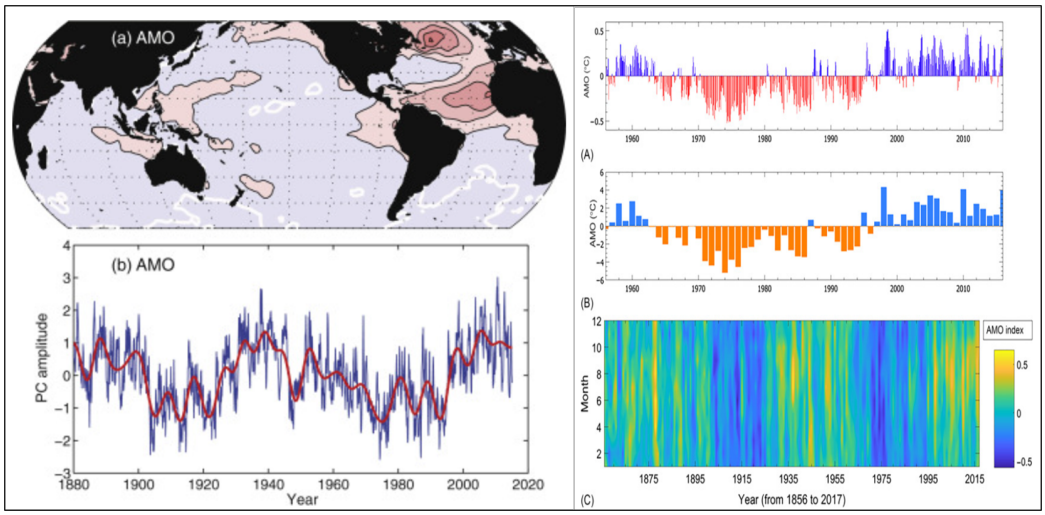


Figure 17. Atlantic Multidecadal Oscillation Index [39]

As mentioned previously AMO has a period frequency of 70 years and encompasses much of the Norther Hemisphere's Atlantic Ocean and is driven by the warming and cooling of Sea Surface Temperatures (SSTs) over such a large area [39]. It has been related to many prominent examples of climate variability in the last century

to include the North Easter and African Sahel rainfalls, the decreased rainfall experienced in the United States in the 1930s-502, and Atlantic hurricane generation in the main hurricane development region (MDR) [39]. Additionally, Figure 18 illustrates a significant correlation between seasonal precipitation amounts and the AMO index. This relationship displays a significant positive relationship for the Mid-Atlantic region and negative correlation for the South-Eastern and Gulf-Coast states [41].

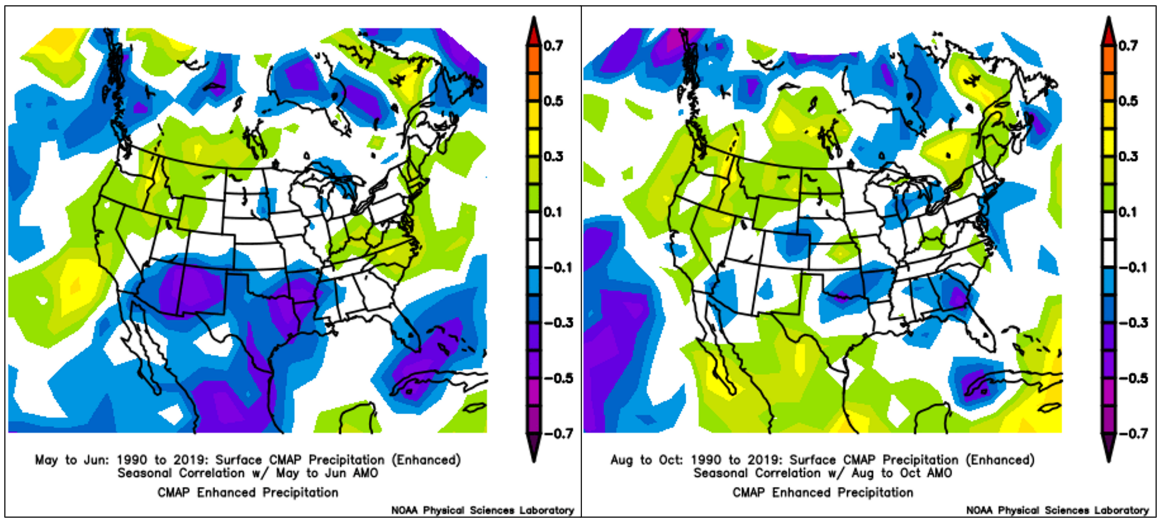


Figure 18. Precipitation and AMO Seasonal Correlation Maps- May-to-Jun & Aug-to-Oct [41]

All three of these oscillations impact extreme weather events and subsequent precipitation amounts due to their combating pressures, wind directions and vertical shear magnitudes which are driven by sea-surface temperatures in their respective regions. While this does not necessarily decrease the risk posed by a flood event such as a hurricane, it does decrease the overall variability of expected flood outcomes and enables appropriate preparations due to its long-lead time of expected magnitude. The cyclical interactions of climate oscillations have significant impacts on the magnitude and frequency of weather events generated in the region but increased sea-surface temperatures magnify these interactive effects, causing increased temperature and pressure differentials, humidity levels, and wind shears, all of which are

ingredients for extreme weather events that often bring with them multi-modal flood conditions through heavy precipitation and storm surges [29, 38, 39].

Storm Surge.

Storm surge is the occurrence of an abnormal rise in local sea-level during a storm, and is measured as the height above the normal predicted astronomical tide as shown in Figure 19 below [32]. This abnormal rise is caused by the expansive winds associated with a large storm such as a hurricane that pushes surface water in towards the coast resulting in storm surge. The amplitude of the surge is affected by a number of variables: the intensity, size, and speed of the storm vary the amount of water pushed towards a coastline by the storm's wind [42]. The angle at which a storm approaches the coast can also affect the magnitude of storm surge; a direct or perpendicular landfall track typically results in the greatest storm surge because large amounts of surge water is pushed directly towards the coast, whereas an angled landfall track allows the surge water to "escape" in a more parallel path along the coast, resulting in lower surge tides.

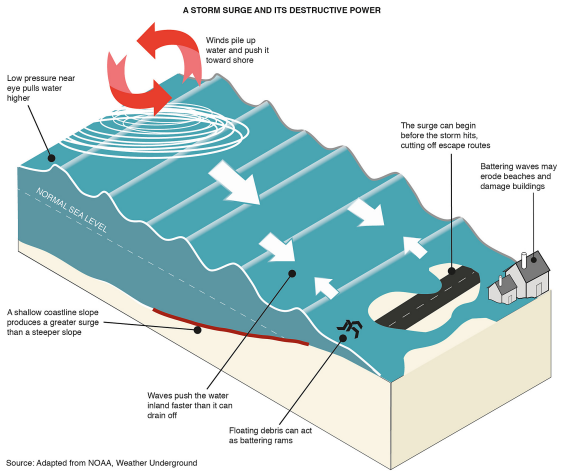


Figure 19. NOAA Storm Surge Diagram

The final major factor that impacts storm surge intensity is an area's topography,

not just overland topography as we typically think of it, but also the submarine topography of the sea floor of an area referred to as bathymetry. Bathymetry includes the volumes, depths, and shape of an area exposed to a storm threat and can vary significantly across small coastal distances. The longer and shallower the sea floor, the greater the storm surge will be [43]. An example of a high-risk storm surge area due to bathymetry is New Orleans, which has a broad, funnel-like exposure area the leading from the Gulf of Mexico to a narrow end made up of Lake Borgne and Lake Pontchartrain. This funnel-shaped bathymetry, shown in Figure 20 below, along with the direct storm path and immense intensity of Hurricane Katrina resulted storm surge of 25-28 ft in Hancock and Harrison counties. Only a few miles away, New Orleans proper saw storm surge of 16-18 ft, leading to over-topping and failure of the levees that protect much of the low-lying city that caused over 1,833 fatalities and over $172.5B in damage [2].

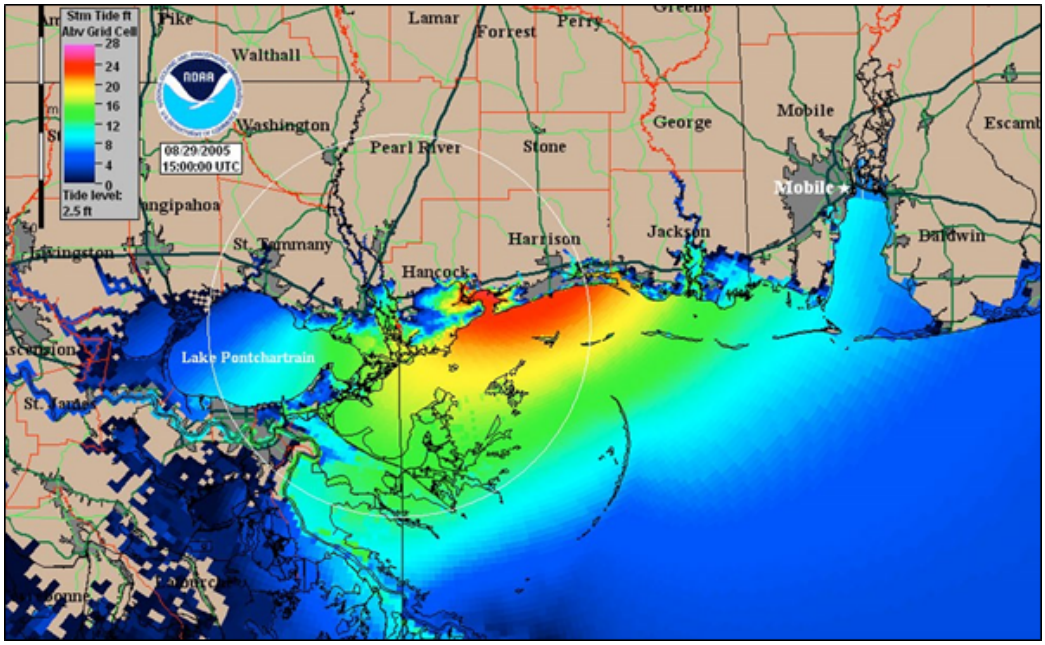


Figure 20. NOAA Peak Storm Surge Map, Hurricane Katrina, 29 August 2005

Tidal Fluctuations, Astronomical Tides.

After a single day on the beach, it is easy to see that the ocean isn't always at the same level. If you happen to lay your towel out on the sand at the wrong time of day, you may come back to it after a short swim to find all your belongings waterlogged. What are commonly referred to simply as "tides" are not due to a change in volume of water in the ocean. Instead, the changes in local sea-level (LSL) or tide differential (difference between high and low tide for a single tide cycle) you experienced are actually due to the entire volume of the ocean, changing location slightly due the combined gravitational pulls of the Sun and Moon on the Earth's Ocean as they revolve around each other and is known as the Astronomical Tide. The Earth's axis is canted 23.44 degrees, because of this cant, as the Earth rotates throughout the day you are actually brought closer to and farther away from the moon resulting in the changing gravitational pull from the Moon which changes the LSL that you can experience in a single day on the beach. This inter-day distance change is also affected by the latitude at which you are located; the farther from the equator you are the higher the tide differential will be on a given day.

The Earth's orbit around the Sun as well as the Moon's orbit around the Earth are elliptical (not perfectly circular) so the distance between the three bodies varies over the course of their orbits as well. Again, this changes the amount of gravitational force "pulling" at Earth's Oceans causing tidal fluctuations. The lunar orbit is 29.5 days, with extremes experienced every 7.3 days. In addition, the Earth's orbit of 365 days and results in a gravitational oscillation between extremes every 90 days. Figure 21 below illustrates the 2 extremes of the combined gravitational pulls from the Sun and Moon. Figure 21 (left), illustrates a Spring Tide, also known as "King Tide" and are effectively the "highest of high tides" because the Moon, Sun, and Earth are all aligned resulting in the highest combined gravitational pull on the Earth's Oceans

and subsequently highest tide differentials. Figure 21 (right), illustrates a Neap Tide which is considered a very moderate tide, and occurs when the tide differential is at its lowest point in a given lunar cycle. This is due to the 90 degree angle between Sun and Moon, which cause some of the gravimetric force to be negated.

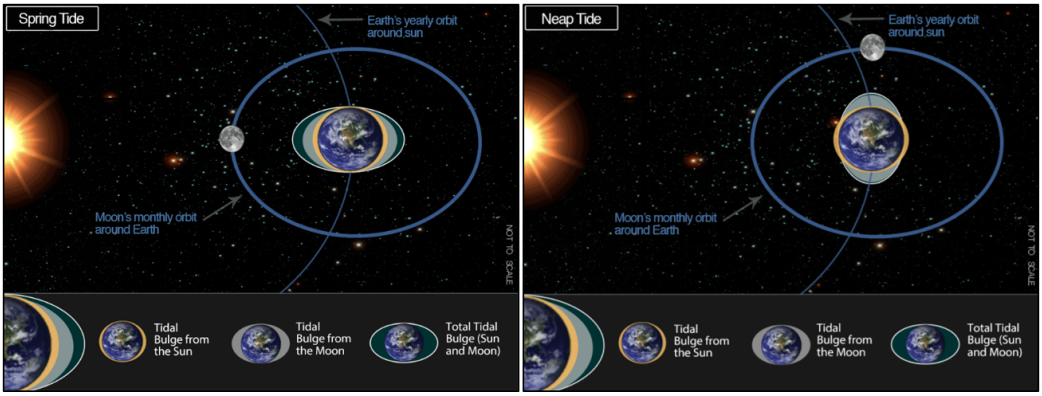


Figure 21. Astronomical diagram of tidal extremes

Since gravitational forces and orbits are inherently constant, tidal fluctuation predictions are highly reliable and well known at coastal locations, so they are never a singular cause of a flooding event. However, if another other hydrologic threat such as a moderate or extreme rainfall event happens to take place at an inopportune such as during a King Tide, it can result in significant riverine flooding near the effluent because the river has nowhere to drain to. Due to their predictable nature, tidal fluctuations are easily incorporated into coastal flood predictions [5].

Multi-modal Recurrent Flooding.

As we have discussed previously, rarely are any of these coastal hydrologic threats a singular cause of recurrent flooding. Instead, combinations of these events exacerbate the extent of the damages and create compound resilience challenges for effective mitigation adaptations [44]. In addition, the combinations of component effects results in a wide variety of multi-modal risks that are also incredibly temporally dynamic,

making large-coastal flooding events extremely challenging to predict and react to effectively [15, 45, 46].

In his 2015 paper, "Increasing Risk of Compound Flooding from Storm Surge and Rainfall for Major US Cities", Dr. Thomas Wahl evaluated the complex interplay between storm surge and precipitation and their impacts to coastal flooding. To do this he evaluated historical data at the cities shown in Figure 22a. below and found two major significant interaction trends referred to as Case 1 and Case 2. Case 1 occurrences were measured using the highest annual storm surge and the highest precipitation within ± 1 day of the tidal event. He found that in these occurrences across all sites along the Gulf and East Coasts, there was a significant correlation between the two variables which is associated with a higher likelihood of compound flooding occurrences (Figure 22b). Case 2 occurrences were defined as the the opposite, instead measuring the highest annual precipitation events and then the highest storm surge ± 1 day of those precipitation events. In this case, he found a significant dependency between the two variables but only in more confined areas; first in the Gulf and Southeast Coast, a single site in the Northeast, and 3 sites on the West coast (Figure 22c) [23].

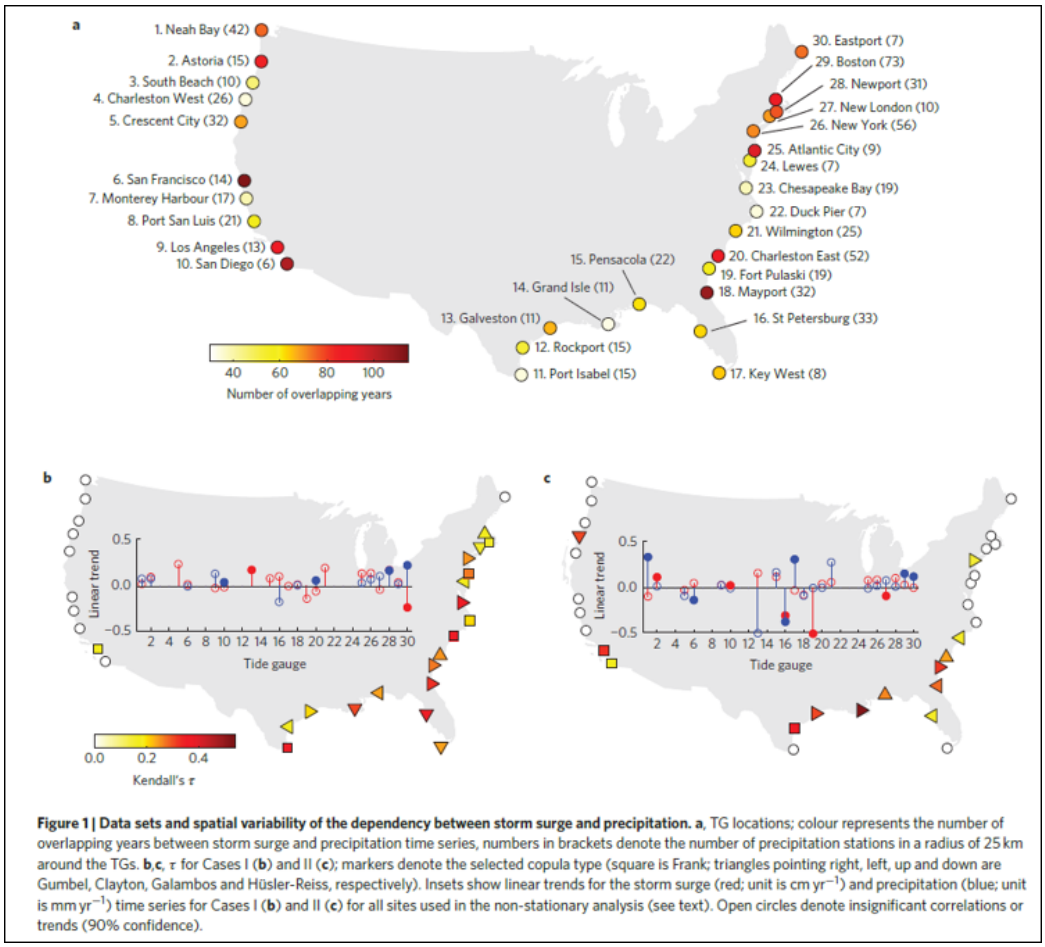


Figure 1 | Data sets and spatial variability of the dependency between storm surge and precipitation. a, TG locations; colour represents the number of overlapping years between storm surge and precipitation time series, numbers in brackets denote the number of precipitation stations in a radius of 25 km around the TGs. **b**,**c**, τ for Cases I (**b**) and II (**c**); markers denote the selected copula type (square is Frank; triangles pointing right, left, up and down are Gumbel, Clayton, Galambos and Hüsler-Reiss, respectively). Insets show linear trends for the storm surge (red; unit is cm yr^{-1}) and precipitation (blue; unit is mm yr^{-1}) time series for Cases I (**b**) and II (**c**) for all sites used in the non-stationary analysis (see text). Open circles denote insignificant correlations or trends (90% confidence).

Figure 22. Tide Surge and Precipitation Interaction Results- Wahl et. al 2015 [23]

These hydrologic relationships and linear trends in the frequencies of compound events made up of extreme precipitation and storm surge highlights the changing (non-stochastic) nature of recurrent flood risk and the need to thoroughly reevaluate the water-control infrastructure at our coastal Air Force Installations because their design lives may prove to be incredibly inaccurate due the changing magnitudes and frequency of these compound hydrologic events.

III. Methodology

3.1 Indicator Selection

My hypothesis is that the rates of change in the precipitation and tidal hydrologic components of recurrent flooding vary regionally. In order to test this theory, I needed to identify meaningful indicators of each flood component that together create a "hydrologic profile" for a given location. This hydrologic profile will highlight any historical trends with respects to magnitude and frequency of events at a given installation. In addition, these indicators must be selected and calculated in a manner that allows statistically sound comparisons between all other indicators' results as well as against indicators' results from other installations to conduct a coast-wide analysis.

Indicators were selected based on (1) their ability accurately illustrate long-term changes in both magnitude and/or frequency of events and (2) their results' ability to be cross evaluated with those of results from another installation without inherit selection bias due to the locations of data collection. For example, it is possible for selection bias to occur in the de-trending of precipitation data when utilizing seasonal indicators because researchers traditionally look at a single location or region that is small enough to share the same "rainy season" across their study area due to proximity and prevailing weather patterns. Since I am evaluating such a large region with wildly varying weather patterns across the study, more localized "rainy" or "dry" season analyses such as a "Total June-July-August Precipitation" indicator across all locations is not an appropriate analysis method because the "rainy season" in Maine or New York may vary significantly from that of Florida and Louisiana. Selecting indicators that are able to highlight long-term trends in both the magnitude and frequency of hydrologic events are critical to illustrating changes in the flood risk components. By normalizing and applying trend-lines to the indicators that meet

both of the criteria above for each installation, we can use the resulting rates of hydrologic profiles to understand how hydrologic components have changed over time and whether or not these changes are occurring regionally.

In the remainder of this chapter, I will describe the datasets used for each of the hydrologic components, the datasets' limitations, which hydrologic indicators were selected, how each of these indicators contributes to a location's overall hydrologic profile. Lastly, I will explain exactly how I calculated each of the indicator values from the raw datasets.

3.2 Precipitation Data

In the previous chapter, I discussed how precipitation results from storm systems. Regardless of the driver behind a rainfall event, both the rainfall accumulation amounts and durations can vary widely from location to location even for the same event and over very short distances. Since precipitation events can cause recurrent flooding through both high-intensity-short-duration and low-intensity-long-duration events, it was important to select indicators that could capture the variety of rainfall events experienced at an installation as well as the installation's climatology. The 17

The first historical climate dataset I attempted to use was from National Oceanic and Atmospheric Administration's (NOAA) Historical Observing Metadata Repository (HOMR) and Integrated Surface Datasets (ISD) databases. This dataset included full suite of meteorological variables such as visibility, humidity, wind speeds etc. recorded at roughly the hourly frequency, some weather stations recorded every 15 minutes, others only every 3 hours. Unfortunately, upon analysis of the resulting total annual precipitation amounts, I found some validation issues associated with units which resulted in calculated values that were higher than the mean annual precipitation historically recorded by the United States Geological Survey (USGS) shown

in Figure 2. Investigating the data further, I found numerous random errors throughout the recorded precipitation values across 13 of the 17 weather stations which I planned to evaluate. I was not able to find any pattern or information about how to parse out these errors, so I was forced to to abandon the dataset. However, the methods developed during the initial analysis, which can be found in the Appendix, provided an initial framework for my precipitation analysis.

The dataset used for my analysis is the Accuweather dataset that was purchased by the ENV department from Accuweather. This 1985-2019 dataset contains "clean" and verified daily weather data for all U.S. weather stations to include daily precipitation accumulation amount in inches. To thoroughly investigate the 35 years worth of daily data, a total of 18 precipitation indicators described below were used to build out an installation's hydrologic profile for precipitation events.

Data Retrieval and Analysis in RStudio.

The Accuweather dataset is structured as a series of Excel Binary Workbook files or .xslb's, one for each weather station in the United States. Each weather station has it's own .xslb workbook labeled according to its 4-character International Civil Aviation Organization (ICAO) Weather Station Code. To locate an appropriate weather station for each target installation I used the "WeatherStationMapv1" GIS interface tool. This interface tool allowed me to search the entire ICAO station index for all weather stations within a set radius of an installation. Fortunately, almost all DoD installations have long standing weather stations located on or immediately adjacent to the installation or airfield. Only stations with complete (1985-2019) data sets located within a 25km radius of the study's target installations were used in this analysis.

I was then able to download each station's .xslb workbook to a local drive manu-

ally. For example, the ICAO for the station at Tyndall AFB is "KPFN" and the .xslb for this station was titled "KPFN-HISTORY-FINAL.XLSB", this naming convention was consistent across all stations. Within each workbook, there are multiple sheets for various climate data types and recording structures. However, for the extent of this analysis only select columns on the "DATA" sheet were necessary. The 'readxslb' package within RStudio was used to retrieve the "DATA" sheet from the .xslb and convert it into a manipulable tabular form. A consistent naming convention of the datasets allowed me to use the "paste" function to combine the ICAO variable "Station" for each target installation and file designator(-HISTORY-FINAL.XLSB) to pull the appropriate .xslb using the read_xslb function for use in my code. The dataset was then subset to only the applicable columns (dates and precipitation amounts) necessary for the analysis. The 'tidyr' package was used throughout this analysis to re-format dates, restructure the raw dataset, and aggregate values for each indicator. I also used the 'paste' function when calling on station titles so that all of my recorded results and .csv exports would be labeled appropriately. Formatting my code in this manner made it possible to run the entire set of code to calculate all indicator values for a given station and only required me to change the "Station" and "Base" names to run the next installation.

To determine a rate of change for each indicator, for each base, I structured my code so that the indicator calculation results were completed for each calendar year and then recorded in a format that could later be re-organized and/or sub-set for plotting and analysis. This proved to be a challenge initially because I would have at least (18 indicators x 40 yearly data-points + 4 summary statistics values that needed to be recorded per indicator) x 17 installations worth of results values. To manage all of these values I chose to build out an long-data-frame which included only 5 columns "station", "base", "year", "measurement" (indicator title), and the

"value" calculated for that year.

I created a for loop that subset the 1985-2019 dataset to a single year and within this loop I calculated all of my indicator values. After each indicator value was calculated, I used the 'rbind' function to append it to the bottom of the 5-column results data frame. At the end of each yearly for-loop cycle, 18 appropriately-labeled indicator values were recorded as 18 rows in the results data frame. The full RStudio Precipitation Analysis Code discussed throughout this section can be viewed in Appendix.

Precipitation Indicators.

The following section will define each of the 18 precipitation indicators listed below, explain the indicator's relevance to an installation's hydroloic profile, and explain how each indicator was calculated within the RStuido construct described above.

Precipitation Indicators
1. Total Annual Precipitation
2. Maximum Monthly Accumulation
3. Month of Maximum Monthly Accumulation Occurrence
4-6. Peak Period Accumulations- 24, 48, 72hr periods
7-18. Number of Threshold Exceedances per year for 24, 48, & 72 hr periods: (4 Thresholds: 1, 1.5, 2, & 3 inches)

Figure 23. Precipitation Indicators

1. Total Annual Precipitation.

The first indicator selected was the total annual precipitation; it is the simplest and most straightforward precipitation indicator that is widely used to classify an area's climatology and along with temperature are the basis of the Köppen–Geiger

climate classification system [47]. Over an extended period, significant changes in an location's Total Annual Precipitation can illustrate a location or area's susceptibility to increased or decreased rainfall beyond the relatively short-term (3-5yr) effects of the El Nino Southern Oscillation (ENSO) discussed in Chapter 2 [40]. Measuring this indicator's change over an extended period can also help to counteract recency bias in decision-making if a given location has experienced a prolonged drought or wet period that may have been influenced by ENSO or other recurring climate patterns. To calculate this indicator a simple sum-aggregation of precipitation amount was run for each year.

2. Maximum Monthly Accumulation.

As I discussed in Chapter 2, precipitation driven-recurrent flooding does not often occur solely due to a single rain rain event, but can be overtaken after a series of rain events fully saturates soils and fills natural or designed holding channels or basins. Capturing the maximum monthly accumulation can help capture some of the changes in flood-risk caused by these possible methods of inundation. In addition, when evaluated in conjunction with Indicator 3, month of maximum accumulation occurrence, it is possible to see not only when the "rainy" season is quantitatively, but whether or not that that season in changing in intensity, or shifting earlier or later in the year.

Identification of such trends could be very valuable to installation planners and design engineers when scoping storm water systems because if they know a certain area is inundated each July, and this analysis shows that July precipitation is trending up at a rate of say 3% annually, they can then increase their design specifications above the current stochastic design standards to be able to withstand the projected monthly precipitation amounts. To calculate this indicator, an additional for-loop was created

to subset the data by month and then sum-aggregate the precipitation totals for each month. The maximum monthly total within each year was then recorded.

3. Month of Maximum Monthly Accumulation Occurrence.

As I just discussed, knowing the month when an installation experiences the greatest rainfall can tell us when the peak of the rainy-season is or when extreme precipitation events occur. By looking at these historical data-points we can see if such events are occurring earlier or later in the year. Such a trend is important to identify because it illustrates the changes to the highest-flood-risk time of year that residents or planners may be accustomed to. To get this indicator value, the month of Indicator 2 result was simply recorded.

4-6. Peak Period Accumulations- 24, 48, & 72hr periods.

In Chapter 2, I discussed the nature of flood classification based on intensity and probabilities of expected return periods for rainfall events of a given size. Storm water system design calculations are often completed using multiple IDF design events that can range from 5 minutes to 60 days depending on the size and slope of the serviced area and intensities that are geospatially subjective. The 30 minute, 1 hour, 6 hour, and 24 hour events are the most common durations evaluated during design of most standard storm water infrastructure as is often seen at an Air Force installations [22]. However, for systems that serve much larger catchment areas, higher duration events are also calculated based on potential extended holding periods caused by downstream events or high volume upstream runoff events that can magnify the localized flooding effects [22].

Since the dataset available for this analysis only contains daily records, I chose to evaluate rainfall event intensities at the 24, 48, and 72 hr duration levels. While it

would have been beneficial to have higher frequency data, such as the 1 hr maximum acclamation, because it is one of the principle design durations, these indicators still provide very relevant and useful insight into a location's hydrologic condition. By applying a linear trend to these annual maxima values, we can see how magnitudes (or intensities) of 1-3 day extreme storm events are changing over time.

7-18. Number of Threshold Exceedances per year for 24, 48, & 72 hr periods: 4 Thresholds- 1, 1.5, 2, & 3 inches.

Indicators 7-18 are a series of annual exceedances indicators that I believe, when evaluated in combination, truly illustrate how rainfall events are changing. As we discussed previously, the magnitude or depth of rainfall used in design storms varies regionally due to the standards imparted by precipitation-frequency atlases such as the NOAA Atlas 14. In order to make cross-comparisons of installation trends in different regions I instead chose to use a set standardized exceedance thresholds of 1, 1.5, 2, and 3 inches that capture the spread of moderate to high rainfall events.

Plotting and comparing these indicators for a given installation on a by-threshold basis (i.e. single duration, all thresholds), one can see how the climatology or number of lower threshold events are changing relative to high threshold events. In comparing each of these indicators over a long period it is possible to determine whether or not the stochastic design assumptions used in precipitation-frequency curves are accurate in capturing the a region's climatology in a rapidly changing climate.

To calculate each of the 24 hour exceedance indicators for a given year, I created a dummy variable vector of all zeros, and then used the greater than function to set all of the instances where the daily accumulation was greater than that indicator's threshold amount equal to 1. I then summed the dummy variable vector to get the total number of exceedances for that year within the greater for-loop. To get the

48 hour exceedance indicators, I first duplicated the daily accumulation column and applied a one row offset and then summed the two daily values to get the 48 hour accumulation and repeated this again to find the 72 hour accumulations. I then applied the same code logic above to get total number of threshold exceedances for each of the three durations at each of the four threshold levels.

3.3 Tidal Data: SLR, Tidal Fluctuations

Data Retrieval and Analysis in RStudio.

Locating appropriate SLR and tidal fluctuation data was harder to find than originally expected. I had assumed that all ocean monitoring buoys in NOAA's National Data Buoy Center database would be equipped with elevation data that could be synthesized to work for my analysis application and that similar to the weather station data. I believed I could simply select buoys that were appropriately close to the target installations and had a complete dataset for the 1985-2019 study period [48]. I used the NOAA Buoy map tool to identify such buoys and used the RNOAA package to interface with the NOAA National Buoy Center database to pull down the raw datasets from the target buoys. Unfortunately, I learned that there are a number of different buoy types and almost none of them record elevation data. Most monitoring buoys simply contain accelerometers that record wave direction, magnitude (height), and frequency. A smaller number of buoys include full weather station suites that in addition to accelerometers, can record weather conditions such as wind speed, temperature, etc., but do not explicitly record elevation.

Instead, tidal elevations and sea-level rise are actually recorded at coastal stations as a part of NOAA's National Water Level Observation Network (NWLON), which is an observation network with more than 200 permanent water level stations like the one in Figure 24 on the U.S. coasts and Great Lakes [49]. These stations are

used to monitor weather, wave characteristics, and tidal fluctuations or elevations at a 6-minute record frequency.



Figure 24. National Water Level Observation Network (NWLON) Tidal Station [49]

To access large quantities of data within NOAA's NWLON database, you must use an Application Programming Interface (API) which is just a manner in which two computer programs interact with one another. I did this in RStudio using the "httr" and "jsonlite" packages. The required NWLON API format uses a long hyperlink that consists of series of data sub-setting characteristics which includes the station identification code, exact variables requested, the datum used to calculate the elevations, and target dates. Unfortunately the NWLON database had a 365-day maximum per API request, so once I found all the correct data parameters to get exactly the data types I needed for a single year as shown in Figure 25 below, I separated the functioning hyperlink into "fixed" and "variable" sections along with the concatenation function, which allowed me to automatically update the API pull dates within my RStudio code using a yearly for-loop. The 'rbind' function was used to append each year's data pull to make a single long data set. Similar to my precipitation code, it then only required a change in station ID to run the entire code on the next target station.

Parameter	Selection
Date:	Annual (1 Jan - 31 Dec)
Product (variable):	Height- Mean Hourly
Datum:	Standard
Units:	Metric
Time Zone:	GMT
Web Services Format:	JSON

Example API concatenation:
https://api.tidesandcurrents.noaa.gov/api/prod/datagetter?begin_date=19850101&end_date=19851231&station=8638610&product=hourly_height&datum=stnd&units=metric&time_zone=gmt&application=web_services&format=json

Figure 25. API Parameters and Example Concatenation

During the NWLON station selection for each of the target Air Force Installations, I found that due to their proximity to the available tidal stations, multiple installations would have to be evaluated using the same station. Additionally, a number of the station records were incomplete and did not include the entire 1985-2019 target period. All possible tidal stations within a 50 km radius of those with incomplete records were evaluated but the limited number of stations with complete datasets left me with only 7 tidal stations to evaluate as shown in Figure 26 below.

Air Force Installation			Tidal Stations		
N to S ID #	Name	State	Tidal Staion #	Station NWLON ID	Station Name
1	Hanscom AFB	MA	1	8443970	Boston, MA
~~2~~	~~Cape Cod AFS~~	~~MA~~		~~8447435~~	~~Chatham, Lydia Cove, MA~~
3	JB McGuire-Dix-Lakehurst	NJ	2	8534720	Atlantic City, NJ
~~4~~	~~Dover AFB~~	~~DE~~		~~8537121~~	~~Ship John Shoal, NJ~~
5	JB Anacostia-Bolling	DC	3	8594900	Washington, DC
6	JB Andrews	MD			
7	JB Langley-Eustis	VA	4	8638610	Sewells Point, VA
~~8~~	~~Seymour Johnson AFB~~	~~NC~~		~~8654467~~	~~USCG Station Hatteras, NC~~
~~9~~	~~Pope AFB~~	~~NC~~		~~8658163~~	~~Wrightsville Beach, NC~~
10	JB Charleston	SC	5	8665530	Charleston, Cooper River Entrance, SC
~~11~~	~~Cape Canaveral AFS~~	~~FL~~		~~8721604~~	~~Trident Pier, Port Canaveral, FL~~
~~12~~	~~Patrick AFB~~	~~FL~~			
~~13~~	~~MacDill AFB~~	~~FL~~		~~8726607~~	~~Old Port Tampa, FL~~
14	Tyndall AFB	FL	6	8729108	Panama City, FL
15	Hurlburt Field	FL	7	8729840	Pensacola, FL
16	Eglin AFB	FL			
~~17~~	~~Keesler AFB~~	~~MS~~		~~8741533~~	~~Pascagoula NOAA Lab, M~~

Figure 26. Selected Tidal Stations

SLR and Tidal Indicators.

Similar to the precipitation indicator selection, the tidal indicators below were selected to enable analyses through the use of means, extremes, and number of exceedances. One series of indicators that I wanted to include in my analysis was the differences between the forecasted and observed elevations. However, there was a very limited number of station records that included this data and those that did often had multi-year gaps, so I omitted these indicators from my analysis.

Sea-Level Rise and Tidal Indicators
1. Mean Annual Sea Level
2. Peak Tide (Highest High Tide)
3. Maximum Tide Differential
4-5. Number of 90% and 95% Quantile Exceedances

Figure 27. Sea-Level Rise and Tidal Indicators

1. Mean Annual Sea Level.

Mean annual sea level is an important indicator because it can provide insight to how the regional sea level (RSL) is changing over time, regardless of the cyclical changes due to lunar tides. Since this data set is at the hourly scale, extreme readings such as from a storm surge (relatively low duration, 12-24 hrs) are not disproportionately weighted in the analysis. When evaluated at a single location this indicator reinforces that sea-levels are, in fact, rising. However, when used to compare multiple installations, it may be possible to identify greater regional trends with certain regions experiencing faster rates of SLR than others.

To calculate this indicator all of the non valid entries such as N/A's and 000's were first removed from the data set, then the mean annual sea level was calculated by simply using the mean function for elevation within the yearly for-loop. This gave a single average sea level for each year.

2. Peak Tide (Highest High Tide).

Peak tide or what is often referred to as the "Highest High Tide" is another extreme value indicator that illustrates the maximum tide levels that a location experiences. These values show the most extreme tidal heights experienced in a given year which, as we discussed in Chapter 2, are often the instances when EWEs and recurrent flooding are experienced. This indicator's trends for a given location can

be compared with the design specifications or tide height capacities of infrastructure such as sea walls or the elevations of existing infrastructures using GIS software to determine extents of intrusions. Similar to the mean annual sea level, I calculated highest high tide by simply using the max function within the yearly for-loop.

3. Maximum Tide Differential.

As I discussed in Chapter 2, the astronomical tide cycle causes two full tide cycles per day. Tidal differentials are often easily forecasted and high versus low differentials are to be expected due to the astronomical cycle. It is unlikely that a changing climate will cause statistically significant differences in day-to-day tide differentials due to the primary drivers being the orbits of the earth, moon and sun. However, the most extreme tide differentials are likely the edge instances that are often the causes of recurrent flooding. This indicator alone is not a great predictor of flood risk because these extreme values do not capture water elevations during the given tide cycle so there is no way to know if flooding occurred or was at high risk even with such a large differential. Establishing flood risk would require a more elaborate evaluation of each instance to determine if these extremes were astronomically forecasted or the result of an EWE such as a tropical storm whose storm surge "hit" or "retreated" at a time that impacted the differential on that day. The worst-case flooding scenario with respects to this indicator is if a large amount of storm surge occurs during an a forecasted very large or King tide scenario. Even without knowing the nature of each value for this indicator, my assumption is that the max tidal differential magnitudes are valid measurements of tidal conditions that occur during extreme conditions such a hurricane or tropical storm.

To calculate this indicator, I aggregated the tidal elevation data by day, month, and year with respects to both the max and min functions. I then took the difference

between the max and min for each day and again used the max function to determine the maximum within that yearly for-loop iteration.

4-5. Number of 90% and 95% Quantile Exceedances.

Tidal indicators number 4 and 5 are the number of 90% and 95% quantile exceedances that occur in each year with respects to the entire 1985-2019 data set. I expected these indicator values to have a significantly positive slopes since it is generally accepted that sea-levels are rising and I expected a larger number of instances to occur in the more recent years. The strength of this indicator for trend analysis is in cross-installation or cross-region comparisons to see if there are any statistical differences in the rates of change such as those shown in Figure 11 due to vertical land movement forces.

To calculate these indicators, I used the quantile function on the entire dataset at the 90% and 95% levels. I then used the sum function within the yearly for-loop for all instances where recorded elevations exceeded these levels to get the number of exceedances in each calendar year.

3.4 Data Analysis & Normalization

Simple Linear Regression.

After completion of the yearly for-loop for both the precipitation and tidal data sets, a long dataset with each row consisting of a single indicator for each year remained. Using the 'dcast' function, I converted the long dataset to a wide dataset where each column was an indicator and each row was the year that the indicator value was calculated for. With the goal of this thesis being to evaluate the rates of change across indicators, I next needed to run a simple linear regression on each of the indicators (columns in my wide dataset), so I then created 4 additional empty

rows to record the linear regression output data. The four rows were: y-intercept, m (slope), p-value, and R^2. The result was a final matrix of values for all 18 indicators for 1985-2019 and the simple linear regression results for each of the indicators which was then exported using the write.csv function.

Normalization.

All of the indicator calculations described thus far were to calculate "raw" numerical values for each indicator at a given installation. These values are easily understood and analyzed for a single indicator at a single installation. For example, if you were to plot an installation's total annual precipitation, applied a trend line, and could see an increase of two inches when comparing the early end of the data set (1985-89) to the late end (2015-19), then you could obviously see a change in magnitude and the resultant p-value would indicate whether or not this change in magnitude for was statistically significant or not. One can also easily compare similar indicators such as the 24 hour and 72 hour max accumulations for an installation because the units and reference location are the same. However, it is not possible to easily compare dissimilar indicators, even for a single installation due to unit and magnitude conflicts that cause an "apples-to-oranges" comparison.

In order to appropriately compare and accurately interpret the indicator results and their potential geospatial trends, they must be normalized using a consistent baseline so that all cross-indicator and cross-installation comparisons are conducted in an "apples-to-apples" manner. I chose to use a 5-year normalization baseline of 1985-89 for each installation. My assumption is that a 5-year baseline is long enough for any extreme edge case magnitude hydrologic events that could occur during the baseline period will not disproportionately skew the normalized data results. By normalizing the indicator values to the 1985-89 baseline, each of the indicator values now becomes

unit-less and each data point can be interpreted as "the percent difference in year X, from the 1985-89 baseline for indicator Y at installation Z". Similarly, the slope of an indicator's trend line can be interpreted as "the percent change per year for indicator Y at installation Z".

To calculate the normalized results for each indicator, I used the long results table within RStudio and subset the table to only indicator results for years 1985-89. I then completed a series of subsets (one for each indicator) and took the mean of the 5 annual values for each and recorded them as the baseline values for each indicator. I then applied a for-loop to the initial long results table with a series of if statements that calculated the percent difference between the yearly indicator value and the appropriate indicator baseline value. The resulting normalized values were then recorded, transformed, and summary statistics were calculated in the same manner as described earlier in this section. Indicator rates of change were evaluated for statistical significance at the $\alpha = 0.2$ confidence level.

3.5 Analysis Structuring and Synthesizing Results

1. Single Installation Analysis.

I conducted three phases of results analysis for this thesis. The first results analysis process was the dissection and summarization of a single installation's hyrdologic profile and any significant trends that exist over the study period. To do this, each of the indicators, in both the raw and normalized value formats, were plotted using Grapher. A trend line and summary statistics were applied and and the resultant plots were cross-analyzed to identify trends in magnitudes and frequency amongst the various indicators. Chapter 4. contains a complete analysis of Joint-Base Charleston's hydrologic profile conducted in this manner.

2. Multi-Installation Trends.

The second phase of my analysis was to identify cross-installation and regional trends in the various indicators. To do this, the resulting rates of change and p-values for the indicators were organized in a wide format with each row being an installation (See Appendix). The installations were placed in an order that follows the coastline from the Northeastern U.S., down around Florida peninsula, and along the Gulf Coast as shown in Figure 2, which is referred to as the "North-to-South" or "N-to-S #" in the results summary tables shown in Chapter 4. Structuring the results in this manner allowed the easiest way of identifying geospatial trends amongst indicators and overall hydrologic profiles. Within this table, all indicator rates of change that failed to meet the statistical significance level of $\alpha = 0.2$ were set to zero so that only significant or effective rates of change would be considered during the visual trend identification. Indicators with 10 or more of the 17 installations having statistically significant rates of change in said indicators were identified as "Significant Indicators". The 7 significant precipitation indicators can be seen in Figure 38 in Chapter 4.

3. K-means Clustering Analyses.

The third phase of results analysis consisted of a series of k-means clustering analyses on the resulting rates of change. These analyses were done first within RStudio using wide-normalized rates of change which provided a way identify any clustering trends quantitatively, using only the rates of change. The second set of clustering analyses were done using ArcGIS so that they also included the geospatial component for analysis.

The 'factoextra', 'reshape2', and 'tidyr' packages were used to conduct the clustering analyses within RStudio. To do so, the wide-normalized rates of change .csv was uploaded and subset to only include the indicators' rates of change. The 'get_dist'

function was used to get the Euclidean distances between data points. The 'fviz_dist' fucntion was used to illustrate the installations' hydrologic profiles likeness. The 'fviz_nbclust' function was used to create an elbow chart that could be used to determine the optimal number of clusters to be used in the k-means clustering analysis. The 'kluster' function was used to actually conduct the clustering analysis and the 'fviz_cluster' function was used to plot the clusters. Since the data set was organized in the "N-to-S" manner, the data points shown in the clustering plots appropriately match the installations shown in Figure 2. This process was completed twice, first using all of the precipitation indicators, the second using only the 7 significant indicators to see if or how much the cluster results varied.

IV. Results

This chapter consists of three sections. First, I will analyze and interpret the indicators' results for a single installation, Joint-Base Charleston, in order to build out the installation's hydrologic profile. Next, the indicator results for all 17 Air Force installations are evaluated to identify regional trends in the hydrologic profiles. Lastly, a series of k-means clustering analyses are applied to identify additional trend analysis.

4.1 Single Installation Analysis

As we discussed in Chapter 3, conducting a single installation analysis of all of the hydrologic indicators through single-indicator and multi-indicator trend analysis allows us to fully understand an installation's climatology and overall hydrologic profile with respects to flood-risk. In this section, I will use the precipitation and tidal indicators results of Joint-Base Charleston to detail the installation's hydrologic profile using both the raw and normalized values to establish an appropriate interpretation of the indicators' results. This interpretation of a single installation's hydrologic profile can then be applied in the following sections when evaluating the results of multiple installations and the identification of regional hydrologic trends.

Precipitation Results.

Total Annual Precipitation.

Figure 28 below shows the observed Total Annual Precipitation values for Joint-Base Charleston from 1985-2019. The top plot illustrates the "raw" data and the bottom plot shows the same data which was normalized to the 1985-89 base line for cross-indicator and cross-installation comparisons. As you can see from the fit line

on the raw data plot (top), the R^2 value recorded is very low, which is to be expected because it is not applicable since we are not using year as a predictor for precipitation. Instead, we are simply running the simple linear regression to determine the historical rates of change of the hydrologic indicators.

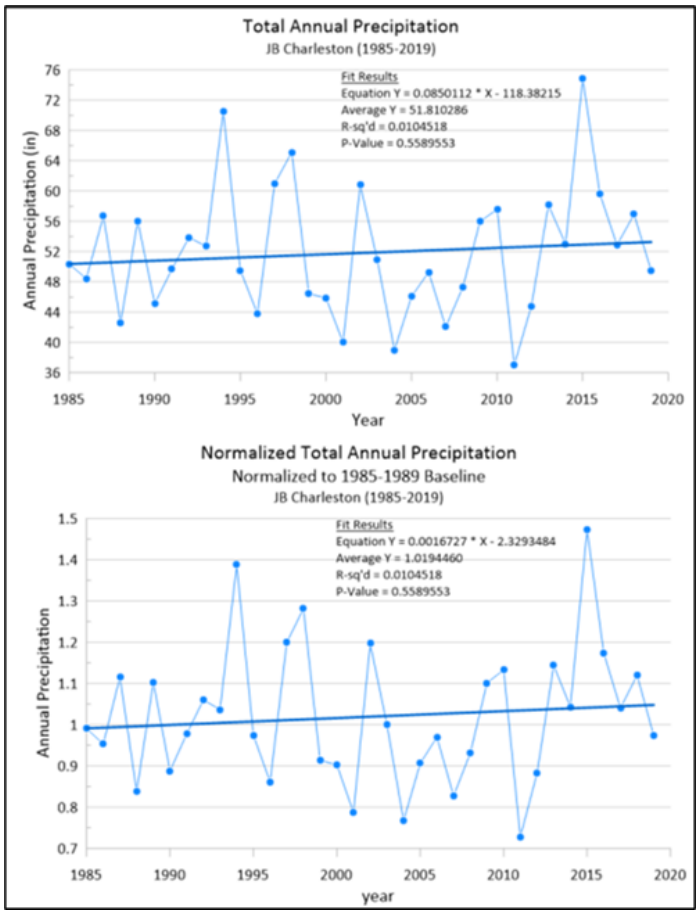


Figure 28. Total Annual Precipitation

The linear fit results show that the data has a slightly positive slope. The fitted line equation shows a slope of 0.085 which can be interpreted as "on average, Joint-Base Charleston has just under 1/10th of an inch of additional precipitation per year since 1985." However, the p-value indicates that the rate of change, while slightly positive at 0.085, is not statistically significant at the $\alpha = 0.2$ confidence level. In comparison to the observed or "raw" data plot, the normalized plot's linear fit shows

a slope of 0.0016. This value has a significantly different interpretation than the observed values' slope. The accurate interpretation of this slope can be described as "JB Charleston has, on average, experienced a 0.16% per year increase in total annual precipitation with respects to the 1985-89 baseline." As discussed above, while the normalized rate of change may be less intuitive, it is necessary to record it in this manner so that the rate change for this indicator can be compared with any other indicators at any location.

The remainder of the indicator results will only be shown and interpreted using the normalized data sets to enable such comparisons. This step is imperative for later evaluation in my thesis when conducting a k-means clustering analysis based off of all of these indicator rates of change. Note: All of the indicator results plot can be found in the "dual" format as shown in Figure 28 in the Appendix, allowing one to determine the magnitudes of a rate of change of interest.

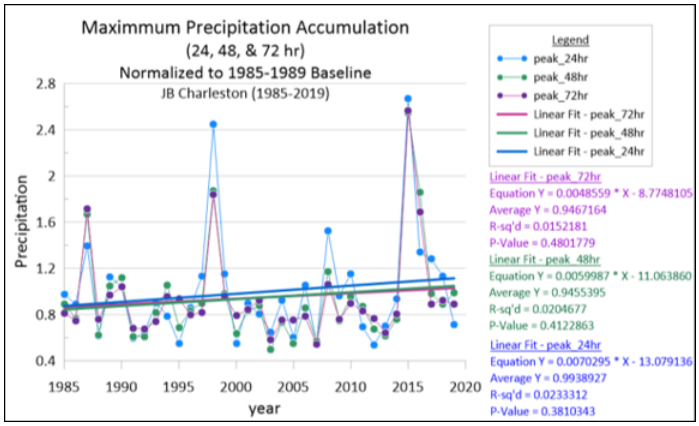


Figure 29. Maximum Accumulation by Period

Figure 29 shows the results for precipitation indicators 4-6: Maximum Precipitation Accumulation at the 24, 48, and 72-hour durations. When looking at the observed data we see a slight increase, likely from the couple of extreme values such as the 16 inch 72-hour event experienced in 2015, but it is not statistically significant. Looking at the slopes of the 3 period lines shows that they are almost perfectly paral-

lel, so there are not any cross-period trends to be observed in the peak accumulations at Joint-Base Charleston.

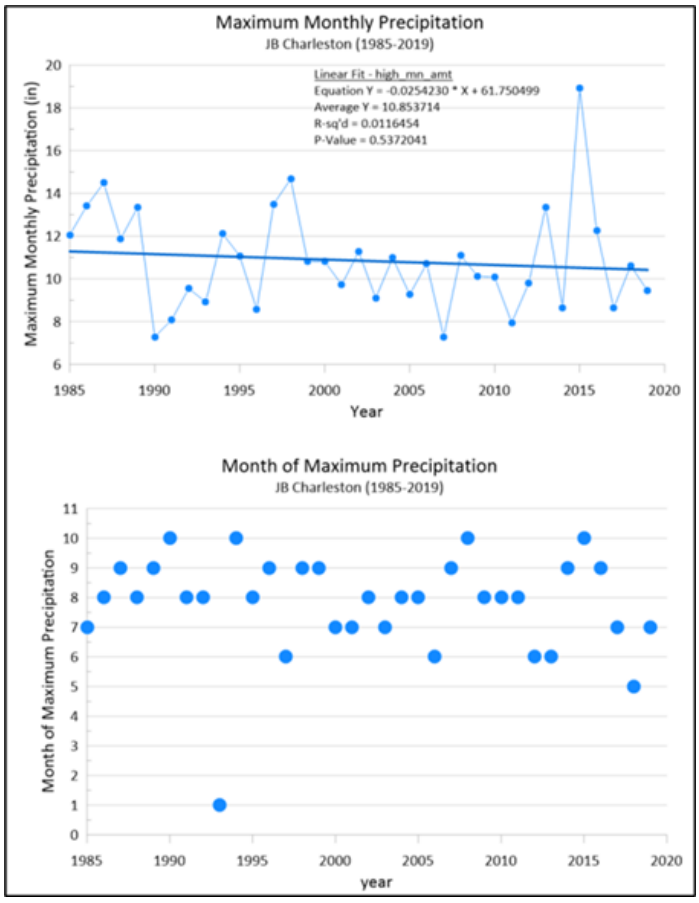


Figure 30. Max Monthly Precipitation & Month

Figure 30 above shows the resulting Maximum Monthly Precipitation Amount and the Month with which it was observed. Figure 4 shows that there has actually been a slight decrease in observed monthly maximums through this period. We can also see that historically August-October is when Joint-Base Charleston experiences its max rainfall, but is beginning to trend earlier in the summer in recent years.

For all of the Number of Threshold Exceedance results, there are two ways to review and interpret the data, both of which give insight into JB Charleston's overall "hydrologic profile." The first manner is by looking at all of the Threshold 1 Exceedances for each of the 3 periods as shown in Figures 31 and 32 below. Reviewing

the data in this format allows us to see one side of the frequency and magnitude coin. By comparing the slopes of the 3 period lines, we can see that they all run approximately parallel, so there are not any major trend diversions between period counts at JB Charleston, but that may not be the case at every installation. If for example, in Figures 31, the 72-hour line had a negative slope, but the other two remained positive as shown, we could observe that "JB Charleston is seeing slightly more annual rainfall (Figure 2), but would be doing so at a higher frequency of low-intensity (Threshold 1) events lasting less than 48 hours". Figures 31 and 32 (Thresholds 1-3) are all very similar, showing slightly positive increases in frequency. Figure 8 (Threshold 4) however, is slightly negative across all 3 periods meaning "JB Charleston is seeing fewer high-intensity (Threshold 4) rainfall events, regardless of time period".

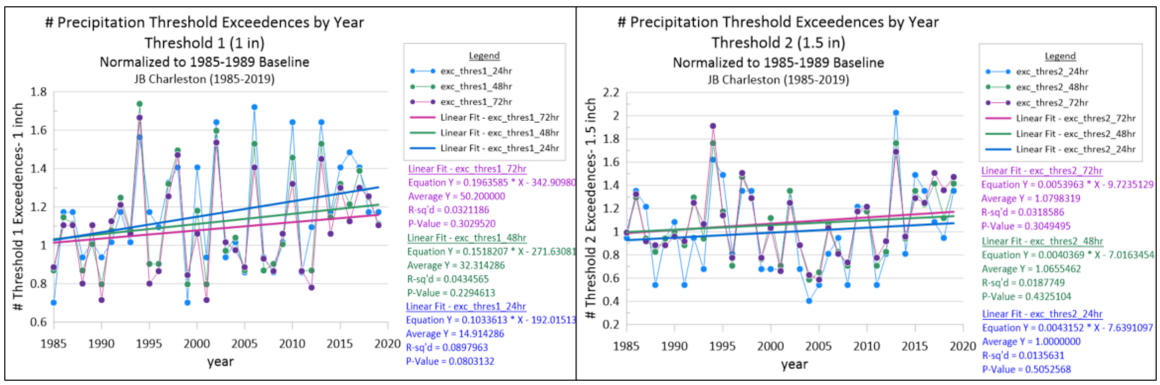


Figure 31. # Threshold Exceedances by Duration- Threshold 1 & 2 respectively

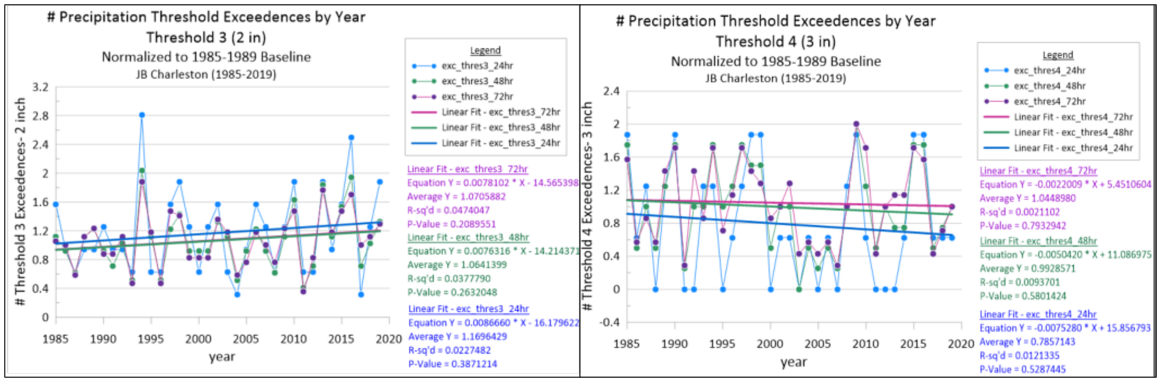


Figure 32. # Threshold Exceedances by Duration- Threshold 3 & 4 respectively

The second manner with which to evaluate the Number Threshold Exceedances is by plotting all 4 threshold exceedances for a given time period on one plot as shown in Figures 33 and 34. By looking at the data in this format we can see that number of low-intensity (Threshold 1) events are increasing faster than the number of medium-intensity (Threshold 2 & 3) events, and the frequency of high-intensity events (Threshold 4) have decreased over time. We arrive at similar conclusions, but by looking at the same data in these two formats we can see all of the indicator interactions at each of the different levels (thresholds and periods).

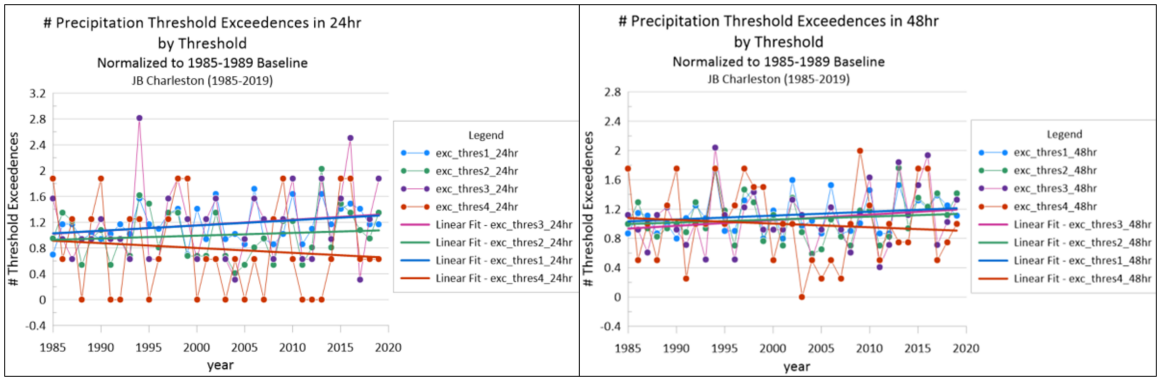


Figure 33. Number Threshold Exceedances by Threshold for 24hr & 48hr Periods

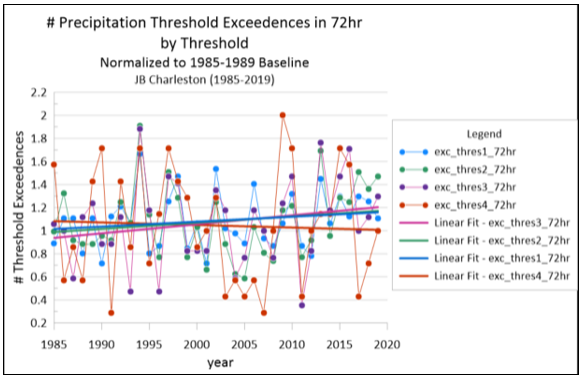


Figure 34. Number Threshold Exceedances by Threshold for 72hr Period

Tidal Results.

Figures 35 & 36 illustrate the tidal and SLR components of JB Charleston's "hydrologic profile." Figure 35 (left) shows that the Mean Sea Level at JB Charleston, has experienced a statistically significant increase over the study period. With an average rate of change of 0.0046m per year or 4.6mm/yr, which is 0.181 inches/yr or just under 3/16 inches of regional sea-level rise per year. At first glance, this SLR rate is almost 50% higher than the generally accepted global sea level rise rate of 3mm/yr that we discussed in Chapter 2 but when we reference the locally experienced Vertical Land Movement (VLM) of between 1-2 mm/yr experienced in the Carolina's as shown in Figure 11 this value is appropriate. Ultimately, this figure reinforces that sea-level at JB Charleston is rising, and while this result may not be surprising, it validates the methodology used for calculating the RSL. It also becomes much more valuable when used to compare the mean sea levels of other installations, and can allow for the identification of coastal trends.

Figure 35 (right) is a plot of Tidal Indicator 2. Peak Tide (Highest High Tide), which also shows a slight increase over the study period, but it is not statistically significant. When evaluating this plot further, I found that the couple of extreme points were the result of EWEs that made landfall directly in the Carolina's: 1989- Hurricane Hugo (Cat 4), 2015- Hurricane Joaquin (Cat 3), 2017- Hurricane Irma, 2018- Hurricane Florence (Cat 2). While this indicator did not yield significant results at JB Charleston, the cross-installation comparison may highlight existing trends.

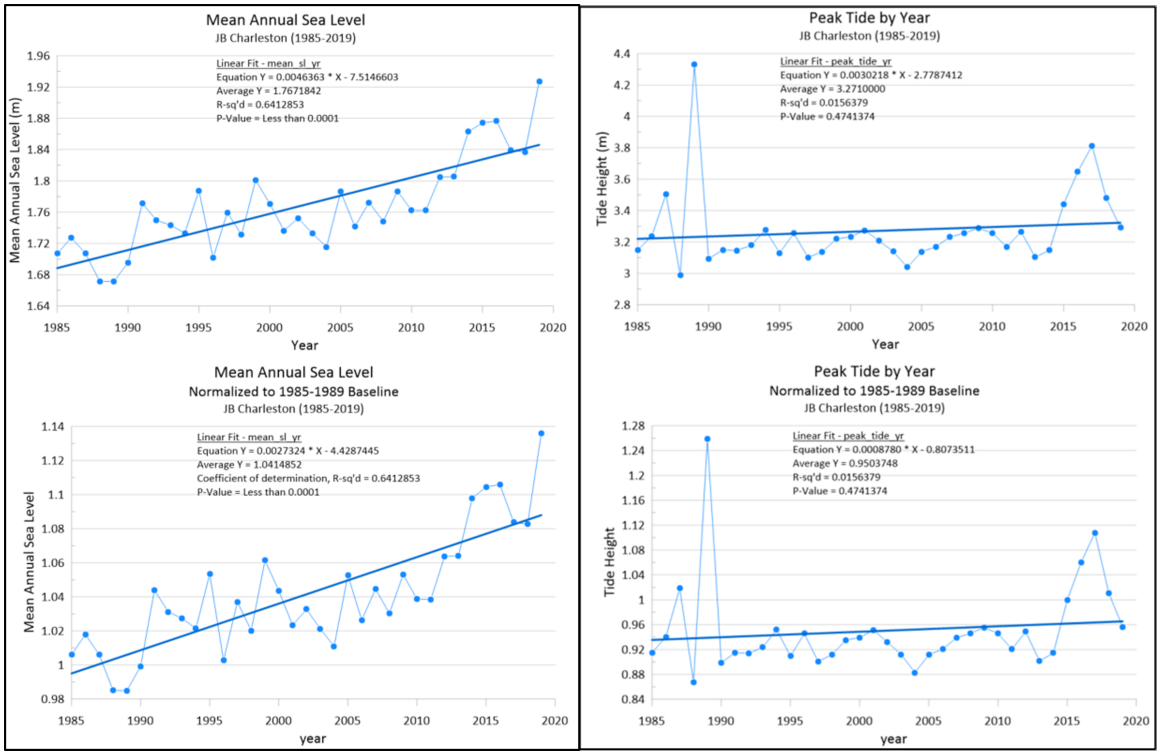


Figure 35. Mean Sea Level & Peak Tides

Figure 36 (left) is the plot of Tidal Indicators 4 & 5, the number of 90 & 95% Quantile exceedances for each year. Because we know that sea level continues to rise, I expected the resulting significant positive slope shown. However, these values will be more valuable when cross-examining with other installations.

Figure 36 (right) shows JB Charleston's Maximum Tide Differential for each year and we can see a slightly negative but insignificant slope. However this is likely caused by the outlier impact of 1989's Hurricane Hugo that fell within the 1985-89 baseline because the remainder of the data looks quite consistent.

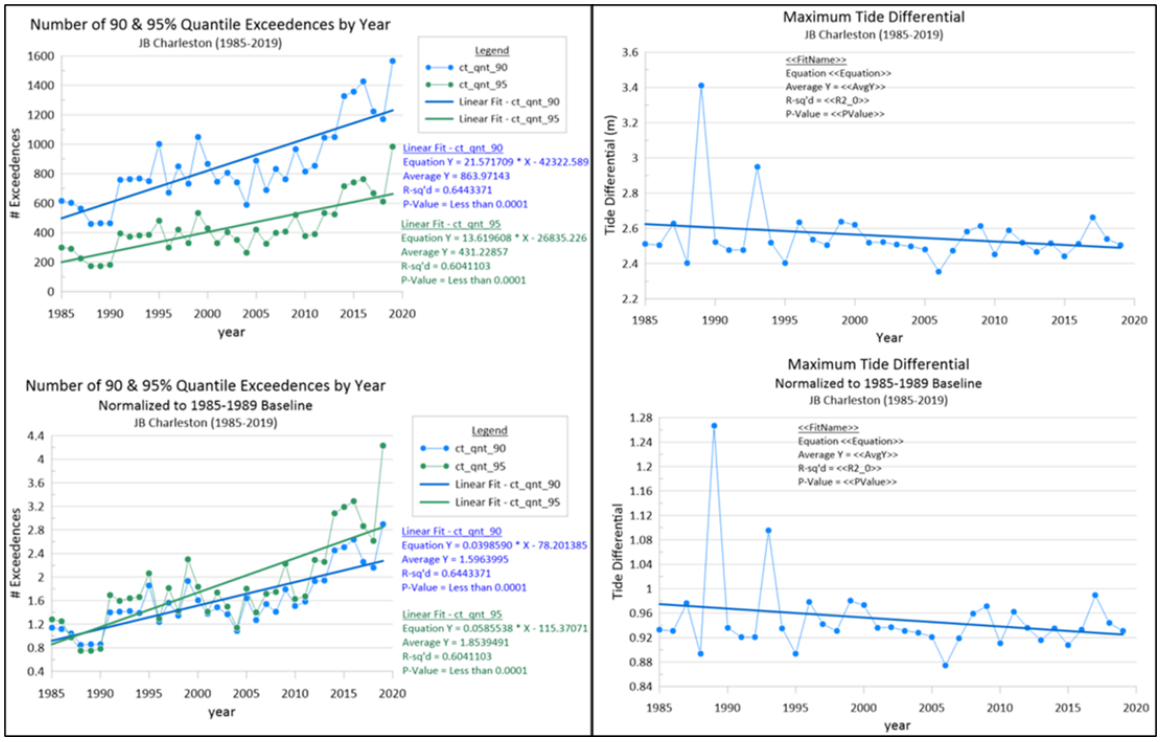


Figure 36. Number of 90 & 95% Quantile Exceedances and Maximum Tide Differential

4.2 Multi-Installation Trends

Tidal Trend Analysis.

Figure 37 below displays the 5 tidal indicators' rates of change results at each of the 7 tidal stations evaluated. Only one installation, Hanscom AFB, showed significant results across all 5 indicators.

Tidal Indicators- Rates of Change Results			Tidal Station #	Mean Sea Level	Peak Tide (Highest High Tide)	Maximum Tide Differential	# of 90% Quantile Exceedances	# of 90% Quantile Exceedances	Total Sig. Indicators	
#	Installation	State								
1	Hanscom AFB	MA	1	0.18%	0.14%	0.08%	2.74%	4.03%	5	
3	JB McGuire-Dix-Lakehurst	NJ	2	0.23%	0.00%	-0.20%	4.19%	5.82%	4	-1%
5	JB Anacostia-Bolling	DC	3	0.27%	0.00%	0.00%	6.61%	9.73%	3	0%
6	JB Andrews	MD								1%
7	JB Langley-Eustis	VA	4	0.38%	0.31%	0.00%	10.49%	14.22%	4	2%
10	JB Charleston	SC	5	0.27%	0.00%	-0.15%	3.99%	5.86%	4	3%
14	Tyndall AFB	FL	6	0.33%	0.43%	0.00%	5.76%	8.06%	4	4%
15	Hurlburt Field	FL	7	0.18%	0.00%	0.00%	9.24%	13.89%	3	>5%
16	Eglin AFB	FL								
# Stations w/ sig. Ind. Results				7	3	3	7	7		

Figure 37. Tidal Indicators- Rates of Change Results Table

The first indicator, mean annual sea-level, showed a slight but statistically significant increase year over year as we would expect. In addition, the variation is sea-level rises by location is very small, with only a 0.2% spread which indicates again indicates that sea-level rise has relatively equivalent impacts across the East and Gulf Coast.

The second indicator, peak tide, only showed 3 locations that had significant results, all of which were slightly positive, indicating that in comparison to the 1985-89 baseline, these installations are now experiencing slightly higher peak tides. Interestingly, the maximum tide differentials for 2 of the 3 significant results showed a slight decrease in the experienced differentials. This trend is plausible, but could also have been caused by an outlier within the baseline. More investigation would be required to make any sound assumptions off of this indicator, but the magnitudes are so small that neither the peak tides or the max tide differentials as I have calculated them can be used to identify any hydrologic trends. The last two indicators, the # of 90% and 95% quantile exceedances are all significantly positive, which reinforces my previous expectation that sea-level over the study period has in fact increased, resulting in the very positive slopes of these indicators.

Unfortunately, when compared to the precipitation data, the limited number of complete tidal station data sets left me with an incomplete picture to try parse out any regional trends. The only true trend that could be identified, or validated, is that mean sea-levels have increased since 1985, but the minute differences in the rates of change do not allow me to identify any significant regional trends as I did with the precipitation indicators.

Precipitation Trend Analysis.

Figure 38 below is the results table of the rates of change (RoC) for every precipitation indicator for each installation using the normalized results and correction for

non-significant rates of change as described in Chapter 3. As I mentioned previously, by ordering the installation results in the "N-to-S" manner following the coast and applying a heat-map color scale to the results we can easily identify a number of trends within the results.

Precipitation Indicators- Rates of Change Results

#	Installation \ Indicator ->	Tot. Annual Precip.	Threshold 1: # Events w/ > 1" in ___			Threshold 2: # Events w/ > 1.5" in ___			Threshold 3: # Events w/ > 2" in ___			Threshold 4: # Events w/ > 3" in ___			Max Monthly Accum.	Median 24hr Accum.	Median 48hr Accum.	Median 72hr Accum.	Peak 24hr Accum.	Peak 48hr Accum.	Peak 72hr Accum.	24hr- 75th %tile	48hr- 75th %tile	72hr- 75th %tile			
			24 hr	48 hr	72 hr	24 hr	48 hr	72 hr	24 hr	48 hr	72 hr	24 hr	48 hr	72 hr														
		A	B	C	D	E	F	G	H	I	J	K	L	M	N	O	P	Q	R	S	T	U	V	W			
1	Hanscom AFB	0.0%	0.0%	0.0%	0.0%	0.0%	0.0%	0.0%	-1.8%	-1.6%	-1.2%	0.0%	-2.8%	-2.1%	0.0%	1.6%	1.1%	1.0%	-1.1%	-1.2%	-1.1%	0.6%	0.0%	0.0%	Tot. Sig. Ind.	12	4	8
2	Cape Cod AFS	-1.6%	-1.7%	-1.9%	-1.9%	-1.4%	-1.8%	-1.9%	-1.6%	-1.9%	-1.9%	-2.2%	-2.1%	-2.1%	-1.6%	-2.1%	-2.2%	-2.4%	-0.9%	-1.3%	-1.6%	-1.7%	-1.5%	-1.5%	Tot. Pos. Sig. Ind.	23	0	23
3	JB McGuire-Dix-Lakehurst	-0.7%	0.0%	-0.9%	-0.9%	0.0%	-1.1%	-1.3%	-1.4%	-1.9%	-2.0%	-2.1%	-2.1%	-1.9%	-0.6%	-0.5%	-0.7%	-0.7%	-0.9%	-0.8%	-0.8%	0.0%	-0.6%	-0.7%	Tot. Neg. Sig. Ind.	20	0	20
4	Dover AFB	0.0%	1.2%	0.0%	0.0%	0.0%	0.0%	0.0%	0.0%	0.0%	0.0%	0.0%	0.0%	0.0%	0.6%	0.0%	0.0%	0.0%	0.0%	0.0%	0.0%	0.0%	0.0%	0.0%		2	2	0
5	JB Anacostia-Bolling	0.7%	0.9%	0.0%	0.0%	2.6%	2.0%	1.6%	7.2%	6.3%	5.8%	10.8%	17.2%	19.4%	1.4%	0.0%	0.0%	0.0%	1.8%	1.9%	2.2%	0.0%	0.0%	0.0%		15	15	0
6	JB Andrews	-0.4%	0.0%	0.0%	0.0%	2.9%	0.0%	0.0%	9.0%	4.1%	2.9%	0.0%	7.8%	8.5%	0.0%	2.6%	1.2%	0.0%	1.4%	1.6%	1.6%	3.6%	1.5%	0.5%		15	14	1
7	JB Langley-Eustis	-0.9%	0.0%	0.0%	0.0%	0.0%	0.0%	0.0%	0.0%	0.0%	0.0%	0.0%	0.0%	0.0%	-1.1%	0.0%	-0.5%	-0.7%	0.0%	0.0%	0.0%	2.1%	0.8%	0.0%		6	2	4
8	Seymour Johnson AFB	0.6%	2.1%	1.4%	1.2%	4.4%	2.4%	1.8%	0.0%	3.0%	2.3%	0.0%	0.0%	6.1%	0.0%	-0.7%	-0.6%	0.0%	1.8%	0.0%	0.0%	0.0%	0.0%	0.0%		13	11	2
9	Pope AFB	0.0%	1.4%	0.0%	0.0%	2.5%	0.0%	0.0%	5.3%	0.0%	0.0%	22.0%	9.2%	7.5%	0.0%	2.5%	1.5%	0.8%	2.5%	2.5%	2.7%	3.9%	2.2%	1.2%		15	15	0
10	JB Charleston	0.0%	0.8%	0.0%	0.0%	0.0%	0.0%	0.0%	0.0%	0.0%	0.0%	0.0%	0.0%	0.0%	0.0%	0.0%	0.0%	0.0%	0.0%	0.0%	0.0%	0.0%	0.0%	0.0%		2	2	0
11	Cape Canaveral AFS	-1.1%	0.0%	0.0%	-0.8%	0.0%	-0.9%	-1.1%	0.0%	0.0%	-1.1%	0.0%	0.0%	0.0%	0.0%	0.0%	0.0%	0.0%	0.0%	0.0%	0.0%	0.8%	0.0%	0.0%		6	1	5
12	Patrick AFB	0.0%	0.0%	0.0%	0.0%	0.0%	0.0%	0.0%	0.0%	0.0%	0.0%	0.0%	0.0%	0.0%	0.0%	0.0%	0.0%	0.0%	0.0%	0.0%	0.0%	0.0%	0.0%	0.0%		0	0	0
13	MacDill AFB	0.0%	0.0%	0.0%	0.0%	2.3%	1.5%	0.8%	2.1%	1.9%	1.9%	6.5%	3.7%	3.4%	1.1%	3.9%	3.6%	2.8%	0.0%	0.0%	0.0%	3.4%	2.6%	1.6%		16	16	0
14	Tyndall AFB	-1.1%	-1.6%	-1.4%	-1.2%	-1.9%	-1.8%	-1.7%	-2.5%	-2.0%	-2.0%	-2.3%	-2.2%	-2.0%	-1.2%	-1.7%	-1.6%	-1.5%	-1.3%	-1.4%	-1.4%	-1.4%	-1.5%	-1.5%		23	0	23
15	Hurlburt Field	-1.2%	-0.8%	-1.0%	-1.2%	0.0%	-0.8%	-1.0%	0.0%	0.0%	-1.0%	0.0%	0.0%	-1.0%	0.0%	0.0%	0.0%	0.0%	0.0%	0.0%	0.0%	0.0%	0.0%	0.0%		7	0	7
16	Eglin AFB	-1.0%	-0.9%	-1.0%	-1.0%	0.0%	-0.7%	-0.9%	0.0%	0.0%	-0.7%	0.0%	0.0%	-1.0%	0.0%	0.0%	-0.6%	-0.7%	0.0%	0.0%	0.0%	0.0%	0.0%	-0.6%		11	0	11
17	Keesler AFB	-1.3%	-0.7%	-1.0%	-1.2%	0.0%	-1.0%	-1.1%	0.0%	-0.8%	-1.2%	0.0%	0.0%	-1.3%	0.0%	0.8%	0.0%	0.0%	0.0%	0.0%	0.0%	1.6%	0.0%	0.0%		11	2	9
	# Bases w/ sig. Ind. Results	11	10	7	8	7	10	10	8	9	12	6	8	11	7	9	10	8	8	7	7	9	8	7				

-5%
-4%
-3%
-2%
-1%
0%
1%
2%
3%
4%
>5%

Significant Indicators: >9 installations w/ sig. results, used in k-means clustering analysis

Figure 38. Precipitation Indicators- Rates of Change Results Table

1. Distinct Zones.

Upon immediate inspection, the results illustrate three distinct zone of overall positive and negative precipitation trends. Zone 1, the northernmost installations (# 1-4) exhibited negative trends across most of the precipitation indicators. Zone 2, consists of the central to southern Atlantic coastal installations (# 5-13) exhibited mostly positive indicator trends. The third zone, consists of installations located on the Gulf of Mexico (# 14-17), also showed negative indicator trends.

These results were surprising to me because much of my literature review had pointed towards the significant increases in both the magnitude and frequency of extreme weather events such as tropical storms and hurricanes. I had assumed these increases would mostly affect the Gulf Coast and Southeastern states such as Louisiana, Florida and Georgia the due the "typical" hurricanes paths and the frequency with which these areas are impacts by such storms. However, the zones and overall trends would suggest that the central East coast is experiencing the brunt of these storm trends and the gulf is actually coast risk profile may even be improving.

2. Significant Indicator Identification.

Following the methodology described in Chapter 3, the overall "Significant Indicators" are the indicators which had more than 10 of the 17 target installations with significant RoCs. The significant indicators are highlighted in green on Figure 38 and are used in the clustering analysis discussed in the next section. It was surprising to find that the vast majority of installations' total annual precipitations actually showed a negative trend in the historical data. It was also interesting to find that indicators G, J, and M which represent 72-hour duration event occurrences at threshold 2-4 magnitudes showed some of the highest changes in both the positive and negative directions. Installation # 5 JB Anacostia-Bolling showed extreme increases in

these indicators which translates to much more frequent high-intensity events which could dramatically increase the installation's overall flood risk when compared to the 1985-89 baseline.

3. Installation- Positive & Negative Indicator Magnitudes.

The last 3 columns of Figure 38 consist of a simple count of the total number of significant RoCs, the number of positive significant RoCs, and the number of negative significant RoCs respectively. I found that the number of significant RoCs varied significantly across the field of target installations. Installation #12, Patrick AFB showed 0 significant indicators, meaning that there have been not any detectable and statistically significant changes in precipitation patterns when compared to its 1985-89 baseline. Installations #2 and 14, Cape Cod AFS and Tyndall AFB respectively, showed significant positive trends in all 23 indicator metrics.

There were only a few installations that resulted in both positive and negative indicator RoC, all of which were installations with relatively low total significant indicator numbers. Installations #7, 11, and 17, JB Langley-Eustis, Cape Canaveral AFS, and Keesler AFB respectively.

4. Single Installation Trends.

Installation's #4 and 12, Dover AFB and Patrick AFB respectively have similar hydrologic profiles with respects to precipitation to that of the JB Charleston (#10) example we analyzed in the previous section, which had almost no significant precipitation indicators. This means that in the precipitation component of the recurrent flood risk has not significantly changed since 1985. Additionally, it is important to note that each of these 3 installations are located on the "edges" of the zones unidentified above, but a lack of significant results makes it hard to speculate on their overall

precipitation driven risk status.

Most installations illustrated sweeping trends in either the positive or negative directions. Installations #5, 8, 9, and 13 all show consistently positive indicator RoCs, signaling an overall increase in precipitation flood risk. Whereas installations #2, 3, 14, 15, and 16 all showed overall decreases in the precipitation RoCs, signaling that the precipitation driven component of recurrent flood risk at these installations has actually decreased in comparison to the 1985-89 baseline.

Installation #6, JB Andrews's results were interesting because they showed an average decrease in total annual precipitation (-0.4%), but it also saw very large increases in higher magnitude (Thresholds 3 and 4) rainfall events across all durations. This means that while JB Andrews is seeing lower total precipitation, which could indicate a lower recurrent flood risk, it is also experiencing more frequent higher intensity events so while these indicators may contradict each other slightly, it is likely that JB Andrew's overall flood risk is still actually increasing. This type of trend can be understood easily through visual inspection of the abundance and magnitude of the color scales used if Figure 38, but could otherwise be easily missed if only on a single indicator was used in decision making.

4.3 K-means Clustering Analyses

The final results analysis method conducted in this research was a series of k-means clustering analyses. As we discussed in the previous section, having only 7 tidal observations made clustering via the tidal indicator results impossible. However, the precipitation indicator results were able to be analyzed. The remainder of figures displayed in this section are in a side-by-side format where all of the left panes are the k-means clustering analysis results using all of the precipitation indicator results and the right panes show the results using only the 7 significant indicators I discussed

previously. This allowed additional comparison between the clusters and allowed me to evaluate whether using the sub-set of significant indicators was appropriate and whether or not either of these cluster series matched the Zones identified in Figure 38.

Quantitative Analysis: RStudio.

Figures 39 & 40 help illustrate the appropriate number of clusters within the precipitation results. Figure 39 (left) shows that when using all of the indicators, there are 3-4 installation clusters where as there are 3 distinct clusters (or 2 clusters with a singular outlier) while using only the 7 significant indicators. The elbow charts in Figure 40 show that using all indicators, the optimal number of clusters is either 2 or 5, whereas the significant indicators likely have 2 or 4 clusters. Due to this discrepancy, and my desire to identify any significant differences between the two series (all versus significant), I ran the k-means clustering analysis using 2, 3, 4, and 5 clusters as shown in Figure 41.

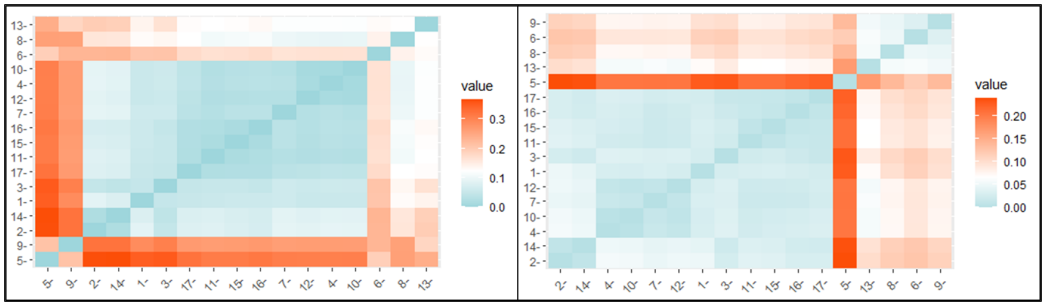


Figure 39. Precipitation Results- Euclidean Distances Heat Maps

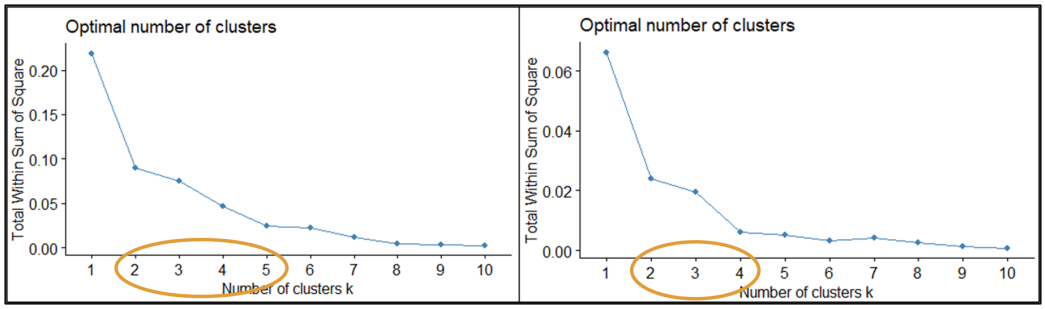


Figure 40. K-Means Optimal Number of Clusters- Elbow Charts

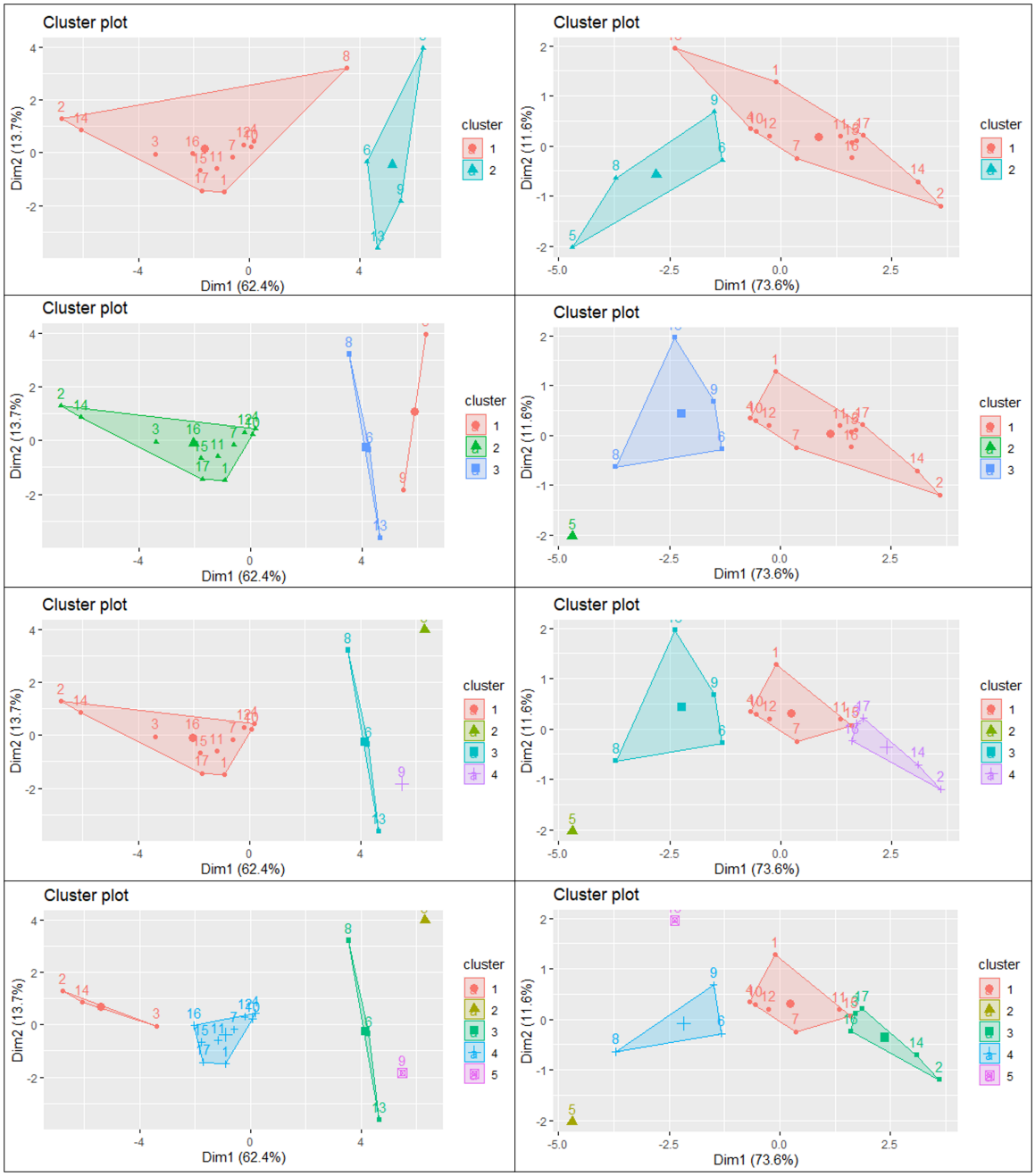


Figure 41. Cluster Results

K-means Clustering Analysis: Rstudio Quantitative Results Summary								
N to S	All Indicators				Significant Indicators			
	# Clusters				# Clusters			
	2	3	4	5	2	3	4	5
1	1	2	1	4	1	1	1	1
2	1	2	1	1	1	1	4	3
3	1	2	1	1	1	1	4	3
4	1	2	1	4	1	1	1	1
5	2	1	2	2	2	2	2	2
6	2	3	3	3	2	3	3	4
7	1	2	1	4	1	1	1	1
8	1	3	3	3	2	3	3	4
9	2	1	4	5	2	3	3	4
10	1	2	1	4	1	1	1	1
11	1	2	1	4	1	1	1	1
12	1	2	1	4	1	1	1	1
13	2	3	3	3	1	3	3	5
14	1	2	1	1	1	1	4	3
15	1	2	1	4	1	1	1	1
16	1	2	1	4	1	1	4	3
17	1	2	1	4	1	1	4	3

Figure 42. Cluster Results Summary Table

Figure 42 above summary table of all of the clustering analyses ran organized again in the "N-to-S" coastal installation order. From this table, you can see that the k-means clustering analysis at 2 & 3 clusters for both series are very similar. Cluster 2 in these iterations, made up of Bolling (#5), Andrews (#6), Seymour-Johnson (#8), Pope (#9), and MacDill (#13) AFBs are consistently clustered together, even in the 4 and 5 cluster iterations across both series. While comparing each of the clustering iteration results, you can easily see the similarities the RStudio results and color outputs shown in Figure 38. These similarities amount to how high-low or red-blue an installation's average precipitation profile looks. Unfortunately, there aren't any additional trends found in these results beyond the Zones identified previously. The 4 and 5 cluster iterations do highlight the extreme values recorded for Bolling (#5) and Seymour-Johnson (#8) in the threshold 4 indicators as installation outliers.

4.4 Key Takeaways

1. Installation hydrologic profiles made up of the rates of change for indicators measuring means, extremes and exceedances of the four hydrologic components illustrates the changing recurrent flood risk conditions of coastal installations.

2. Sea-levels appear to be rising uniformly for all 7 tidal stations (9 Air Force Installations) evaluated.

3. This analysis did not display any discernible changes to tidal fluctuations.

4. Tide height extremes during storm surge events are increasing slightly, but only slightly faster that of sea-level rise.

5. Hydrologic profiles of the 17 coastal Air Force installations illustrate 3 distinct trend zones for the precipitation indicators. The Mid-Atlantic installations are showing significant increases in recurrent flood risk conditions for precipitation.

V. Discussion

5.1 Hurricane Isabel, Langley AFB and Adaptation Effectiveness

At Langley AFB there had not been any extreme flooding events prior to Hurricane Isabel since the Chesapeake Potomac Hurricane in 1933 so a sort of reverse-frequency bias existed within the region that had not cultivated or forced adequate flood mitigation measures. This was especially true on Langley AFB itself, as the limited funding availability climate within the DoD, and lack of experience in evaluating compound flood threats had led to the significant deterioration of what little storm water infrastructure the installation had.

Fortunately, Isabel's rapid growth to a Category 5 whilst still in the middle of the Atlantic garnered immediate attention and the threat was taken very seriously, well in advance of landfall. Oftentimes, impact areas receive only 2-3 days' notice of an impending threat, so Isabel was unique in that the Carolinas and Virginia had an entire week to prepare for the storm. This allowed ample time for targeted evacuations of high-risk areas (to include the entirety of Langley), the hardening of facilities as best as possible by placing over 35,000 sandbags, and placing of barriers on roads that were expected to be flooded [10]. Emergency response and recovery crews were also organized for deployment following the storm. While the base's efforts resulted in no loss of life on the installation, the infrastructure hardening measures were ineffective against the compound threat of $\tilde{8}$ft of storm surge and 8-12 inches rainfall experienced.

Recovery following a natural disaster such as this begins with meeting the immediate needs of the community to return to normalcy as well as the long-term recovery goals of reducing future vulnerabilities of the experienced (or similar) threats [43]. Langley had three major recovery milestones that in all, took several years to com-

plete. The first milestone, was to regain airfield operations capabilities due to the strategic mission importance of Langley and its support of Washington D.C.. It took 4 days for Langley to recover its airfield, primarily due to power outages and loss of back-up generators to flooding, but persisting flood waters, debris, and airfield facility damage also contributed to this timeline. The second milestone was to be able to reopen the installation in order to meet the community's basic human needs which took nearly 10 days due to the immense facility and road damage caused by the flooding as well as safe power restoration across the facility.

The third milestone of Langley's recovery effort was to get all of its facilities and infrastructure back to full operating capacity while embedding resiliency against future flooding events as a part of the rebuild. The installation embraced the "build back better" mentality by incorporating mitigation techniques into all of its repairs. It updated its building codes for all new construction and where possible on renovations for the first floor to be located at a minimum of 10 ft above sea level. Numerous projects were completed to robust storm water drainage systems including a new high-capacity pump station to pull water off the installation and airfield [10]. Many power lines were located underground, protected from high winds and transformers were relocated to elevated platforms to avoid being flooded. Low lying facilities were even fitted with panel flood barriers at all entrances to provide much more rapid and effective protection.

In addition, the base's most exposed shorelines were reinforced using combinations of sea walls and living shorelines designed to mitigate wide-spread storm surge infiltration. The installation also partnered with NASA's Jet Propulsion Laboratory and the Virginia Institute of Marine Science to develop state of the art flood models and mapping capabilities that have enabled targeted adaptation of infrastructure bolstering the base's flood resilience and built-preparedness [12, 13, 34].

On November 13th, 2009, the installation's efforts were tested when a Nor'easter that descended after Hurricane Ida unleashed two days of torrential downpours and over 55 mph winds on the installation. During this storm, nearly 18 inches of precipitation fell and the storm surge reached 8 feet, yet the installation was able to keep power on throughout the storm and the airfield was recovered in just 2 days after being submerged in nearly 3 feet of water. The threats experienced during this storm varied from those of Hurricane Isabel, but the mitigation measures implemented resulted in only $44M of damage compared to Isabel's $156M. Following these investments, Langley has seen minimal damage costs even when exposed to numerous serious threats listed below [10].

- 2011- Hurricane Irene, $1.5M
- 2012- Superstorm Sandy, $40k
- 2015- Hurricane Joaquin, $6.5M (mostly from Fort Eustis side of base, post-Joint-Basing)
- 2016- Hurricane Hermione, $9k and Hurricane Mathew, $168k

These impressive reductions in damage costs against considerable hydrologic threats show that effective implementation of water-control adaptations and threat evaluation practices can save money and minimize disruptions to our DoD missions even in face of the extremely complex risks posed by recurrent coast flooding and extreme weather events. Unfortunately, the coastal flooding battle space is continuously deteriorating as sea-levels rise and climate change increases both the frequency and intensity of these complex hydrologic events. It is imperative that the DoD proactively begin prioritizing high-risk installations for climate change resilience adaptations to prevent or mitigate damage from recurrent flooding. Doing so would reduce the DoD's flood-risk

exposure and reduce the probability of having to pay a multi-hundred million dollar repair bill to recover Langley in 2003, or multi-billion dollar bill to rebuild Tyndall in 2018.

5.2 Air Force Application of Hydrologic Profiles

1. DOD Risk Identification and Analysis.

The Intergovernmental Panel on Climate Change (IPCC) 6th Assessment Report warned that the warming of the Earth's atmosphere is indisputable, and is responsible for an increase in the number of Extreme Weather Events (EWEs) globally [4]. The projected increase in such climate threats poses significant societal threats, given that large proportions of global populations live near coastlines [37]. The Department of Defense (DoD) and USAF recognizes the risks that climate change imposes these risks and their corresponding influence on installation planning as laid out in the DoD's 2019 Report on Effects of a Changing Climate and the 2019 Inspector General's Audit on the DoD's Preparation for Natural Disasters.

SLR projections are one tool that offer civil planners a means to assess current and future infrastructure impacts. GIS can support infrastructure decisions by identifying the regions and infrastructure at risk to future conditions that may impact our installations' ability to execute their missions [50, 51]. For example, electrical systems are a form of critical infrastructure that both our coastal communities and Air Forces installations are incredibly dependent upon but which climate change jeopardizes. Power plants, transmission lines, and substations are all at risk of flooding and can seriously impact system functionality and operability of our installations. However, by utilizing simple geospatial analysis techniques in GIS and the National Oceanic and Atmospheric Administration's (NOAA) Sea-Level Rise (SLR) Projections datasets, we are able to to evaluate the exposure of electrical infrastructure such as trans-

mission lines, substations, and power plants that support our installations at various water levels and flood conditions. Figure 43 below illustrates a simple GIS application of NOAA's SLR projections for six USAF installations (Hurlburt Field, Eglin AFB, Tyndall AFB, MacDill AFB, Cape Canaveral, and Patrick AFB) identify probable impacts stemming from flood hazards on these critical infrastructure components.

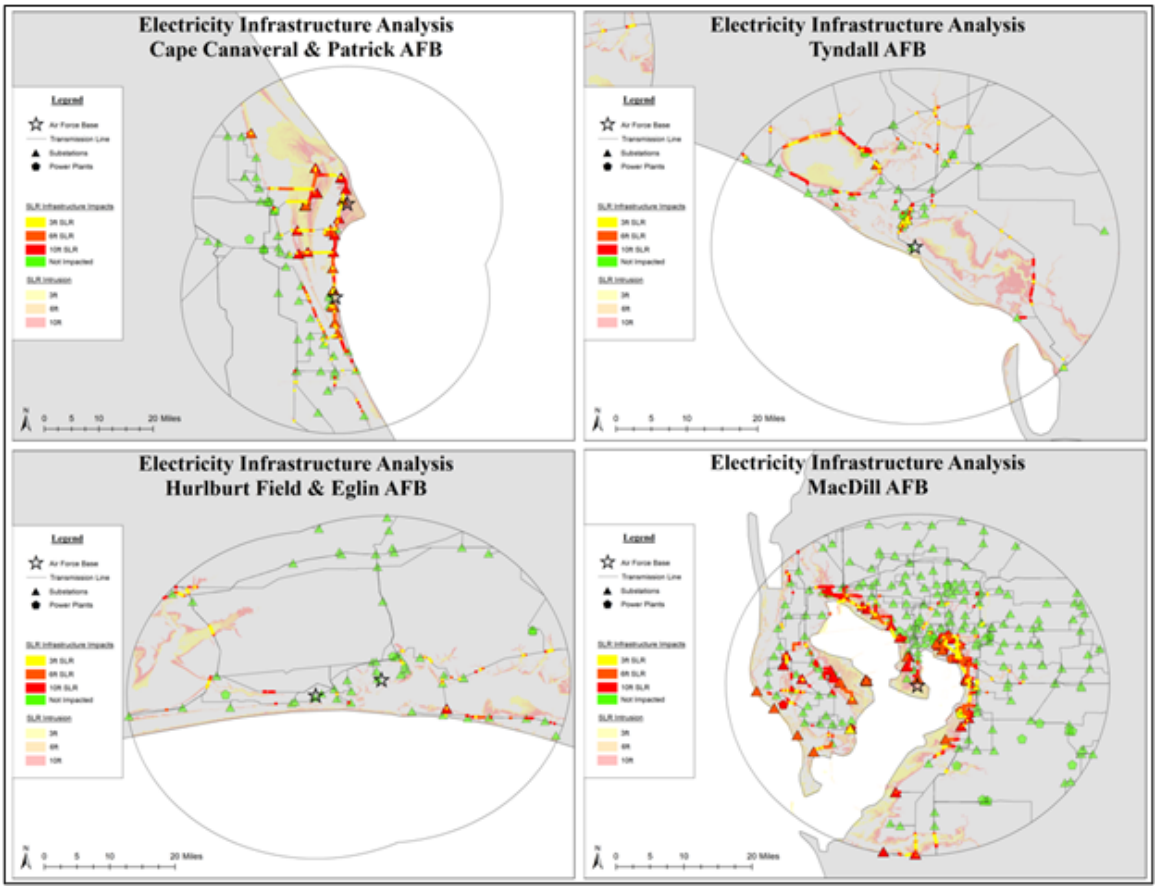


Figure 43. Electricity Infrastructure Flood Analysis – Florida USAF Installations

By applying this low-cost analysis could help the USAF installations identify critical areas or systems that at risk from flooding. Not only is the method practical and approachable, but GIS integration also helps produce visualizations that can simplify analysis and present the hazards in a more consumable manner. USAF planners could pair GIS visualizations and quantitative infrastructure impacts to enhance asset analysis and support investment decisions.

2. Adaptation Efforts.

Various mitigation strategies or Lines of Effort (LOEs) can be implemented to address the hazards hazards of a changing climate. However, their efficacy for implementation of LOEs and adaptations at U.S. Air Force Bases fluctuates based on complexity and cost of adaptations. Figure 44 is a resilience resilience LOE matrix for aimed at adapting an installation's electricity system. The matrix organizes realistic mitigation efforts based on their respective cost and complexity of implementation. Ideally, planners will seek out and act upon solutions that expend minimal cost and effort while yielding the greatest resilience return on investment (ROI). However, circumstances where logistics, politics, geospatial constraints, and other factors complicate electricity resilience actionability, requiring more rigorous and costly solutions to be explored.

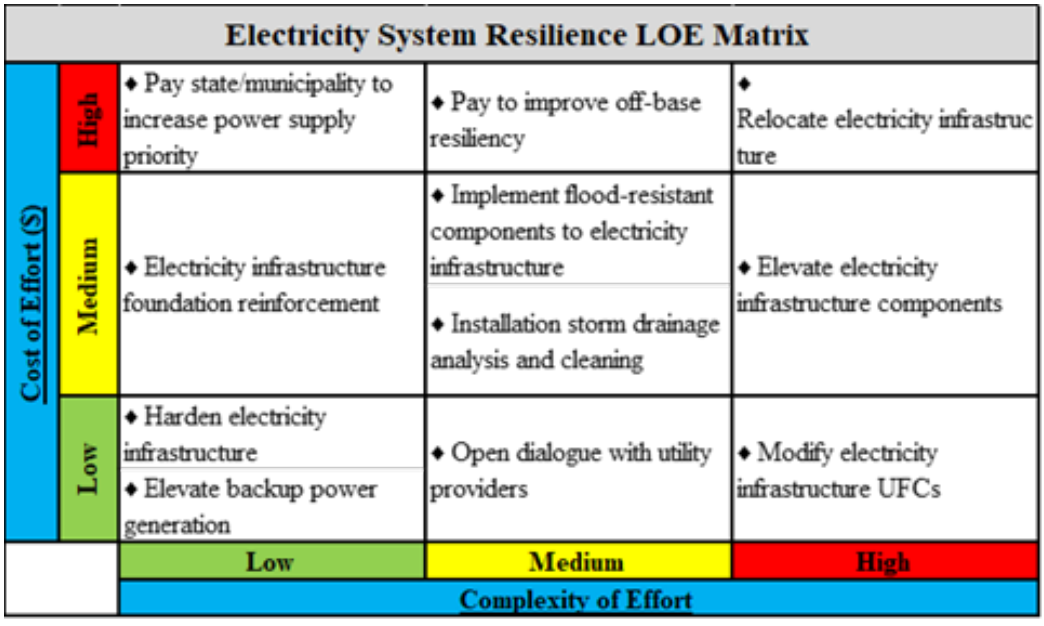


Figure 44. Electricity Infrastructure Line-of-Effort Matrix for Flood Mitigation

Efficacy or planned implementation of each of the LOEs above can also be significantly impacted by timing with respect to an installation's condition status. Timing of LOE implementation could be life cycle in nature, where the age and condition

of existing infrastructure warrant repair or replacement, during which LOEs can be included. However, timing can also play a large part when an installation is recovering from an adverse event such as an EWE, giving ample opportunity and leadership enthusiasm to implement such measures, making both the costs and efforts more palatable. Unfortunately, the Air Force has historically operated in this manner, only significantly investing in resilience in reaction to a costly destructive EWE event.

3. Prioritizing Installations for Adaptation.

The methodology developed in this study enabled the evaluation of 40 years' worth of historical precipitation and tidal data to determine rates of change and geospatial trends for each of the four hydrologic components by establishing hydrologic profiles for each of the 17 Air Force installations.

The tidal indicator results in Figure 37 show that one of hydrologic components of recurrent flooding, tidal fluctuations, has not changed significantly over the 1985-2019 study. Storm surge from extreme weather events was not able to be directly measured in this study because the data sets available only included the experienced tide elevations but were lacking the expected lunar tide heights for comparison. A future study could further analyze this hydrologic component by using historical astronomical tide books (using appropriate datums) and taking the differences between the experienced hourly tidal data and forecasted elevations could be used to directly measure storm surge intensities and relative frequencies.

The results from this study reinforce that sea-level rise is in fact occurring at a measurable and statistically significant rate. In addition, there is no discernible regional variability in the magnitude of sea-level rise along the East and Gulf Coasts. This means that all of our low-lying coastal installations are experiencing an equivalent, but rapidly increasing risk of recurrent flood due to sea-level rise. There are a

number of factors that can impact an installation's risk or susceptibility to sea-level rise, an increase in sea-level rise also dramatically increase the damage potential of the other three hydrologic components.

Within this study, Cape Cod AFS, Dover, Bolling, Langley, Cape Canaveral, Patrick, MacDill, Tyndall, Hurlburt, Eglin, and Keesler AFB's are all essentially "beach-front-bases." These installations are located at extremely low elevations and are directly exposed to recurrent flood threats from SLR and storm surge. It would be prudent of the Air Force to take immediate action to thoroughly investigate these changing threats, determine the current capacities of coastal flood prevention infrastructure, and plan the timely implementation of adaptations using climate change projections.

The precipitation indicator results in Figure 38 showed significant regional trends. The Mid-Atlantic coastal installations, which we referred to as Zone 2, showed the highest rates of change for all of the precipitation indicators through the 1985-2019 study period. These results alone do not infer that the Zone 2 installations have suddenly all become flood zones, nor that they are now to be considered higher-risk than their Zone 1 and 3 counterparts. However, the results do illustrate that the climate and flood conditions are changing significantly and the stochastic hydrologic design scales that our water-control infrastructure are built to, may inadequate for the new flood threats occurring at these installations. The Mid-Atlantic "beach-front-bases" are Bolling, Langley, Cape Canaveral, Patrick, MacDill. Of the 17 coastal installations evaluated in this study, these five should be the highest priority for additional flood-risk evaluation and potential adaptation investments because in addition to SLR and increasing storm surges, they are also experiencing significantly increased precipitation driven flood risk.

VI. Conclusions

In conclusion, a changing climate impacts the frequency and magnitude of extreme weather events and creates long-term changes in the hydrologic environment, altering the threats of recurrent flooding at our coastal Air Force installations. In this study I defined the four components of recurrent flooding: sea-level rise, tidal fluctuations, storm surges, and precipitation and explored how climate change is impacting each component.

I analyzed 40 years of historical precipitation and tidal data for 17 coastal U.S. Air Force installations and developed a series of hydrologic indicators using both peak and threshold exceedance frequencies to identify long-term temporal trends in the hydrologic components that drive recurrent flooding. These indicator results were used to establish an installation's "hydrologic profile" allowing for a thorough evaluation of changing hydrologic conditions and enabling the identification of installations with rapidly changing flood risk conditions.

The results from this analysis demonstrated that hydrologic conditions for three of the recurrent flooding components (SLR, storm surge, and precipitation) are displaying significant trends away from the historical norms. Since the water-control infrastructure on our Air Force installations were designed assuming stochastic threat condition of the past, the trends identified in this study suggest that our infrastructure portfolio may not be able to handle the climate conditions of the future.

Finally, the hydrologic profiles developed in this study determined that sea-level rise is a persistent and increasing threat that is impacting all of the coastal Air Force installations similarly. However, precipitation conditions appear to be worsening in the Mid-Atlantic region the fastest, placing these coastal installations at the greatest risk of recurrent in a changing climate.

VII. Appendix

```
##### Precipitation Pull and Analysis
# Analysis V2- Updates 2
# Now "fully automate", just have to change Station ID and Base name
# 6 August 2021

### To be changed for each installation ####

Station<-"KPFN"         # CHANGE ME
Base<-'Tyndall AFB'    # CHANGE ME

################################################################################
setwd("C:/Users/dylan/Documents/AA. AFIT/Thesis/R Sets/Analysis_v2/
Precip_Data")

#install.packages("readxlsb")
library(readxlsb)
library(tidyr)

#### Keep same, but allow multiple iterations via paste ####
xslb<-"-HISTORY-FINAL.XLSB" # back end of root prcp data file
root_file<-paste0(Station, xslb) # creates root file name

#### pull from XZLB ####
data<-read_xlsb(root_file, sheet="DATA", col_names=TRUE) # works


### subset to cols req'd ####
data<-subset(data, select = c("WEATHER.STATION.CODE",
                              "DATA.DATE",
                              "X30.YEAR.NORMAL.TOTAL.DAILY.WATER.EQUIVALENT..Inches.",
                              "OBSERVED.TOTAL.DAILY.WATER.EQUIVALENT.AWXCLIMO..Inches."))

colnames(data)<-c("station", "date", "mean precip 30 yr", "precip")

### format date to cols ####
date.format<-"%Y,%m,%d"
data$date<-as.Date(data$date, date.format)
data<- separate(data, date, c("Year", "Month", "Day"))

###establishing 48 & 72 hr accum columns ####
data$accum_48hr<-0
data$accum_72hr<-0

### estab. precip Thresholds (in) ####
thres1<-1
thres2<-1.5
thres3<-2
thres4<-3

### Estab Results dataframe ####
results<-data.frame(station=character(), base=character(), year=numeric(),
measurment=character(), value=numeric())

#### Setting Year For-loop parameters
```

```
yr_min<-min(data$Year)
yr_max<-max(data$Year)

yr<-yr_min

######## Start of yrly for loops ######
for(yr in yr_min:yr_max){
  #### subset to 1 year ####
  data_yr<-data[data$Year==yr,]

  ### Total Annual Accumulations #####
  prcp_ann_tot_yr<-sum(data_yr$precip) # in inches
  ## how /where to record
  results<-rbind(results,c( Station, Base,  yr, 'annual.precip',
prcp_ann_tot_yr ))

  ### Peak 24 hr ####
  peak_24hr_rainfall_yr<-max(data_yr$precip)
  results<-rbind(results,c( Station, Base,  yr, 'peak.24hr',
peak_24hr_rainfall_yr ))

  ### Median of 24hr acccum>0 ####
  med_24hr_rainfall_yr<-median(data_yr$precip[data_yr$precip>0])
  results<-rbind(results,c( Station, Base,  yr, 'median.24hr',
med_24hr_rainfall_yr ))

  ### 75% of 24hr acccum>0 ####
  qnt_24hr_75_yr<-quantile(data_yr$precip[data_yr$precip>0], probs = c(0.75),
na.rm = TRUE)
  results<-rbind(results,c( Station, Base,  yr, 'q.75pct.24hr', qnt_24hr_75_yr
))

    ### finding 48 & 72 hr amounts ####
  rows<-nrow(data_yr)

  dum48<-c(data_yr$precip[2:rows],0) #creates dumb variable vector, sets = to
precip
  # starting at row 2 to #rows, and put a 0 as last value
  data_yr$accum_48hr<- dum48+ data_yr$precip # sets col to sum or precip &
dumb var
  dum72<-c(data_yr$precip[3:rows],0,0) # same but 2 rows for
  data_yr$accum_72hr<- dum48+ data_yr$precip +dum72 # adds all 3

  rm(dum48) #removes from GE
  rm(dum72)

  ### 24hr exceedences ####
  exc_thres1_24<-sum(data_yr$precip > thres1)
  results<-rbind(results,c(  Station, Base, yr, 'exc.thres1.24hr',
exc_thres1_24 ))

  exc_thres2_24<-sum(data_yr$precip > thres2)
  results<-rbind(results,c(  Station, Base, yr, 'exc.thres2.24hr',
exc_thres2_24 ))
```

```
  exc_thres3_24<-sum(data_yr$precip > thres3)
  results<-rbind(results,c(  Station, Base, yr, 'exc.thres3.24hr',
exc_thres3_24 ))

  exc_thres4_24<-sum(data_yr$precip > thres4)
  results<-rbind(results,c(  Station, Base, yr, 'exc.thres4.24hr',
exc_thres4_24 ))

  ### 48hr exceedances ####
  #exc_thres1<-sum(data_yr$accum_48hr > thres1) # give T/F for thresh 1 (T=1),
  #sums Ts for #instances the 48hr total exceeds thres 1  #exc_thres1<-
sum(dum_thres1)

  exc_thres1_48<-sum(data_yr$accum_48hr > thres1)
  results<-rbind(results,c(  Station, Base, yr, 'exc.thres1.48hr',
exc_thres1_48 ))

  exc_thres2_48<-sum(data_yr$accum_48hr > thres2)
  results<-rbind(results,c(  Station, Base, yr, 'exc.thres2.48hr',
exc_thres2_48 ))

  exc_thres3_48<-sum(data_yr$accum_48hr > thres3)
  results<-rbind(results,c(  Station, Base, yr, 'exc.thres3.48hr',
exc_thres3_48 ))

  exc_thres4_48<-sum(data_yr$accum_48hr > thres4)
  results<-rbind(results,c(  Station, Base, yr, 'exc.thres4.48hr',
exc_thres4_48 ))

  ### 72hr exceedances ####
  exc_thres1_72<-sum(data_yr$accum_72hr > thres1)
  results<-rbind(results,c(  Station,Base, yr, 'exc.thres1.72hr',
exc_thres1_72 ))

  exc_thres2_72<-sum(data_yr$accum_72hr > thres2)
  results<-rbind(results,c(  Station, Base, yr, 'exc.thres2.72hr',
exc_thres2_72 ))

  exc_thres3_72<-sum(data_yr$accum_72hr > thres3)
  results<-rbind(results,c(  Station, Base, yr, 'exc.thres3.72hr',
exc_thres3_72 ))

  exc_thres4_72<-sum(data_yr$accum_72hr > thres4)
  results<-rbind(results,c(  Station,Base, yr, 'exc.thres4.72hr',
exc_thres4_72 ))

  ### Peak 48 hr ####
  peak_48hr_rainfall_yr<-max(data_yr$accum_48hr)
  results<-rbind(results,c(  Station, Base, yr, 'peak.48hr',
peak_48hr_rainfall_yr ))

  ### Median of 48hr acccum>0 ####
  med_48hr_rainfall_yr<-median(data_yr$accum_48hr[data_yr$accum_48hr>0])
```

```
  results<-rbind(results,c( Station, Base,  yr, 'median.48hr',
med_48hr_rainfall_yr ))

  ### 75% of 48hr acccum>0 ####
  qnt_48hr_75_yr<-quantile(data_yr$accum_48hr[data_yr$accum_48hr>0], probs =
c(0.75), na.rm = TRUE)
  results<-rbind(results,c( Station, Base,  yr, 'q.75pct.48hr', qnt_48hr_75_yr
))

    ### Peak 72 hr ####
  peak_72hr_rainfall_yr<-max(data_yr$accum_72hr)
  results<-rbind(results,c(  Station, Base, yr, 'peak.72hr',
peak_72hr_rainfall_yr ))

  ### Median of 72hr acccum>0 ####
  med_72hr_rainfall_yr<-median(data_yr$accum_72hr[data_yr$accum_72hr>0])
  results<-rbind(results,c( Station, Base,  yr, 'median.72hr',
med_72hr_rainfall_yr ))

  ### 75% of 72hr acccum>0 ####
  qnt_72hr_75_yr<-quantile(data_yr$accum_72hr[data_yr$accum_72hr>0], probs =
c(0.75), na.rm = TRUE)
  results<-rbind(results,c( Station, Base,  yr, 'q.75pct.72hr', qnt_72hr_75_yr
))

    #### Monthly Precip Extremes- amt and month #######
  ### Monthly Precip Extreme ###
  #a. Highest mean monthly accumulation - ID month, plot 1 data-pt per year
  #b. Lowest mean monthly accumulation - ID month, plot 1 data-pt per year
  cat1<-c("precip")
  agg1<-aggregate(data_yr[cat1], by=list(Year=data_yr$Year,
                                         Month=data_yr$Month), FUN=sum)
  high_mn_amt<-max(agg1$precip)
  results<-rbind(results,c(  Station, Base, yr, 'high.mn.amt', high_mn_amt ))

  high_mn_mn<-agg1$Month[agg1$precip==high_mn_amt]
  results<-rbind(results,c( Station, Base,  yr, 'high.mn.mn', high_mn_mn ))

}
colnames(results)<-c("station","base" ,"year","measurement","value")
results$value<-as.numeric(results$value)

# ###### Overall Peak Accumulation- Median and 75%iles ######
# ### Overall Peak 24hr accumulation- 75 %ile & Median####
# peak_24_data<-results[results$measurement=='peak.24hr',]
# qnt_24_75<-quantile(peak_24_data$value, probs = c(0.75), na.rm=TRUE)
# qnt_24_75<-as.numeric(qnt_24_75)
# results<-rbind(results,c( Station, Base,  'All', 'ov.qnt.24hr.75ile',
qnt_24_75 ))
#
# med_peak_24<-median(peak_24_data$value)
# results<-rbind(results,c( Station, Base, 'All', 'ov.med.24hr', med_peak_24))
#
# ### Overall Peak 48hr accumulation- 75 %ile & Median####
```

```
# results$value<-as.numeric(results$value)
# peak_48_data<-results[results$measurement=='peak.48hr',]
# qnt_48_75<-quantile(peak_48_data$value, probs = c(0.75), na.rm=TRUE)
# qnt_48_75<-as.numeric(qnt_48_75)
# results<-rbind(results,c( Station, Base, 'All', 'ov.qnt.48hr.75ile',
qnt_48_75 ))
#
# med_peak_48<-median(peak_48_data$value)
# results<-rbind(results,c( Station, Base,  'All', 'ov.med.48hr',
med_peak_48))
#
# ### Overall Peak 72hr accumulation- 75 %ile & Median####
# results$value<-as.numeric(results$value)
# peak_72_data<-results[results$measurement=='peak.72hr',]
# qnt_72_75<-quantile(peak_72_data$value, probs = c(0.75), na.rm=TRUE)
# qnt_72_75<-as.numeric(qnt_72_75)
# results<-rbind(results,c( Station, Base, 'All', 'ov.qnt.72hr.75ile',
qnt_72_75 ))
#
# med_peak_72<-median(peak_72_data$value)
# results<-rbind(results,c( Station, Base, 'All', 'ov.med.72hr', med_peak_72))

##### write.csv- Single location results ####
csv1_loc_front<-"C:/Users/dylan/Documents/AA. AFIT/Thesis/R Sets/Analysis_v2/
Precip_Data/"
csv1_loc_back<-"_res_csv1.csv"
csv1_all<-paste0(csv1_loc_front,Station,csv1_loc_back)
csv1<-paste0(Station,csv1_loc_back)
# automates write.csv
write.csv(results,csv1_all, row.names = FALSE)

#### End XLSB conversion ####

################################################################################
################################################################################
####### Baselines & Normalizing Data Start#######
#rm(list=ls(all.names = TRUE))

# read the .csv ####
results<-read.csv(csv1, sep=",", header=TRUE)

res_base<-results[results$year <= 1989,]
# establish baseline years (1985-89, 5 year mean)

#### Establish Baselines for each indicator#####
#annual.precip
annual.precip<-res_base[res_base$measurement =='annual.precip',]
annual.precip_base<-mean(annual.precip$value)

### Peaks ####
#peak 24
peak.24hr<-res_base[res_base$measurement =='peak.24hr',]
peak.24hr_base<-mean(peak.24hr$value)
```

```
#peak 48
peak.48hr<-res_base[res_base$measurement =='peak.48hr',]
peak.48hr_base<-mean(peak.48hr$value)

#peak 72
peak.72hr<-res_base[res_base$measurement =='peak.72hr',]
peak.72hr_base<-mean(peak.72hr$value)

### Medians ####
# med 24hr
med.24hr<-res_base[res_base$measurement =='median.24hr',]
med.24hr_base<-mean(med.24hr$value)

# med 48hr
med.48hr<-res_base[res_base$measurement =='median.48hr',]
med.48hr_base<-mean(med.48hr$value)

# med 72hr
med.72hr<-res_base[res_base$measurement =='median.72hr',]
med.72hr_base<-mean(med.72hr$value)

### 75%iles ####
# 75%- 24hr
qnt75.24hr<-res_base[res_base$measurement =='q.75pct.24hr',]
qnt75.24hr_base<-mean(qnt75.24hr$value)

# 75%- 48hr
qnt75.48hr<-res_base[res_base$measurement =='q.75pct.48hr',]
qnt75.48hr_base<-mean(qnt75.48hr$value)

# 75%- 72hr
qnt75.72hr<-res_base[res_base$measurement =='q.75pct.72hr',]
qnt75.72hr_base<-mean(qnt75.72hr$value)



#24 excd ####
exc.thres1.24hr<-res_base[res_base$measurement =='exc.thres1.24hr',]
exc.thres1.24hr_base<-mean(exc.thres1.24hr$value)

exc.thres2.24hr<-res_base[res_base$measurement =='exc.thres2.24hr',]
exc.thres2.24hr_base<-mean(exc.thres2.24hr$value)

exc.thres3.24hr<-res_base[res_base$measurement =='exc.thres3.24hr',]
exc.thres3.24hr_base<-mean(exc.thres3.24hr$value)

exc.thres4.24hr<-res_base[res_base$measurement =='exc.thres4.24hr',]
exc.thres4.24hr_base<-mean(exc.thres4.24hr$value)

#48 excd ####
exc.thres1.48hr<-res_base[res_base$measurement =='exc.thres1.48hr',]
exc.thres1.48hr_base<-mean(exc.thres1.48hr$value)

exc.thres2.48hr<-res_base[res_base$measurement =='exc.thres2.48hr',]
```

```
exc.thres2.48hr_base<-mean(exc.thres2.48hr$value)

exc.thres3.48hr<-res_base[res_base$measurement =='exc.thres3.48hr',]
exc.thres3.48hr_base<-mean(exc.thres3.48hr$value)

exc.thres4.48hr<-res_base[res_base$measurement =='exc.thres4.48hr',]
exc.thres4.48hr_base<-mean(exc.thres4.48hr$value)

#72 excd ####
exc.thres1.72hr<-res_base[res_base$measurement =='exc.thres1.72hr',]
exc.thres1.72hr_base<-mean(exc.thres1.72hr$value)

exc.thres2.72hr<-res_base[res_base$measurement =='exc.thres2.72hr',]
exc.thres2.72hr_base<-mean(exc.thres2.72hr$value)

exc.thres3.72hr<-res_base[res_base$measurement =='exc.thres3.72hr',]
exc.thres3.72hr_base<-mean(exc.thres3.72hr$value)

exc.thres4.72hr<-res_base[res_base$measurement =='exc.thres4.72hr',]
exc.thres4.72hr_base<-mean(exc.thres4.72hr$value)

# high.mn.amt ####
high.mn.amt<-res_base[res_base$measurement =='high.mn.amt',]
high.mn.amt_base<-mean(high.mn.amt$value)
# high.mn.mn doesn't get normalized b/c it is a categorical variable
#### end Estab. Baseline ###


###### Normalizing data ######

results$value_norm<-0
idx<-1
res_nrow<-nrow(results)

if (results$measurement[idx] == 'peak.24hr') {
  results$value_norm[idx]<- (results$value[idx] - peak.24hr_base) / peak.
24hr_base}


for(idx in 1:res_nrow){
  # peak amts
  if (results$measurement[idx] == 'peak.24hr') {
    results$value_norm[idx]<- results$value[idx] / peak.24hr_base}
  if (results$measurement[idx] == 'peak.48hr') {
    results$value_norm[idx]<- results$value[idx] / peak.48hr_base}
  if (results$measurement[idx] == 'peak.72hr') {
    results$value_norm[idx]<- results$value[idx] / peak.72hr_base}
  # annual.precip
  if (results$measurement[idx] == 'annual.precip') {
    results$value_norm[idx]<- results$value[idx] / annual.precip_base}

  # medians
  if (results$measurement[idx] == 'median.24hr') {
    results$value_norm[idx]<- results$value[idx] / med.24hr_base}
```

```
if (results$measurement[idx] == 'median.48hr') {
  results$value_norm[idx]<- results$value[idx] / med.48hr_base}
if (results$measurement[idx] == 'median.72hr') {
  results$value_norm[idx]<- results$value[idx] / med.72hr_base}

# 75%iles
if (results$measurement[idx] == 'q.75pct.24hr') {
  results$value_norm[idx]<- results$value[idx] / qnt75.24hr_base}
if (results$measurement[idx] == 'q.75pct.48hr') {
  results$value_norm[idx]<- results$value[idx] / qnt75.48hr_base}
if (results$measurement[idx] == 'q.75pct.72hr') {
  results$value_norm[idx]<- results$value[idx] / qnt75.72hr_base}




#thresh 1 exc
if (results$measurement[idx] == 'exc.thres1.24hr') {
  results$value_norm[idx]<- results$value[idx] / exc.thres1.24hr_base}
if (results$measurement[idx] == 'exc.thres1.48hr') {
  results$value_norm[idx]<- results$value[idx] / exc.thres1.48hr_base}
if (results$measurement[idx] == 'exc.thres1.72hr') {
  results$value_norm[idx]<- results$value[idx] / exc.thres1.72hr_base}
#thresh 2 exc
if (results$measurement[idx] == 'exc.thres2.24hr') {
  results$value_norm[idx]<- results$value[idx] / exc.thres2.24hr_base}
if (results$measurement[idx] == 'exc.thres2.48hr') {
  results$value_norm[idx]<- results$value[idx] / exc.thres2.48hr_base}
if (results$measurement[idx] == 'exc.thres2.72hr') {
  results$value_norm[idx]<- results$value[idx] / exc.thres2.72hr_base}
#thresh 3 exc
if (results$measurement[idx] == 'exc.thres3.24hr') {
  results$value_norm[idx]<- results$value[idx] / exc.thres3.24hr_base}
if (results$measurement[idx] == 'exc.thres3.48hr') {
  results$value_norm[idx]<- results$value[idx] / exc.thres3.48hr_base}
if (results$measurement[idx] == 'exc.thres3.72hr') {
  results$value_norm[idx]<- results$value[idx] / exc.thres3.72hr_base}
#thresh 3 exc
if (results$measurement[idx] == 'exc.thres3.24hr') {
  results$value_norm[idx]<- results$value[idx] / exc.thres3.24hr_base}
if (results$measurement[idx] == 'exc.thres3.48hr') {
  results$value_norm[idx]<- results$value[idx] / exc.thres3.48hr_base}
if (results$measurement[idx] == 'exc.thres3.72hr') {
  results$value_norm[idx]<- results$value[idx] / exc.thres3.72hr_base}
#thresh 4 exc
if (results$measurement[idx] == 'exc.thres4.24hr') {
  results$value_norm[idx]<- results$value[idx] / exc.thres4.24hr_base}
if (results$measurement[idx] == 'exc.thres4.48hr') {
  results$value_norm[idx]<- results$value[idx] / exc.thres4.48hr_base}
if (results$measurement[idx] == 'exc.thres4.72hr') {
  results$value_norm[idx]<- results$value[idx] / exc.thres4.72hr_base}
# high.mn.amt
if (results$measurement[idx] == 'high.mn.amt') {
```

```
    results$value_norm[idx]<- results$value[idx] / high.mn.amt_base}
} #works


##### write.csv- Single location- NORMALIZED results ####
csv2_loc_front<-"C:/Users/dylan/Documents/AA. AFIT/Thesis/R Sets/Analysis_v2/
Precip_Data/"
csv2_loc_back<-"_res_norm_csv2.csv"
csv2_all<-paste0(csv2_loc_front,Station,csv2_loc_back)
csv2<-paste0(Station,csv2_loc_back)

# automates write.csv2 (normalized results)
write.csv(results,csv2_all, row.names = FALSE)

################################################################################
#### dcast- take from long to wide ####
#590A- lesson 3 slides, Character Manipulation and Functions in R
setwd("C:/Users/dylan/Documents/AA. AFIT/Thesis/R Sets/Analysis_v2/
Precip_Data")
library(tidyr)
library(reshape2)


prcp_data<-read.csv(csv2,sep=",", header = TRUE)

#### dcast- norm and value ####
#https://www.youtube.com/watch?v=hP7EWk09POg
#thank you, you beautiful human being you.

wide_prcp_norm<-dcast(prcp_data, formula = year~measurement, value.var =
"value_norm")
# (long data set, formula=1st col wanted+ 2nd col wanted(none for me) ~column
# that you want each entry to be seperated into its own column, value.var=
value
# you want filled in

wide_prcp_value<-dcast(prcp_data, formula = year~measurement, value.var =
"value")



# write.csv wide_prcp_norm ####
csv3_loc_front<-"C:/Users/dylan/Documents/AA. AFIT/Thesis/R Sets/Analysis_v2/
Precip_Data/"
csv3_loc_back<-"_res_norm_wide_csv3.csv"
csv3_all<-paste0(csv3_loc_front,Station,csv3_loc_back)
csv3<-paste0(Station,csv3_loc_back)

# automates write.csv2 (normalized results)
write.csv(wide_prcp_norm,csv3_all, row.names = FALSE)

# write.csv(wide_prcp_norm,'C:/Users/dylan/Documents/AA. AFIT/Thesis/R Sets/
Analysis_v2/Precip_Data/wide_precip_data_norm_Char_UPDATE.csv',
#           row.names = FALSE)
```

```
# write.csv wide_prcp_value ####
# write.csv(wide_prcp_value,'C:/Users/dylan/Documents/AA. AFIT/Thesis/R Sets/
Analysis_v2/Precip_Data/wide_precip_data_value_Char_UPDATE.csv',
#           row.names = FALSE)

csv4_loc_front<-"C:/Users/dylan/Documents/AA. AFIT/Thesis/R Sets/Analysis_v2/
Precip_Data/"
csv4_loc_back<-"_res_value_wide_csv4.csv"
csv4_all<-paste0(csv4_loc_front,Station,csv4_loc_back)
csv4<-paste0(Station,csv4_loc_back)

# automates write.csv2 (normalized results)
write.csv(wide_prcp_value,csv4_all, row.names = FALSE)

#### End of dcast ####

################################################################################
################################################################################
#### Summary Statistics #####
### x is the normalized data ###
n_row<-nrow(wide_prcp_norm)

x<-wide_prcp_norm #creates new data frame
x[n_row +1,]<-"" #creates 3 new blank rows for intercept, m, and p-value
x[n_row +2,]<-""
x[n_row +3,]<-""
x[n_row +4,]<-""

x$year[n_row +1]<- "int" # titles them
x$year[n_row +2]<- "m"
x$year[n_row +3]<- "p-value"
x$year[n_row +4]<- "r-sq'd"

# run lm
fit_x<-lm(formula= annual.precip ~ year, data=wide_prcp_norm)
summary<-summary(fit_x)
x$annual.precip[n_row +1]<-summary$coefficients[1] # intercept
x$annual.precip[n_row +2]<-summary$coefficients[2] # m (slope)
x$annual.precip[n_row +3]<-summary$coefficients[8] # p-value
x$annual.precip[n_row +4]<-summary$r.squared       # r-squared

# exc.thres1
fit_x<-lm(exc.thres1.24hr ~ year, data=wide_prcp_norm)
summary<-summary(fit_x)
x$exc.thres1.24hr[n_row +1]<-summary$coefficients[1] # intercept
x$exc.thres1.24hr[n_row +2]<-summary$coefficients[2] # m (slope)
x$exc.thres1.24hr[n_row +3]<-summary$coefficients[8] # p-value
x$exc.thres1.24hr[n_row +4]<-summary$r.squared       # r-squared

fit_x<-lm(exc.thres1.48hr ~ year, data=wide_prcp_norm)
summary<-summary(fit_x)
x$exc.thres1.48hr[n_row +1]<-summary$coefficients[1] # intercept
```

```
x$exc.thres1.48hr[n_row +2]<-summary$coefficients[2] # m (slope)
x$exc.thres1.48hr[n_row +3]<-summary$coefficients[8] # p-value
x$exc.thres1.48hr[n_row +4]<-summary$r.squared       # r-squared

fit_x<-lm(exc.thres1.72hr ~ year, data=wide_prcp_norm)
summary<-summary(fit_x)
x$exc.thres1.72hr[n_row +1]<-summary$coefficients[1] # intercept
x$exc.thres1.72hr[n_row +2]<-summary$coefficients[2] # m (slope)
x$exc.thres1.72hr[n_row +3]<-summary$coefficients[8] # p-value
x$exc.thres1.72hr[n_row +4]<-summary$r.squared       # r-squared

# exc.thres2
fit_x<-lm(exc.thres2.24hr ~ year, data=wide_prcp_norm)
summary<-summary(fit_x)
x$exc.thres2.24hr[n_row +1]<-summary$coefficients[1] # intercept
x$exc.thres2.24hr[n_row +2]<-summary$coefficients[2] # m (slope)
x$exc.thres2.24hr[n_row +3]<-summary$coefficients[8] # p-value
x$exc.thres2.24hr[n_row +4]<-summary$r.squared       # r-squared

fit_x<-lm(exc.thres2.48hr ~ year, data=wide_prcp_norm)
summary<-summary(fit_x)
x$exc.thres2.48hr[n_row +1]<-summary$coefficients[1] # intercept
x$exc.thres2.48hr[n_row +2]<-summary$coefficients[2] # m (slope)
x$exc.thres2.48hr[n_row +3]<-summary$coefficients[8] # p-value
x$exc.thres2.48hr[n_row +4]<-summary$r.squared       # r-squared

fit_x<-lm(exc.thres2.72hr ~ year, data=wide_prcp_norm)
summary<-summary(fit_x)
x$exc.thres2.72hr[n_row +1]<-summary$coefficients[1] # intercept
x$exc.thres2.72hr[n_row +2]<-summary$coefficients[2] # m (slope)
x$exc.thres2.72hr[n_row +3]<-summary$coefficients[8] # p-value
x$exc.thres2.72hr[n_row +4]<-summary$r.squared       # r-squared

# exc.thres3
fit_x<-lm(exc.thres3.24hr ~ year, data=wide_prcp_norm)
summary<-summary(fit_x)
x$exc.thres3.24hr[n_row +1]<-summary$coefficients[1] # intercept
x$exc.thres3.24hr[n_row +2]<-summary$coefficients[2] # m (slope)
x$exc.thres3.24hr[n_row +3]<-summary$coefficients[8] # p-value
x$exc.thres3.24hr[n_row +4]<-summary$r.squared       # r-squared

fit_x<-lm(exc.thres3.48hr ~ year, data=wide_prcp_norm)
summary<-summary(fit_x)
x$exc.thres3.48hr[n_row +1]<-summary$coefficients[1] # intercept
x$exc.thres3.48hr[n_row +2]<-summary$coefficients[2] # m (slope)
x$exc.thres3.48hr[n_row +3]<-summary$coefficients[8] # p-value
x$exc.thres3.48hr[n_row +4]<-summary$r.squared       # r-squared

fit_x<-lm(exc.thres3.72hr ~ year, data=wide_prcp_norm)
summary<-summary(fit_x)
x$exc.thres3.72hr[n_row +1]<-summary$coefficients[1] # intercept
x$exc.thres3.72hr[n_row +2]<-summary$coefficients[2] # m (slope)
x$exc.thres3.72hr[n_row +3]<-summary$coefficients[8] # p-value
x$exc.thres3.72hr[n_row +4]<-summary$r.squared       # r-squared
```

```
# exc.thres4
fit_x<-lm(exc.thres4.24hr ~ year, data=wide_prcp_norm)
summary<-summary(fit_x)
x$exc.thres4.24hr[n_row +1]<-summary$coefficients[1] # intercept
x$exc.thres4.24hr[n_row +2]<-summary$coefficients[2] # m (slope)
x$exc.thres4.24hr[n_row +3]<-summary$coefficients[8] # p-value
x$exc.thres4.24hr[n_row +4]<-summary$r.squared       # r-squared

fit_x<-lm(exc.thres4.48hr ~ year, data=wide_prcp_norm)
summary<-summary(fit_x)
x$exc.thres4.48hr[n_row +1]<-summary$coefficients[1] # intercept
x$exc.thres4.48hr[n_row +2]<-summary$coefficients[2] # m (slope)
x$exc.thres4.48hr[n_row +3]<-summary$coefficients[8] # p-value
x$exc.thres4.48hr[n_row +4]<-summary$r.squared       # r-squared

fit_x<-lm(exc.thres4.72hr ~ year, data=wide_prcp_norm)
summary<-summary(fit_x)
x$exc.thres4.72hr[n_row +1]<-summary$coefficients[1] # intercept
x$exc.thres4.72hr[n_row +2]<-summary$coefficients[2] # m (slope)
x$exc.thres4.72hr[n_row +3]<-summary$coefficients[8] # p-value
x$exc.thres4.72hr[n_row +4]<-summary$r.squared       # r-squared

# high.mn.amt
fit_x<-lm(high.mn.amt ~ year, data=wide_prcp_norm)
summary<-summary(fit_x)
x$high.mn.amt[n_row +1]<-summary$coefficients[1] # intercept
x$high.mn.amt[n_row +2]<-summary$coefficients[2] # m (slope)
x$high.mn.amt[n_row +3]<-summary$coefficients[8] # p-value
x$high.mn.amt[n_row +4]<-summary$r.squared       # r-squared

# high.mn.mn
fit_x<-lm(high.mn.mn ~ year, data=wide_prcp_norm)
summary<-summary(fit_x)
x$high.mn.mn[n_row +1]<-summary$coefficients[1] # intercept
x$high.mn.mn[n_row +2]<-summary$coefficients[2] # m (slope)
x$high.mn.mn[n_row +3]<-summary$coefficients[8] # p-value
x$high.mn.mn[n_row +4]<-summary$r.squared       # r-squared

# median
fit_x<-lm(median.24hr ~ year, data=wide_prcp_norm)
summary<-summary(fit_x)
x$median.24hr[n_row +1]<-summary$coefficients[1] # intercept
x$median.24hr[n_row +2]<-summary$coefficients[2] # m (slope)
x$median.24hr[n_row +3]<-summary$coefficients[8] # p-value
x$median.24hr[n_row +4]<-summary$r.squared       # r-squared

fit_x<-lm(median.48hr ~ year, data=wide_prcp_norm)
summary<-summary(fit_x)
x$median.48hr[n_row +1]<-summary$coefficients[1] # intercept
x$median.48hr[n_row +2]<-summary$coefficients[2] # m (slope)
x$median.48hr[n_row +3]<-summary$coefficients[8] # p-value
x$median.48hr[n_row +4]<-summary$r.squared       # r-squared
```

```
fit_x<-lm(median.72hr ~ year, data=wide_prcp_norm)
summary<-summary(fit_x)
x$median.72hr[n_row +1]<-summary$coefficients[1] # intercept
x$median.72hr[n_row +2]<-summary$coefficients[2] # m (slope)
x$median.72hr[n_row +3]<-summary$coefficients[8] # p-value
x$median.72hr[n_row +4]<-summary$r.squared       # r-squared

# peak
fit_x<-lm(peak.24hr ~ year, data=wide_prcp_norm)
summary<-summary(fit_x)
x$peak.24hr[n_row +1]<-summary$coefficients[1] # intercept
x$peak.24hr[n_row +2]<-summary$coefficients[2] # m (slope)
x$peak.24hr[n_row +3]<-summary$coefficients[8] # p-value
x$peak.24hr[n_row +4]<-summary$r.squared       # r-squared

fit_x<-lm(peak.48hr ~ year, data=wide_prcp_norm)
summary<-summary(fit_x)
x$peak.48hr[n_row +1]<-summary$coefficients[1] # intercept
x$peak.48hr[n_row +2]<-summary$coefficients[2] # m (slope)
x$peak.48hr[n_row +3]<-summary$coefficients[8] # p-value
x$peak.48hr[n_row +4]<-summary$r.squared       # r-squared

fit_x<-lm(peak.72hr ~ year, data=wide_prcp_norm)
summary<-summary(fit_x)
x$peak.72hr[n_row +1]<-summary$coefficients[1] # intercept
x$peak.72hr[n_row +2]<-summary$coefficients[2] # m (slope)
x$peak.72hr[n_row +3]<-summary$coefficients[8] # p-value
x$peak.72hr[n_row +4]<-summary$r.squared       # r-squared

# q.75pct
fit_x<-lm(q.75pct.24hr ~ year, data=wide_prcp_norm)
summary<-summary(fit_x)
x$q.75pct.24hr[n_row +1]<-summary$coefficients[1] # intercept
x$q.75pct.24hr[n_row +2]<-summary$coefficients[2] # m (slope)
x$q.75pct.24hr[n_row +3]<-summary$coefficients[8] # p-value
x$q.75pct.24hr[n_row +4]<-summary$r.squared       # r-squared

fit_x<-lm(q.75pct.48hr ~ year, data=wide_prcp_norm)
summary<-summary(fit_x)
x$q.75pct.48hr[n_row +1]<-summary$coefficients[1] # intercept
x$q.75pct.48hr[n_row +2]<-summary$coefficients[2] # m (slope)
x$q.75pct.48hr[n_row +3]<-summary$coefficients[8] # p-value
x$q.75pct.48hr[n_row +4]<-summary$r.squared       # r-squared

fit_x<-lm(q.75pct.72hr ~ year, data=wide_prcp_norm)
summary<-summary(fit_x)
x$q.75pct.72hr[n_row +1]<-summary$coefficients[1] # intercept
x$q.75pct.72hr[n_row +2]<-summary$coefficients[2] # m (slope)
x$q.75pct.72hr[n_row +3]<-summary$coefficients[8] # p-value
x$q.75pct.72hr[n_row +4]<-summary$r.squared       # r-squared


csv5_loc_front<-"C:/Users/dylan/Documents/AA. AFIT/Thesis/R Sets/Analysis_v2/
Precip_Data/"
```

```
csv5_loc_back<-"_res_norm_wide_p_csv5.csv"
csv5_all<-paste0(csv5_loc_front,Station,csv5_loc_back)
csv5<-paste0(Station,csv5_loc_back)

# automates write.csv2 (normalized results)
write.csv(x,csv5_all, row.names = FALSE)

#### End of wide_norm_p-values ####
################################################################################

n_row<-nrow(wide_prcp_value)

x<-wide_prcp_value #creates new data frame
x[n_row +1,]<-"" #creates 3 new blank rows for intercept, m, and p-value
x[n_row +2,]<-""
x[n_row +3,]<-""
x[n_row +4,]<-""

x$year[n_row +1]<- "int" # titles them
x$year[n_row +2]<- "m"
x$year[n_row +3]<- "p-value"
x$year[n_row +4]<- "r-sq'd"

#### run lm ####
# annual.precip
fit_x<-lm(formula= annual.precip ~ year, data=wide_prcp_value)
summary<-summary(fit_x)
x$annual.precip[n_row +1]<-summary$coefficients[1] # intercept
x$annual.precip[n_row +2]<-summary$coefficients[2] # m (slope)
x$annual.precip[n_row +3]<-summary$coefficients[8] # p-value
x$annual.precip[n_row +4]<-summary$r.squared       # r-squared

# exc.thres1
fit_x<-lm(exc.thres1.24hr ~ year, data=wide_prcp_value)
summary<-summary(fit_x)
x$exc.thres1.24hr[n_row +1]<-summary$coefficients[1] # intercept
x$exc.thres1.24hr[n_row +2]<-summary$coefficients[2] # m (slope)
x$exc.thres1.24hr[n_row +3]<-summary$coefficients[8] # p-value
x$exc.thres1.24hr[n_row +4]<-summary$r.squared       # r-squared

fit_x<-lm(exc.thres1.48hr ~ year, data=wide_prcp_value)
summary<-summary(fit_x)
x$exc.thres1.48hr[n_row +1]<-summary$coefficients[1] # intercept
x$exc.thres1.48hr[n_row +2]<-summary$coefficients[2] # m (slope)
x$exc.thres1.48hr[n_row +3]<-summary$coefficients[8] # p-value
x$exc.thres1.48hr[n_row +4]<-summary$r.squared       # r-squared

fit_x<-lm(exc.thres1.72hr ~ year, data=wide_prcp_value)
summary<-summary(fit_x)
x$exc.thres1.72hr[n_row +1]<-summary$coefficients[1] # intercept
x$exc.thres1.72hr[n_row +2]<-summary$coefficients[2] # m (slope)
x$exc.thres1.72hr[n_row +3]<-summary$coefficients[8] # p-value
x$exc.thres1.72hr[n_row +4]<-summary$r.squared       # r-squared
```

```
# exc.thres2
fit_x<-lm(exc.thres2.24hr ~ year, data=wide_prcp_value)
summary<-summary(fit_x)
x$exc.thres2.24hr[n_row +1]<-summary$coefficients[1] # intercept
x$exc.thres2.24hr[n_row +2]<-summary$coefficients[2] # m (slope)
x$exc.thres2.24hr[n_row +3]<-summary$coefficients[8] # p-value
x$exc.thres2.24hr[n_row +4]<-summary$r.squared       # r-squared

fit_x<-lm(exc.thres2.48hr ~ year, data=wide_prcp_value)
summary<-summary(fit_x)
x$exc.thres2.48hr[n_row +1]<-summary$coefficients[1] # intercept
x$exc.thres2.48hr[n_row +2]<-summary$coefficients[2] # m (slope)
x$exc.thres2.48hr[n_row +3]<-summary$coefficients[8] # p-value
x$exc.thres2.48hr[n_row +4]<-summary$r.squared       # r-squared

fit_x<-lm(exc.thres2.72hr ~ year, data=wide_prcp_value)
summary<-summary(fit_x)
x$exc.thres2.72hr[n_row +1]<-summary$coefficients[1] # intercept
x$exc.thres2.72hr[n_row +2]<-summary$coefficients[2] # m (slope)
x$exc.thres2.72hr[n_row +3]<-summary$coefficients[8] # p-value
x$exc.thres2.72hr[n_row +4]<-summary$r.squared       # r-squared

# exc.thres3
fit_x<-lm(exc.thres3.24hr ~ year, data=wide_prcp_value)
summary<-summary(fit_x)
x$exc.thres3.24hr[n_row +1]<-summary$coefficients[1] # intercept
x$exc.thres3.24hr[n_row +2]<-summary$coefficients[2] # m (slope)
x$exc.thres3.24hr[n_row +3]<-summary$coefficients[8] # p-value
x$exc.thres3.24hr[n_row +4]<-summary$r.squared       # r-squared

fit_x<-lm(exc.thres3.48hr ~ year, data=wide_prcp_value)
summary<-summary(fit_x)
x$exc.thres3.48hr[n_row +1]<-summary$coefficients[1] # intercept
x$exc.thres3.48hr[n_row +2]<-summary$coefficients[2] # m (slope)
x$exc.thres3.48hr[n_row +3]<-summary$coefficients[8] # p-value
x$exc.thres3.48hr[n_row +4]<-summary$r.squared       # r-squared

fit_x<-lm(exc.thres3.72hr ~ year, data=wide_prcp_value)
summary<-summary(fit_x)
x$exc.thres3.72hr[n_row +1]<-summary$coefficients[1] # intercept
x$exc.thres3.72hr[n_row +2]<-summary$coefficients[2] # m (slope)
x$exc.thres3.72hr[n_row +3]<-summary$coefficients[8] # p-value
x$exc.thres3.72hr[n_row +4]<-summary$r.squared       # r-squared

# exc.thres4
fit_x<-lm(exc.thres4.24hr ~ year, data=wide_prcp_value)
summary<-summary(fit_x)
x$exc.thres4.24hr[n_row +1]<-summary$coefficients[1] # intercept
x$exc.thres4.24hr[n_row +2]<-summary$coefficients[2] # m (slope)
x$exc.thres4.24hr[n_row +3]<-summary$coefficients[8] # p-value
x$exc.thres4.24hr[n_row +4]<-summary$r.squared       # r-squared

fit_x<-lm(exc.thres4.48hr ~ year, data=wide_prcp_value)
summary<-summary(fit_x)
```

```
x$exc.thres4.48hr[n_row +1]<-summary$coefficients[1] # intercept
x$exc.thres4.48hr[n_row +2]<-summary$coefficients[2] # m (slope)
x$exc.thres4.48hr[n_row +3]<-summary$coefficients[8] # p-value
x$exc.thres4.48hr[n_row +4]<-summary$r.squared       # r-squared

fit_x<-lm(exc.thres4.72hr ~ year, data=wide_prcp_value)
summary<-summary(fit_x)
x$exc.thres4.72hr[n_row +1]<-summary$coefficients[1] # intercept
x$exc.thres4.72hr[n_row +2]<-summary$coefficients[2] # m (slope)
x$exc.thres4.72hr[n_row +3]<-summary$coefficients[8] # p-value
x$exc.thres4.72hr[n_row +4]<-summary$r.squared       # r-squared

# high.mn.amt
fit_x<-lm(high.mn.amt ~ year, data=wide_prcp_value)
summary<-summary(fit_x)
x$high.mn.amt[n_row +1]<-summary$coefficients[1] # intercept
x$high.mn.amt[n_row +2]<-summary$coefficients[2] # m (slope)
x$high.mn.amt[n_row +3]<-summary$coefficients[8] # p-value
x$high.mn.amt[n_row +4]<-summary$r.squared       # r-squared

# high.mn.mn
fit_x<-lm(high.mn.mn ~ year, data=wide_prcp_value)
summary<-summary(fit_x)
x$high.mn.mn[n_row +1]<-summary$coefficients[1] # intercept
x$high.mn.mn[n_row +2]<-summary$coefficients[2] # m (slope)
x$high.mn.mn[n_row +3]<-summary$coefficients[8] # p-value
x$high.mn.mn[n_row +4]<-summary$r.squared       # r-squared

# median
fit_x<-lm(median.24hr ~ year, data=wide_prcp_value)
summary<-summary(fit_x)
x$median.24hr[n_row +1]<-summary$coefficients[1] # intercept
x$median.24hr[n_row +2]<-summary$coefficients[2] # m (slope)
x$median.24hr[n_row +3]<-summary$coefficients[8] # p-value
x$median.24hr[n_row +4]<-summary$r.squared       # r-squared

fit_x<-lm(median.48hr ~ year, data=wide_prcp_value)
summary<-summary(fit_x)
x$median.48hr[n_row +1]<-summary$coefficients[1] # intercept
x$median.48hr[n_row +2]<-summary$coefficients[2] # m (slope)
x$median.48hr[n_row +3]<-summary$coefficients[8] # p-value
x$median.48hr[n_row +4]<-summary$r.squared       # r-squared

fit_x<-lm(median.72hr ~ year, data=wide_prcp_value)
summary<-summary(fit_x)
x$median.72hr[n_row +1]<-summary$coefficients[1] # intercept
x$median.72hr[n_row +2]<-summary$coefficients[2] # m (slope)
x$median.72hr[n_row +3]<-summary$coefficients[8] # p-value
x$median.72hr[n_row +4]<-summary$r.squared       # r-squared

# peak
fit_x<-lm(peak.24hr ~ year, data=wide_prcp_value)
summary<-summary(fit_x)
x$peak.24hr[n_row +1]<-summary$coefficients[1] # intercept
```

```
x$peak.24hr[n_row +2]<-summary$coefficients[2] # m (slope)
x$peak.24hr[n_row +3]<-summary$coefficients[8] # p-value
x$peak.24hr[n_row +4]<-summary$r.squared       # r-squared

fit_x<-lm(peak.48hr ~ year, data=wide_prcp_value)
summary<-summary(fit_x)
x$peak.48hr[n_row +1]<-summary$coefficients[1] # intercept
x$peak.48hr[n_row +2]<-summary$coefficients[2] # m (slope)
x$peak.48hr[n_row +3]<-summary$coefficients[8] # p-value
x$peak.48hr[n_row +4]<-summary$r.squared       # r-squared

fit_x<-lm(peak.72hr ~ year, data=wide_prcp_value)
summary<-summary(fit_x)
x$peak.72hr[n_row +1]<-summary$coefficients[1] # intercept
x$peak.72hr[n_row +2]<-summary$coefficients[2] # m (slope)
x$peak.72hr[n_row +3]<-summary$coefficients[8] # p-value
x$peak.72hr[n_row +4]<-summary$r.squared       # r-squared

# q.75pct
fit_x<-lm(q.75pct.24hr ~ year, data=wide_prcp_value)
summary<-summary(fit_x)
x$q.75pct.24hr[n_row +1]<-summary$coefficients[1] # intercept
x$q.75pct.24hr[n_row +2]<-summary$coefficients[2] # m (slope)
x$q.75pct.24hr[n_row +3]<-summary$coefficients[8] # p-value
x$q.75pct.24hr[n_row +4]<-summary$r.squared       # r-squared

fit_x<-lm(q.75pct.48hr ~ year, data=wide_prcp_value)
summary<-summary(fit_x)
x$q.75pct.48hr[n_row +1]<-summary$coefficients[1] # intercept
x$q.75pct.48hr[n_row +2]<-summary$coefficients[2] # m (slope)
x$q.75pct.48hr[n_row +3]<-summary$coefficients[8] # p-value
x$q.75pct.48hr[n_row +4]<-summary$r.squared       # r-squared

fit_x<-lm(q.75pct.72hr ~ year, data=wide_prcp_value)
summary<-summary(fit_x)
x$q.75pct.72hr[n_row +1]<-summary$coefficients[1] # intercept
x$q.75pct.72hr[n_row +2]<-summary$coefficients[2] # m (slope)
x$q.75pct.72hr[n_row +3]<-summary$coefficients[8] # p-value
x$q.75pct.72hr[n_row +4]<-summary$r.squared       # r-squared


csv6_loc_front<-"C:/Users/dylan/Documents/AA. AFIT/Thesis/R Sets/Analysis_v2/
Precip_Data/csv6/"
csv6_loc_back<-"_res_value_wide_p_csv6.csv"
csv6_all<-paste0(csv6_loc_front,Station,csv6_loc_back)
csv6<-paste0(Station,csv6_loc_back)

# automates write.csv2 (valuealized results)
write.csv(x,csv6_all, row.names = FALSE)

#### End of wide_value_p-values ####
####### works sooooooooo gooooooooooddddddd ###########
```

```
###### Tidal Data- Pull and Analysis
# Analysis V2- Updates 2
# Now "fully automate", just have to change Station ID and Base name
# 6 Dec 2021

### To be changed for each installation ####

hyp_num<-12        # CHANGE ME
station<-8447435  # CHANGE ME
base<-"Cape Cod AFS"  # CHANGE ME

################################################################################
setwd("C:/Users/dylan/Documents/AA. AFIT/Thesis/R Sets/Analysis_v2/
Tidal_Data")
library(tidyr)
#https://www.dataquest.io/blog/r-api-tutorial/     API tutorial
#install.packages(c("httr","jsonlite"))
library(httr)
library(jsonlite)
library(reshape2)

######################
hyp_frnt<-"Tidal_hyperlinks"
hyp_back<-".csv"

hyps<-read.csv(paste0(hyp_frnt, hyp_num, hyp_back)) # pull hyperlinks created
in excel

colnames(hyps)<-c("links")
nrow_hyps<-nrow(hyps)

# entry<- hyps$links[1]
#
res = GET(hyps$links[1])
data = fromJSON(rawToChar(res$content))
#names(data)
raw_data<-data$data
data_fin<-raw_data
# ### worksssssssss

for (idx in 2:nrow_hyps){
  res = GET(hyps$links[idx])
  data = fromJSON(rawToChar(res$content))
  names(data)
  raw_data<-data$data

  data_fin<-rbind(data_fin, raw_data)
} ###### ohhhhhhhh yyyyyyeeeeeaaaahhhhhhhhh

##### write.csv- Single location results ####
csv1_loc_front<-"C:/Users/dylan/Documents/AA. AFIT/Thesis/R Sets/Analysis_v2/
Tidal_Data/tide_data_fin_"
csv1_loc_back<-"_csv1.csv"
```

```
csv1_all<-paste0(csv1_loc_front,hyp_num,csv1_loc_back)
csv1<-paste0("tide_data_fin_", hyp_num,csv1_loc_back)

# automates write.csv
write.csv(data_fin,csv1_all, row.names = FALSE)
#### End Data Pull ####

######################################################################
######## Data Analysis ########
# have to seperate date & time
data<-read.csv(csv1, sep=",", header = TRUE)

data<-separate(data= data, col = t, into = c("date", "time"), sep=" ")

### format date to cols ####
date.format<-"%Y,%m,%d"
data<- separate(data, date, c("Year", "Month", "Day"))

# v, units=metric in meters
# I think i can get the predicted vs. observed click on "Web Services"
# https://tidesandcurrents.noaa.gov/waterlevels.html?
id=8665530&units=metric&bdate=20210525&edate=20210526&timezone=GMT&datum=MLLW&interval=6&a

#############################################################################
### Estab Results dataframe ####
results<-data.frame(station=character(), base=character(), year=numeric(),
measurment=character(), value=numeric())

#### Setting Year For-loop parameters
yr_min<-min(data$Year)
yr_max<-max(data$Year)

yr<-yr_min

#### Establishing full quantiles, 0.90, 0.95) ####
# quantile(data$v, probs = c(0.90, 0.95), na.rm=TRUE)
qnt_90<-quantile(data$v, probs = c(0.90), na.rm=TRUE)
qnt_90<-as.numeric(qnt_90)

qnt_95<-quantile(data$v, probs = c(0.95), na.rm=TRUE)
qnt_95<-as.numeric(qnt_95)

######## Start of yrly for loops ######
for(yr in yr_min:yr_max){

#### subset to 1 year ####
data_yr<-data[data$Year==yr,]

#### data completeness ####
row1<-nrow(data_yr)
data_yr<-data_yr[!is.na(data_yr$v),]
row2<-nrow(data_yr)

obs_perc_cmplt<- (row2/row1)*100
```

```
# a bunch of NA values: f/ 1985 orig 8760 obs for July & Aug,
# with NAs removed, 8268, 94.38% complete for 1985
results<-rbind(results,c( station, base, yr, 'obs_perc_cmplt', obs_perc_cmplt
))

### 1. Peak tide per year- Highest high tide ####
peak_tide_yr<-max(data_yr$v)
results<-rbind(results,c( station, base, yr, 'peak_tide_yr', peak_tide_yr ))

### 2. Mean sea level (annual) ####
mean_sl_yr<-mean(data_yr$v)
results<-rbind(results,c( station, base, yr, 'mean_sl_yr', mean_sl_yr ))

### 3. Highest tide differential ####
  # goingt to be harder, have to determine "local" max and mins, subtract to
get
#differntial
# for each day, find the maximum v & min v, take difference, save in diff_res
df
# then report the max of the differences
# yr<- 1985 # testing

cat1<- "v"
agg_max<-aggregate(data_yr[cat1], by=list(Year= data_yr$Year,
Month=data_yr$Month,
                                          Day=data_yr$Day), FUN=max)
agg_min<-aggregate(data_yr[cat1], by=list(Year= data_yr$Year,
Month=data_yr$Month,
                                          Day=data_yr$Day), FUN=min)
diff<-agg_max$v -agg_min$v
max_td_diff_yr<-max(diff)
results<-rbind(results,c( station, base, yr, 'max_td_diff_yr', max_td_diff_yr
))

### 4. Maximum difference between observed and predicted tide levels
  # I don't think that we have predicted with this data set, when we looked
last
  #time we couldn't find it as an option on the site
    #https://api.tidesandcurrents.noaa.gov/api/prod/  has "predictions" at 6
#min interval

### 5. # of instances per year above 90% cumulative ####
#distribution function for entire data record period
# find percentiles of full data set 95_full, create dummy variable & sum like
#24hr exceedences,
## full data set quantiles are established at beginning of code
ct_qnt_90<-sum(data_yr$v > qnt_90)
results<-rbind(results,c( station, base, yr, 'ct_qnt_90', ct_qnt_90 ))

### 6. # of instances per year above 95% cumulative ####
# distribution function for entire data record period
ct_qnt_95<-sum(data_yr$v > qnt_95)
results<-rbind(results,c( station, base, yr, 'ct_qnt_95', ct_qnt_95 ))
```

```
} #### End of For loop ####

results$value<-as.numeric(results$value)

colnames(results)<-c("station","base", "year","measurement","value")

##########################################################################
##### Baselines & Normalization ##########################################

res_base<-results[results$year <= 1989,]

res_base$value<-as.numeric(res_base$value)
#### Establish Baselines for each indicator####
### peak_tide_yr
peak_tide_yr<-res_base[res_base$measurement =='peak_tide_yr',]
peak_tide_yr_base<-mean(peak_tide_yr$value)

### mean_sl_yr
mean_sl_yr<-res_base[res_base$measurement =='mean_sl_yr',]
mean_sl_yr_base<-mean(mean_sl_yr$value)

### max_td_diff_yr
max_td_diff_yr<-res_base[res_base$measurement =='max_td_diff_yr',]
max_td_diff_yr_base<-mean(max_td_diff_yr$value)

### ct_qnt_90
ct_qnt_90<-res_base[res_base$measurement =='ct_qnt_90',]
ct_qnt_90_base<-mean(ct_qnt_90$value)

### ct_qnt_95
ct_qnt_95<-res_base[res_base$measurement =='ct_qnt_95',]
ct_qnt_95_base<-mean(ct_qnt_95$value)
## all indicator bases found##
#### end Estab. Baseline ###


#### Normalizing data####
results$value<-as.numeric(results$value)
results$value_norm<-0
idx<-1
res_nrow<-nrow(results)

#if (results$measurement[idx] == 'peak.24hr') {
#  results$value_norm[idx]<- (results$value[idx] - peak.24hr_base) /
#peak.24hr_base}


for(idx in 1:res_nrow){
  # peak_tide_yr
  if (results$measurement[idx] == 'peak_tide_yr') {
    results$value_norm[idx]<- results$value[idx] / peak_tide_yr_base}
  if (results$measurement[idx] == 'mean_sl_yr') {
    results$value_norm[idx]<- results$value[idx] / mean_sl_yr_base}
  if (results$measurement[idx] == 'max_td_diff_yr') {
```

```
    results$value_norm[idx]<- results$value[idx] / max_td_diff_yr_base}
  # annual.precip
  if (results$measurement[idx] == 'ct_qnt_90') {
    results$value_norm[idx]<- results$value[idx] / ct_qnt_90_base}
  #thresh 1 exc
  if (results$measurement[idx] == 'ct_qnt_95') {
    results$value_norm[idx]<- results$value[idx] / ct_qnt_95_base}
} #works
#### End Normalization ####



##### write.csv- Single location results ####
csv2_loc_front<-"C:/Users/dylan/Documents/AA. AFIT/Thesis/R Sets/Analysis_v2/
Tidal_Data/tide_data_fin_"
csv2_loc_back<-"_csv2.csv"

csv2_all<-paste0(csv2_loc_front,hyp_num,csv2_loc_back)
csv2<-paste0("tide_data_fin_", hyp_num,csv2_loc_back)

# automates write.csv
write.csv(results,csv2_all, row.names = FALSE)

# write.csv(results,'C:/Users/dylan/Documents/AA. AFIT/Thesis/R Sets/Analysis_
# v2/Tidal_Data/tide_data_norm_Tyndall.csv',
#           row.names = FALSE)
#### End normalization ####
################################################################################
#### dcast- take from long to wide ####
#590A- lesson 3 slides, Character Manipulation and Functions in R

tide_data<-read.csv(csv2, sep=",", header = TRUE)

#### dcast- norm and value ####
#https://www.youtube.com/watch?v=hP7EWk09POg
#thank you, you beautiful human being you.

wide_tide_norm<-dcast(tide_data, formula = year~measurement, value.var =
"value_norm")
# (long data set, formula=1st col wanted+ 2nd col wanted(none for me) ~column
# that you want each entry to be seperated into its own column, value.var=
value
# you want filled in

wide_tide_value<-dcast(tide_data, formula = year~measurement, value.var =
"value")

### write.csv wide_tide_norm ####
csv3_loc_front<-"C:/Users/dylan/Documents/AA. AFIT/Thesis/R Sets/Analysis_v2/
Tidal_Data/tide_data_fin_wide_norm_"
csv3_loc_back<-"_csv3.csv"

csv3_all<-paste0(csv3_loc_front,hyp_num,csv3_loc_back)
csv3<-paste0("tide_data_fin_wide_norm", hyp_num,csv3_loc_back)
```

```
# automates write.csv
write.csv(wide_tide_norm,csv3_all, row.names = FALSE)


### write.csv wide_tide_value ####
csv4_loc_front<-"C:/Users/dylan/Documents/AA. AFIT/Thesis/R Sets/Analysis_v2/
Tidal_Data/tide_data_fin_wide_value_"
csv4_loc_back<-"_csv4.csv"

csv4_all<-paste0(csv4_loc_front,hyp_num,csv4_loc_back)
csv4<-paste0("tide_data_fin_wide_value", hyp_num,csv4_loc_back)

# automates write.csv
write.csv(wide_tide_value,csv4_all, row.names = FALSE)

#############################################################################

#### run lms for: int, m, p-value & r-squared ####

#### normalized ####
n_row<-nrow(wide_tide_norm)

x<-wide_tide_norm #creates new data frame
x[n_row +1,]<-"" #creates 3 new blank rows for intercept, m, and p-value
x[n_row +2,]<-""
x[n_row +3,]<-""
x[n_row +4,]<-""

x$year[n_row +1]<- "int" # titles them
x$year[n_row +2]<- "m"
x$year[n_row +3]<- "p-value"
x$year[n_row +4]<- "r-sq'd"

#### run lm's ####
# ct_qnt_90
fit_x<-lm(formula= ct_qnt_90 ~ year, data=wide_tide_norm)
summary<-summary(fit_x)
x$ct_qnt_90[n_row +1]<-summary$coefficients[1] # intercept
x$ct_qnt_90[n_row +2]<-summary$coefficients[2] # m (slope)
x$ct_qnt_90[n_row +3]<-summary$coefficients[8] # p-value
x$ct_qnt_90[n_row +4]<-summary$r.squared       # r-squared

# ct_qnt_95
fit_x<-lm(formula= ct_qnt_95 ~ year, data=wide_tide_norm)
summary<-summary(fit_x)
x$ct_qnt_95[n_row +1]<-summary$coefficients[1] # intercept
x$ct_qnt_95[n_row +2]<-summary$coefficients[2] # m (slope)
x$ct_qnt_95[n_row +3]<-summary$coefficients[8] # p-value
x$ct_qnt_95[n_row +4]<-summary$r.squared       # r-squared

# max_td_diff_yr
fit_x<-lm(formula= max_td_diff_yr ~ year, data=wide_tide_norm)
summary<-summary(fit_x)
```

```
x$max_td_diff_yr[n_row +1]<-summary$coefficients[1] # intercept
x$max_td_diff_yr[n_row +2]<-summary$coefficients[2] # m (slope)
x$max_td_diff_yr[n_row +3]<-summary$coefficients[8] # p-value
x$max_td_diff_yr[n_row +4]<-summary$r.squared       # r-squared

# mean_sl_yr
fit_x<-lm(formula= mean_sl_yr ~ year, data=wide_tide_norm)
summary<-summary(fit_x)
x$mean_sl_yr[n_row +1]<-summary$coefficients[1] # intercept
x$mean_sl_yr[n_row +2]<-summary$coefficients[2] # m (slope)
x$mean_sl_yr[n_row +3]<-summary$coefficients[8] # p-value
x$mean_sl_yr[n_row +4]<-summary$r.squared       # r-squared

# obs_perc_cmplt
fit_x<-lm(formula= obs_perc_cmplt ~ year, data=wide_tide_norm)
summary<-summary(fit_x)
x$obs_perc_cmplt[n_row +1]<-summary$coefficients[1] # intercept
x$obs_perc_cmplt[n_row +2]<-summary$coefficients[2] # m (slope)
x$obs_perc_cmplt[n_row +3]<-summary$coefficients[8] # p-value
x$obs_perc_cmplt[n_row +4]<-summary$r.squared       # r-squared

# peak_tide_yr
fit_x<-lm(formula= peak_tide_yr ~ year, data=wide_tide_norm)
summary<-summary(fit_x)
x$peak_tide_yr[n_row +1]<-summary$coefficients[1] # intercept
x$peak_tide_yr[n_row +2]<-summary$coefficients[2] # m (slope)
x$peak_tide_yr[n_row +3]<-summary$coefficients[8] # p-value
x$peak_tide_yr[n_row +4]<-summary$r.squared       # r-squared

### write.csv wide_tide_norm_p ####
csv5_loc_front<-"C:/Users/dylan/Documents/AA. AFIT/Thesis/R Sets/Analysis_v2/
Tidal_Data/tide_data_fin_wide_norm_p_"
csv5_loc_back<-"_csv5.csv"

csv5_all<-paste0(csv5_loc_front,hyp_num,csv5_loc_back)
csv5<-paste0("tide_data_fin_wide_norm_p_", hyp_num,csv5_loc_back)

# automates write.csv
write.csv(x,csv5_all, row.names = FALSE)

#### value ####
n_row<-nrow(wide_tide_value)

x<-wide_tide_value #creates new data frame
x[n_row +1,]<-"" #creates 3 new blank rows for intercept, m, and p-value
x[n_row +2,]<-""
x[n_row +3,]<-""
x[n_row +4,]<-""

x$year[n_row +1]<- "int" # titles them
x$year[n_row +2]<- "m"
x$year[n_row +3]<- "p-value"
x$year[n_row +4]<- "r-sq'd"
```

```
#### run lm's ####
# ct_qnt_90
fit_x<-lm(formula= ct_qnt_90 ~ year, data=wide_tide_value)
summary<-summary(fit_x)
x$ct_qnt_90[n_row +1]<-summary$coefficients[1] # intercept
x$ct_qnt_90[n_row +2]<-summary$coefficients[2] # m (slope)
x$ct_qnt_90[n_row +3]<-summary$coefficients[8] # p-value
x$ct_qnt_90[n_row +4]<-summary$r.squared       # r-squared

# ct_qnt_95
fit_x<-lm(formula= ct_qnt_95 ~ year, data=wide_tide_value)
summary<-summary(fit_x)
x$ct_qnt_95[n_row +1]<-summary$coefficients[1] # intercept
x$ct_qnt_95[n_row +2]<-summary$coefficients[2] # m (slope)
x$ct_qnt_95[n_row +3]<-summary$coefficients[8] # p-value
x$ct_qnt_95[n_row +4]<-summary$r.squared       # r-squared

# max_td_diff_yr
fit_x<-lm(formula= max_td_diff_yr ~ year, data=wide_tide_value)
summary<-summary(fit_x)
x$max_td_diff_yr[n_row +1]<-summary$coefficients[1] # intercept
x$max_td_diff_yr[n_row +2]<-summary$coefficients[2] # m (slope)
x$max_td_diff_yr[n_row +3]<-summary$coefficients[8] # p-value
x$max_td_diff_yr[n_row +4]<-summary$r.squared       # r-squared

# mean_sl_yr
fit_x<-lm(formula= mean_sl_yr ~ year, data=wide_tide_value)
summary<-summary(fit_x)
x$mean_sl_yr[n_row +1]<-summary$coefficients[1] # intercept
x$mean_sl_yr[n_row +2]<-summary$coefficients[2] # m (slope)
x$mean_sl_yr[n_row +3]<-summary$coefficients[8] # p-value
x$mean_sl_yr[n_row +4]<-summary$r.squared       # r-squared

# obs_perc_cmplt
fit_x<-lm(formula= obs_perc_cmplt ~ year, data=wide_tide_value)
summary<-summary(fit_x)
x$obs_perc_cmplt[n_row +1]<-summary$coefficients[1] # intercept
x$obs_perc_cmplt[n_row +2]<-summary$coefficients[2] # m (slope)
x$obs_perc_cmplt[n_row +3]<-summary$coefficients[8] # p-value
x$obs_perc_cmplt[n_row +4]<-summary$r.squared       # r-squared

# peak_tide_yr
fit_x<-lm(formula= peak_tide_yr ~ year, data=wide_tide_value)
summary<-summary(fit_x)
x$peak_tide_yr[n_row +1]<-summary$coefficients[1] # intercept
x$peak_tide_yr[n_row +2]<-summary$coefficients[2] # m (slope)
x$peak_tide_yr[n_row +3]<-summary$coefficients[8] # p-value
x$peak_tide_yr[n_row +4]<-summary$r.squared       # r-squared

### write.csv wide_tide_value ####
csv6_loc_front<-"C:/Users/dylan/Documents/AA. AFIT/Thesis/R Sets/Analysis_v2/
Tidal_Data/csv6/tide_data_fin_wide_value_p_"
csv6_loc_back<-"_csv6.csv"
```

```
csv6_all<-paste0(csv6_loc_front,hyp_num,csv6_loc_back)
csv6<-paste0("tide_data_fin_wide_value_p_", hyp_num,csv6_loc_back)

# automates write.csv
write.csv(x,csv6_all, row.names = FALSE)

################################## Fin.
#####################################
```

```
###### Precip Data Table, Results Analysis ####
# 26 Oct 21 #
setwd("C:/Users/dylan/Documents/AA. AFIT/Thesis/R Sets/Analysis_v2/Results
Analysis")

library(tidyr)
library(reshape2)
library(factoextra)

data<-read.csv("Precip.5.csv")
names(data)[1]<-'Base' # gets rid of i...base name

n.col<-ncol(data)
data<-data[4:n.col]

data<-data[c(1,2,6,7,10,13,17)]
# subsets indicators to only ones that had 10 or more bases with significant
m's
# turn this off to run across all indicators
      # data<-data[c(1,2,6,7,9,10,13,16,17,22)]
      # if you want indicators w/ 9 or more sig bases

dist.bases<-get_dist(data, method = "euclidean")
#fviz_dist(dist.bases, gradient=list(low="blue", mid="white", high="red"))
fviz_dist(dist.bases, gradient=list(low="#00AFBB", mid="white",
high="#FC4E07"))

# Elbow method- image
fviz_nbclust(data, kmeans, method = "wss")

kluster2<-kmeans(data, centers = 2, nstart = 25)
kluster3<-kmeans(data, centers = 3, nstart = 25)
kluster4<-kmeans(data, centers = 4, nstart = 25)

fviz_cluster(kluster2, data=data)
fviz_cluster(kluster3, data=data)
fviz_cluster(kluster4, data=data)
```

Bibliography

1. Inspector General. Inspector general's audit of the dod's preparation for natural disasters (2019). 2019. URL https://www.dodig.mil/reports.html/Article/1850764/audit-of-the-dods-preparation-for-natural-disasters-dodig-2019-086/.

2. David Muhlbaum and Michael Korsh. The most expensive natural disasters in u.s. history, Jul 2021. URL https://www.kiplinger.com/slideshow/business/t019-s001-most-expensive-natural-disasters-in-u-s-history/index.html.

3. Office of the Under Secretary of Defense for Acquisition and comp Sustainment. *Report on Effects of a Changing Climate to the Department of Defense*. Report no 9-D30BE5A. U.S. Department of Defense, January 2019.

4. Paola Arias, Nicolas Bellouin, Erika Coppola, Richard Jones, Gerhard Krinner, Jochem Marotzke, Vaishali Naik, Matthew Palmer, G-K Plattner, Joeri Rogelj, et al. Climate change 2021: The physical science basis. contribution of working group14 i to the sixth assessment report of the intergovernmental panel on climate change; technical summary. 2021.

5. William William VanderVeer Sweet, Greg Dusek, JTB Obeysekera, and John J Marra. Patterns and projections of high tide flooding along the us coastline using a common impact threshold. 2018.

6. Rajendra K Pachauri, Myles R Allen, Vicente R Barros, John Broome, Wolfgang Cramer, Renate Christ, John A Church, Leon Clarke, Qin Dahe, Purnamita Dasgupta, et al. *Climate change 2014: synthesis report. Contribution of Working Groups I, II and III to the fifth assessment report of the Intergovernmental Panel on Climate Change*. Ipcc, 2014.

7. Michael T Montgomery, Michael M Bell, Sim D Aberson, and Michael L Black. Hurricane isabel (2003): New insights into the physics of intense storms. part i: Mean vortex structure and maximum intensity estimates. *Bulletin of the American Meteorological Society*, 87(10):1335–1348, 2006.

8. Corbett M Smith and Charles S Graffeo. Regional impact of hurricane isabel on emergency departments in coastal southeastern virginia. *Academic Emergency Medicine*, 12(12):1201–1205, 2005.

9. Jack Beven and Hugh Cobb. Tropical cyclone report- hurricane isabel, al132003, Sep 2003. URL https://www.nhc.woc.noaa.gov/data/tcr/AL132003_Isabel.pdf.

10. Tamara Dietrich. Langley air force base battles sea level rise, Apr 2018. URL https://www.dailypress.com/news/dp-nws-lafb-flood-mitigation-20180406-story.html.

11. Yves Quilfen, Jean Tournadre, and Bertrand Chapron. Altimeter dual-frequency observations of surface winds, waves, and rain rate in tropical cyclone isabel. *Journal of Geophysical Research: Oceans*, 111(C1), 2006.

12. Harry V Wang, Jon Derek Loftis, David Forrest, Wade Smith, and Barry Stamey. Modeling storm surge and inundation in washington, dc, during hurricane isabel and the 1936 potomac river great flood. *Journal of Marine Science and Engineering*, 3(3):607–629, 2015.

13. Jon Derek Loftis, Harry Ven-Chieh Wang, and Russell J DeYoung. *A storm surge and inundation model of the Back River watershed at NASA Langley Research Center*. National Aeronautics and Space Administration, Langley Research Center, 2013.

14. On the front lines of rising seas: Joint base langley-eustis, virginia. URL https://www.ucsusa.org/resources/front-lines-rising-seas-joint-base-langley-eustis-virginia.

15. Jakob Zscheischler, Seth Westra, Bart JJM Van Den Hurk, Sonia I Seneviratne, Philip J Ward, Andy Pitman, Amir AghaKouchak, David N Bresch, Michael Leonard, Thomas Wahl, et al. Future climate risk from compound events. *Nature Climate Change*, 8(6):469–477, 2018.

16. JR Hunter, John A Church, Neil J White, and Xuebin Zhang. Towards a global regionally varying allowance for sea-level rise. *Ocean Engineering*, 71:17–27, 2013.

17. Thomas Schinko, Laurent Drouet, Zoi Vrontisi, Andries Hof, Jochen Hinkel, Junko Mochizuki, Valentina Bosetti, Kostas Fragkiadakis, Detlef Van Vuuren, and Daniel Lincke. Economy-wide effects of coastal flooding due to sea level rise: a multi-model simultaneous treatment of mitigation, adaptation, and residual impacts. *Environmental Research Communications*, 2(1):015002, 2020.

18. Reinhard E Flick, Joseph F Murray, and Lesley C Ewing. Trends in united states tidal datum statistics and tide range. *Journal of Waterway, Port, Coastal, and Ocean Engineering*, 129(4):155–164, 2003.

19. Davina L Passeri, Scott C Hagen, Nathaniel G Plant, Matthew V Bilskie, Stephen C Medeiros, and Karim Alizad. Tidal hydrodynamics under future sea level rise and coastal morphology in the northern gulf of mexico. *Earth's Future*, 4(5):159–176, 2016.

20. William V Sweet and Joseph Park. From the extreme to the mean: Acceleration and tipping points of coastal inundation from sea level rise. *Earth's Future*, 2 (12):579–600, 2014.

21. National Research Council et al. *Opportunities in the hydrologic sciences*. National Academies Press, 1991.

22. Larry W Mays. *Ground and surface water hydrology*. Wiley, 2012.

23. Thomas Wahl, Shaleen Jain, Jens Bender, Steven D Meyers, and Mark E Luther. Increasing risk of compound flooding from storm surge and rainfall for major us cities. *Nature Climate Change*, 5(12):1093–1097, 2015.

24. Kristina A Dahl, Melanie F Fitzpatrick, and Erika Spanger-Siegfried. Sea level rise drives increased tidal flooding frequency at tide gauges along the us east and gulf coasts: Projections for 2030 and 2045. *PloS one*, 12(2):e0170949, 2017.

25. Molly Mitchell, Carl Hershner, Julie Herman, Daniel E Schatt, Emily Eggington, et al. Recurrent flooding study for tidewater virginia. 2013.

26. USFEM FEMA. Design guide for improving critical facility safety from flooding and high winds: providing protection to people and buildings, 2007.

27. Ewa Lechowska. What determines flood risk perception? a review of factors of flood risk perception and relations between its basic elements. *Natural Hazards*, 94(3):1341–1366, 2018.

28. V Te Chow, DR Maidment, and LW Mays. Applied hydrology. *Journal of Engineering Education*, 308:1959, 1962.

29. I Annex. Managing the risks of extreme events and disasters to advance climate change adaptation. *Sciences*, 10:97–104, 2012.

30. Sabine Fuss, Josep G Canadell, Glen P Peters, Massimo Tavoni, Robbie M Andrew, Philippe Ciais, Robert B Jackson, Chris D Jones, Florian Kraxner, Nebosja Nakicenovic, et al. Betting on negative emissions. *Nature climate change*, 4(10): 850–853, 2014.

31. Kristen Brown. *The dynamics of coral-algal interactions on coral reef ecosystems*. PhD thesis, 06 2018.

32. National Oceanic, Atmospheric Administration, United States Geological Survey, Environmental Protection Agency, and Rutgers University.

33. John D Boon, Molly Mitchell, Jon Derek Loftis, and David M Malmquist. Anthropocene sea level change: A history of recent trends observed in the us east, gulf, and west coast regions. 2018.

34. Jon Derek Loftis, Harry V Wang, Russell J DeYoung, and William B Ball. Using lidar elevation data to develop a topobathymetric digital elevation model for subgrid inundation modeling at langley research center. *Journal of coastal Research*, (76 (10076)):134–148, 2016.

35. National Oceanic US Department of Commerce and Atmospheric Administration. Noaa's national ocean service ocean facts category, May 2016. URL `https://oceanservice.noaa.gov/facts/oceanfacts-tidescurrents.php`.

36. Guy Wöppelmann and Marta Marcos. Vertical land motion as a key to understanding sea level change and variability. *Reviews of Geophysics*, 54(1):64–92, 2016.

37. Stephanie C Herring, Nikolaos Christidis, Andrew Hoell, James P Kossin, Carl J Schreck III, and Peter A Stott. Explaining extreme events of 2016 from a climate perspective. *Bulletin of the American Meteorological Society*, 99(1):S1–S157, 2018.

38. James W Hurrell and Clara Deser. North atlantic climate variability: the role of the north atlantic oscillation. *Journal of marine systems*, 79(3-4):231–244, 2010.

39. Jeff R Knight, Chris K Folland, and Adam A Scaife. Climate impacts of the atlantic multidecadal oscillation. *Geophysical Research Letters*, 33(17), 2006.

40. NOAA. Multivariate enso index version 2 (mei.v2). URL `https://psl.noaa.gov/enso/mei/`.

41. Dennis L Hartmann. *Global physical climatology*, volume 103. Newnes, 2015.

42. Jun-Whan Lee, Jennifer L Irish, Michelle T Bensi, and Douglas C Marcy. Rapid prediction of peak storm surge from tropical cyclone track time series using machine learning. *Coastal Engineering*, 170:104024, 2021.

43. George D. Haddow, Jane A. Bullock, and Damon P. Coppola. *Introduction to emergency management*. Butterworth-Heinemann is an imprint of Elsevier, 2021.

44. Déborah Idier, Xavier Bertin, Philip Thompson, and Mark D Pickering. Interactions between mean sea level, tide, surge, waves and flooding: mechanisms and contributions to sea level variations at the coast. *Surveys in Geophysics*, 40(6): 1603–1630, 2019.

45. Mohsen Taherkhani, Sean Vitousek, Patrick L Barnard, Neil Frazer, Tiffany R Anderson, and Charles H Fletcher. Sea-level rise exponentially increases coastal flood frequency. *Scientific reports*, 10(1):1–17, 2020.

46. Heidi Kreibich, Giuliano Di Baldassarre, Sergiy Vorogushyn, Jeroen CJH Aerts, Heiko Apel, Giuseppe T Aronica, Karsten Arnbjerg-Nielsen, Laurens M Bouwer, Philip Bubeck, Tommaso Caloiero, et al. Adaptation to flood risk: Results of international paired flood event studies. *Earth's Future*, 5(10):953–965, 2017.

47. Murray C Peel, Brian L Finlayson, and Thomas A McMahon. Updated world map of the köppen-geiger climate classification. *Hydrology and earth system sciences*, 11(5):1633–1644, 2007.

48. National Oceanic National Data Buoy Center, US Department of Commerce and Atmospheric Administration, Nov 1996. URL https://www.ndbc.noaa.gov/.

49. NOAA Tides amp; Currents. Tides amp; great lakes water levels - noaa tides amp; currents. URL https://tidesandcurrents.noaa.gov/water_level_info.html.

50. Daniel Sánchez Muñoz and Jose Luis Dominguez García. Gis-based tool development for flooding impact assessment on electrical sector. *Journal of Cleaner Production*, 320:128793, 2021.

51. Lara Hawchar, Owen Naughton, Paul Nolan, Mark G Stewart, and Paraic C Ryan. A gis-based framework for high-level climate change risk assessment of critical infrastructure. *Climate Risk Management*, 29:100235, 2020.

REPORT DOCUMENTATION PAGE

Form Approved
OMB No. 0704-0188

The public reporting burden for this collection of information is estimated to average 1 hour per response, including the time for reviewing instructions, searching existing data sources, gathering and maintaining the data needed, and completing and reviewing the collection of information. Send comments regarding this burden estimate or any other aspect of this collection of information, including suggestions for reducing the burden, to Department of Defense, Washington Headquarters Services, Directorate for Information Operations and Reports (0704-0188), 1215 Jefferson Davis Highway, Suite 1204, Arlington, VA 22202-4302. Respondents should be aware that notwithstanding any other provision of law, no person shall be subject to any penalty for failing to comply with a collection of information if it does not display a currently valid OMB control number.
PLEASE DO NOT RETURN YOUR FORM TO THE ABOVE ADDRESS.

1. REPORT DATE *(DD-MM-YYYY)*	2. REPORT TYPE	3. DATES COVERED *(From - To)*
02/25/2022	Master's Thesis	September 2020 - March 2022

4. TITLE AND SUBTITLE
Hydrologic Profiles and Geospatial Trend Analysis Evaluating Recurrent Flooding at Coastal U.S. Air Force Installations

5a. CONTRACT NUMBER

5b. GRANT NUMBER

5c. PROGRAM ELEMENT NUMBER

6. AUTHOR(S)
Bechen, Dylan D., Captain, USAF

5d. PROJECT NUMBER

5e. TASK NUMBER

5f. WORK UNIT NUMBER

7. PERFORMING ORGANIZATION NAME(S) AND ADDRESS(ES)
Air Force Institute of Technology
Graduate School of Engineering and Management (AFIT/ENV)
2950 Hobson Way, Building 640
WPAFB OH 45433-8865

8. PERFORMING ORGANIZATION REPORT NUMBER
AFIT-ENV-22-M-181

9. SPONSORING/MONITORING AGENCY NAME(S) AND ADDRESS(ES)
Air Force Civil Engineering Center
2261 Hughes Ave, Ste.155
JBSA Lackland, TX 78236-9853

10. SPONSOR/MONITOR'S ACRONYM(S)
AFCEC

11. SPONSOR/MONITOR'S REPORT NUMBER(S)

12. DISTRIBUTION/AVAILABILITY STATEMENT
DISTRIBUTION A. Approved for public release: distribution unlimited.

13. SUPPLEMENTARY NOTES

14. ABSTRACT
Military installations are exposed to numerous threats, including a changing climate and the risk of recurrent flooding. The four components of recurrent flooding are sea-level rise, tidal fluctuations, storm surges, and precipitation. This research analyzed 40 years of historical precipitation and tidal data at 17 coastal U.S. Air Force installations using indicators of both peak and threshold exceedances to identify long-term temporal trends in the hydrologic components that make up recurrent flood risk, establishing an installation's "hydrologic profile" which can be used to better inform decision makers when evaluating portfolio-wide adaptation strategies and prioritization of long-term infrastructure investments.

15. SUBJECT TERMS
recurrent flooding, climate change, sea-level rise, tidal fluctuations, storm surge, precipitation, water-control infrastructure

16. SECURITY CLASSIFICATION OF:			17. LIMITATION OF ABSTRACT	18. NUMBER OF PAGES	19a. NAME OF RESPONSIBLE PERSON
a. REPORT	b. ABSTRACT	c. THIS PAGE			Dr. Christopher M. Chini, AFIT/ENV
					19b. TELEPHONE NUMBER *(Include area code)*
U	U	U	U	126	(937)255-3636 x4568